SYNTHESES OF FUNCTIONAL MATERIALS FOR ORGANIC PHOTOVOLTAIC AND ELECTROCHROMIC DEVICE APPLICATIONS

A THESIS SUBMITTED TO
THE GRADUATE SCHOOL OF NATURAL AND APPLIED SCIENCES
OF
MIDDLE EAST TECHNICAL UNIVERSITY

BY

FİGEN VARLIOĞLU

IN PARTIAL FULFILLMENT OF THE REQUIREMENTS
FOR
THE DEGREE OF MASTER OF SCIENCE
IN
POLYMER SCIENCE AND TECHNOLOGY

SEPTEMBER 2017

Approval of the thesis:

SYNTHESES OF FUNCTIONAL MATERIALS FOR ORGANIC PHOTOVOLTAIC AND ELECTROCHROMIC DEVICE APPLICATIONS

submitted by Figen VARLIOĞLU in partial fulfillment of the requirements for the degree of Master of Science in Chemistry Department, Middle East Technical University by,

Prof. Dr. Mevlüde Gülbin Dural Ünver _____
Dean, **Graduate School of Natural and Applied Sciences**

Prof. Dr. Necati Özkan _____
Head of Department, **Polymer Science & Technology**

Assist. Prof. Dr. Emrullah Görkem Günbaş _____
Supervisor, **Chemistry Dept., METU**

Examining Committee Members:

Prof. Dr. Levent Toppare _____
Chemistry Dept., METU

Assist. Prof. Dr. Emrullah Görkem Günbaş _____

Chemistry Dept., METU

Prof. Dr. Ali Çırpan _____
Chemistry Dept., METU

Assist. Prof. Dr. Salih Özçubukçu _____

Chemistry Dept., METU

Yrd. Doç. Dr. Safacan KÖLEMEN _____
Chemistry Dept., KOÇ University

Date:08/09/2017

I hereby declare that all information in this document has been obtained and presented in accordance with academic rules and ethical conduct. I also declare that, as required by these rules and conduct, I have fully cited and referenced all material and results that are not original to this work.

Name, Last name: Figen VARLIOĞLU

Signature:

ABSTRACT

SYNTHESES OF FUNCTIONAL MATERIALS FOR ORGANIC PHOTOVOLTAIC AND ELECTROCHROMIC DEVICE APPLICATIONS

VARLIOĞLU, Figen

M. Sc., Department of Polymer Science and Technology

Supervisor: Assist. Prof. Dr. Emrullah Görkem GÜNBAŞ

September 2017, 123 pages

Thienothiophene based moities are widely investigated for organic solar cell applications. In this study, after synthesizing 2-ethylhexyl 4,6-dibromothieno [3,4-b]thiophene-2-carboxylate successfully, copolymerization with commercially available donor 4-(2-ethylhexyl)-2,6-bis(trimethylstannyl)-4H-dithieno[3,2-b:2',3'-d]pyrrole, DTPy, was performed via Stille coupling. At each step, Nuclear Magnetic Resonance (NMR) Spectroscopy were performed for structural analysis. Cyclic voltammogram was used for investigation of electrochemical behaviors. Oxidation potentials of the polymer were monitored at 0.25 V/ 0.81 V for p-doping and 0.08 V/ 0.52 V for p-dedoping. Moreover, spectroelectrochemical analysis was done in order to obtain λ_{max} value which was determined to be 728 nm. Optical band gap was calculated to be 1.2 eV. This clearly shows that a strong NIR absorbing polymer was successfully synthesized. Kinetic studies show optical contrast of PTTDTPy is 14 % at 1055 nm and 17% at 720 nm with 1.43 at 1055 nm and 0.9 at 720 nm switching times. The performance of the polymer in organic solar cells is currently being investigated.

In the field of conjugated polymer systems, PEDOT has a special place. PEDOT and its derivatives are used in a variety of applications, spanning from electrochromic devices to bulk-heterojunction solar cells. Even though there is an immense interest surrounding this family of compounds the long pursued symmetric bifunctional derivative PDiEDOT (poly-dithieno[3,4-b:3',4'-e][1,4]dioxine and ProSOT (poly-3,4-dihydro-2H-thieno[3,4-b]oxathiephine) have not been realized. An eight step synthesis was envisioned in this study for realization of DiEDOT. Seven steps of this synthesis were successfully completed. Future studies will be concerned with finalization of the synthesis and investigation of electrochemical and electrochromic properties. The novel corresponding monomer of ProSOT was successfully synthesized for the first time in this study. However the monomer was not electrochemically active. Hence this monomer was brominated and moiety was coupled with stannylated 3,4-ethylenedioxythiophene EDOT to realize a novel electroactive monomer. For structural analysis NMR spectroscopy and HRMS were used. Electrochemical polymerization was performed with cyclic voltammogram with 0.1 DCM/ACN/$NaClO_4$/$LiClO_4$ systems. Oxidation potentials of the polymer was detected at 0.26 V for p-doping and 0.04 V for p-dedoping. Spectroelectrochemical results reveal that λ_{max} values were 515 nm and 555 nm and optical band gap of the polymer was calculated as 1.60 eV. Moreover, kinetic studies were conducted. At 515 nm, optical contrast of corresponding polymer was founded as 49% fast switching time of 0.8 seconds. This optical contrast value is superior to the corresponding homopolymer of EDOT, PEDOT.

Keywords: conjugated polymers, electrochemistry, organic solar cell, PEDOT, synthesis, thienothiophene.

ÖZ

ORGANİK FOTOVOLTAİK VE ELEKTROKROMİK CİHAZ UYGULAMALARI İÇİN FONKSİYONEL MALZEMELERİN SENTEZİ

VARLIOĞLU, Figen
Yüksek Lisans, Polimer Bilim ve Teknolojisi
Tez yöneticisi: Assist. Prof. Dr. Emrullah Görkem GÜNBAŞ

Eylül 2017, 123 sayfa

Tiyenotiyofen tabanlı monomerlerin araştırma ve uygulamaları organik güneş hücrelerinden OLED teknolojilerine kadar pek çok alanda yer almaktadır. Bu çalışmada, 2-etilheksil 4,6-dibromotiyeno [3,4-b]tiyofen-2-karboksilat monomerinin sentezlenmesinin ardından 4-(2-etilheksil)-2,6-bis(trimetilstannil)-4H-ditiyeno[3,2-b:2',3'-d]pirol, DTPy, donörü ile Stille kenetlenme reaksiyonu yöntemi ile kopolimerizasyonu yapılmıştır. Her sentez aşamasında yapısal analiz için Nükleer Manyetik Rezonans (NMR) spektroskopisi uygulanmış. Elektrokimyasal özelliklerinin belirlenebilmesi için dönüşümlü voltamogram kullanılmış, yükseltgenme potansiyelleri p-doping için 0.25 V/ 0.81 V ve p-dedoping için 0.08 V/ 0.52 V olarak belirlenmiştir. Spektroelektrokimyasal özellikleri incelenmiş ve λ_{max} değeri 728 nm olarak bulunmuştur. Optik bant aralığı 1.2 eV olarak hesaplanmıştır. Bu durum açıkça göstermektedir ki yakın kızıl ötesi bölgede soğurma yapabilen polimer başarılı bir şekilde sentezlenmiştir. Kinetik çalışmaları sonucunda, PTTDTPy polimerinin optik kontrast değeri 1055 nm de 1.43 sn açıp kapama süresi ile %14 ve 720 nm de 0.9 sn açıp kapama süresi ile % 17 olarak belirlenmiştir. Sentezlenen polimerin organik güneş hücresi performansı şu an çalışılmaktadır.

Konjuge, iletken, polimer sistemleri üzerine, birden çok akademik disiplinde, son 20 yılda yapılan çalışmalarda önemli bir artış olmuştur. Yapılan bu çalışmaların önemli bir çoğunluğu elektrokimyasal anlamda kararlı bir konjuge polimer olan ve bu sayede elektrokromik aygıtlardan organik tabanlı bulk heterojunction güneş hücrelerine kadar pek çok alanda uygulama olanağı sunan Poli(3,4-ethylenedioxythiophene) ve türevleri üzerine olmaktadır. PEDOT ve türevlerine karşı olan bu ilgiye rağmen, (Poli-ditiyeno[3,4-b:3',4'-e][1,4]diyoksin ve (Poli-3,4-dihidro-2H-tiyeno[3,4-b]oksatiyefin) ProSOT, monomerleri henüz araştırılmamıştır. Sekiz adım olarak tasarlanan DiDOT monomerinin sentezinin yedi adımı başarılı bir şekilde tamamlanmıştır. İlerleyen çalışmalarda sentezin tamamlanmasının ardından elektrokimyasal ve elektrokromik özellikleri araştırılacaktır. Diğer özgün malzeme olan ProSOT un monomeri ilk defa bu çalışmada başarılı bir şekilde sentezlenmiştir. Fakat monomer elektrokimyasal olarak aktif değildir. Bu nedenden dolayı monomer bromlanmış ve bu ünite tinli EDOT ile kenetlenme reaksiyonuna sokulmuştur. Elde edilen ürünün dönüşümlü voltamogram yardımı ile elektrokimyasal olarak polimerleştirilmesi sağlanmış ve malzemenin elektroaktif bir özgün malzeme olduğu belirlenmiştir. Her aşamada yapısal analizi için NMR spektroskopisi ve HRMS kullanılmıştır. Elektrokimyasal çalışmaları sonucunda yükseltgenme potansiyelleri p-doping için 0.26 V ve p-dedoping için 0.04 V olarak belirlenmiştir. Spektroelektrokimyasal sonuçlara göre λ_{max} değerleri 515 nm ve 555 nm olarak belirlenmiş optik bant aralığı 1.60 eV olarak hesaplanmıştır. Ayrıca 515 nm de optik kontrast değeri 0.8 sn gibi hızlı bir açıp kapama süre ile birlikte % 49 bulunmuştur. Elde edilen optik kontrast değeri EDOT un homopolimeri olan PEDOT' a göre daha üstün bir değere sahiptir.

Anahtar Kelimeler: elektrokimya, konjuge polimerler, organik güneş hücresi, PEDOT, sentez, tiyenotiyofen.

ACKNOWLEDGMENTS

Firstly, I would like to express my sincere thanks to my supervisor Assist. Prof. Dr. Görkem GÜNBAŞ for giving me chance to work with him. His continuous support, all advices and encouragement helped me a lot throughout the research and writing the thesis. Moreover, I want to thank him for being so energetic that always makes me feel motivated.

I must express my deepest gratitude to Prof. Dr. Levent TOPPARE for sharing his knowledge, experiences and critics about both life and this field.

I would like to thank to Özlem ÜNAL and Dr. Şerife ÖZDEMİR HACIOĞLU for all electrochemical and spectroelectrochemical studies.

Moreover, I would like to thank Prof. Dr. Ali ÇIRPAN, Assist. Prof. Dr. Salih ÖZÇUBUKÇU and Assist. Prof. Dr. Safacan KÖLEMEN for their evaluations and advices.

I would like to thank to Gizem ATAKAN, Cansu İĞCİ and Aliekber KARABAĞ for their patience about answering all illogical questions of mine and endless support since the beginning. Also thanks for making all worse and boring moments to funny events even without noticing.

I would like to thank to Osman KARAMAN, Begüm ÖZBAKIŞ, Sultan ÇETİN, Esra BAĞ, Mustafa YAŞA, Gülce ÖKLEM, Kia Ghasemi , Betül ŞEKER for their cooperation and friendship.

I would like to thank to Gamze ÖZER, my sister, for always being there for me, unconditionally, and for all the endless supports and advices since the beginning of the university.

Mehmet VAROL, my kind soul, thanks for each delicious meals and houseworks during this process. I would like to thank to Betül ÇETİNKAYA for all timeless FaceTime conversations that listen to me patiently. Most importantly, thanks for being with me whenever I feel down and their infinite sympathy.

I would like to thank to Onur ÇETİNKAYA and Kübra KOÇAK for giving me the love of chemistry and for being a great role model to me.

I would also like to thank Harun and Aykut VARLIOĞLU, my dearest brothers, for all kind of supports that gave me and also thanks for every single precious second that we are together.

I would also to thank Burçin and Feyza ANIL for their endless understanding and helps, efforts that make this summer more perfect and thanks for being such a great sisters to me.

Bilgehan YAYLALI, my husband, thanks for always being supportive and patient. Thanks for your love and wisdom that you always generously share with me, understanding my all senseless actions and, most importantly, always standing by me.

I would like to thank deeply to my father, Doğan VARLIOĞLU for giving me discipline of study as possible with being also a headteacher at home and to my mother, Serap VARLIOĞLU to give support spiritually during both education and life in general. Words could not express my thoughts and feelings regarding to your endless love, support and everything you have done for me.

To My Family

TABLE OF CONTENTS

LIST OF FIGURES

LIST OF SCHEMES

CHAPTER 1

CHAPTER 2

LIST OF TABLES

LIST OF ABBREVIATIONS

ACN Acetonitrile

Ag Silver

BT Benzothiadiazole

CE Counter Electrode

CIGS Copper Indium Gallium Di-Selenide

D-A Donor Acceptor

DCM Dichloromethane

DMF Dimethylformamide

DMSO Dimethylsulfoxide

DSSC Dye sensitized solar cell

DTPy 4-(2-ethylhexyl)-2,6-bis(trimethylstannyl)-4H-dithieno[3,2-b:2',3'-d]pyrrole

EDOT 3,4-ethylenedioxythiophene

E_g Band gap

E_g^{el} Electronic Band Gap

E_g^{op} Optical Band Gap

FTO Fluorine Tin Oxide

GPC Gel Permeation Chromatography

HOMO Highest Occupied Molecular Orbital

HRMS High Resolution Mass Spectrometry

ITO Indium Tin Oxide

I_{SC} Short circuit current

LUMO Lowest Unoccupied Molecular Orbital

NBS N-bromosuccinimide

NIR Near Infrared

NMR Nuclear Magnetic Resonance

OLED Organic Light Emitting Diodes

OPV Organic Photovoltaic

OSC Organic Solar Cell

PCE Power Conversion Efficiency

PSC Perovskite Solar Cell

Pt Platinum

PTSA p-toluenesulfonic acid

RE Reference electrode

THF Tetrahydrofuran

WE Working electrode

V_{OC} Open circuit voltage

CHAPTERS

1. SYNTHESIS OF THIENOTHIOPHENE-BASED MONOMERS

1.1 Introduction

1.1.1 Energy Problem

For obtaining energy, most of the countries around the world strongly rely on finite resources as coal, oil and natural gas. As with increasing population, demand for energy is also inevitably increase. Consequence of this situation is that the consumption of resources becomes quite expensive and more importantly detrimental effects for environment that hard to recover are on the rise. Situations such as air pollution, ozone depletion and emission of radioactive substances are some of the examples that faced with and should be taken into considerations for the future of the Earth[1-3].

Alternative energy sources are the only solutions for diminishing these effects. There are various types of renewable energy resources exist such as wind energy, solar energy, geothermal energy, bioenergy, hydropower energy and ocean energy.

1.1.1.1 Why Solar Energy is Important?

Among all of renewable energy resources, solar energy is the most promising and feasible in the aspect of sustainability which is also highly suitable for meeting the current energy demand[4]. Basically, conversion of sunlight directly into electricity is called as photovoltaics. Solar energy is the most abundant clean energy resource. It can be suitable for using in portable electronics and also by integrating solar panel at building, clean energy can be supplied at homes and businesses. These would mean

energy produced by means that is harmless to environment, no emission, no combustion or radioactive contamination and this also gives opportunity to homeowners to attain energy in a non-dependent way.

1.1.2 Solar Cells

The first observation about organic photovoltaic effect was done by Alexandre-Edmond Becquerel in 1839[5]. After years of further research conducted on the photovoltaic effect, the first modern Silicon-based solar cell was designed by Russel Ohl in 1946. In silicon solar cells thin silicon wafers are used as the active component for current generation from sunlight.

A pioneering organic photovoltaic cell was realized as anthracene single crystal being the active layer which was reported in 1959 by Kellmann and Pope[6]. However, power conversion efficiency of device was quite low due to the fact that operation of organic solar cell is mainly dependent on charge separation of electron-hole pairs (excitons) to create external current and in single layer design; it was not achievable in an efficient way. Therefore, PCE values of this type of solar cells were not above 0.1 %.

Another breakthrough approach in organic solar cell design was realized by Tang in order to address this efficiency problem. Basically, two semi-conductive materials one being an electron donor and the other an electron acceptor, were brought in contact with each other. Under this modification, power conversion efficiency was raised to 1% under simulated AM2 illumination. However, as Tang also emphasized the generation of free charge carriers are strongly depend on interface area[7]. Since then, modifications related with device design and introduction of different materials were pursued and significant developments have been achieved in area of organic photovoltaics.

1.1.2.1 First Generation Solar Cell

This type of solar cell is the earliest developed type -which is most widely used by industry due to high conversion efficiencies. Each solar panel consists of silicon wafers that can provide power about 2 to 3 watts.

There are three main categories exist due to ratio of crystalline used.

1.1.2.1.1 Single Crystalline Silicon Solar Cell

Every modules consist of only single crystal silicon which produced by a process named Czochralski[8,9]. The best efficiency that reached so far is 24.7% yet production of silicon wafer process is not cost effective[10].

1.1.2.1.2 Polycrystalline Silicon Solar Cell

Unlike in single crystalline solar cell, this type of design involves numerous crystals in single wafer that is easier and more cost effective to fabricate. However efficiencies are slightly lower (20.3%) [10] . Production is provided by liquefied silicon being filled into a mold, mainly graphite, and cooled down[11].

1.1.2.2 Second Generation Solar Cell

Amorphous silicon and most thin film based technologies are in this generation. In second generation, thickness of each layer is commonly 1 μm whereas in single crystalline silicon based cells 350 μm thickness is common[12]. Three general categories are explained below;

1.1.2.2.1 Amorphous Silicon Solar Cell (a-Si)

a-Si solar cells cost less and the silicon used devices are much thinner compared to single crystalline silicon devices. The most important feature is that manufacturing energy is much lower since low temperature processes can be applied for production of amorphous silicon. Additional different types of materials, i.e polymers, or flexible substances can be used as substrate. However, main problem of amorphous

silicon is that devices produced by using these materials have much lower efficiency (4% to 10.1%) [10].

1.1.2.2.2 Cadmium Telluride/Cadmium Sulfide Solar Cell (CdTe/CdS)

Characteristic properties of CdTe such as having 1.5 eV band gap and being stable make material suitable for solar cell applications[11]. Efficiency of designed solar cells that based on CdTe has reached to 22.1% [10]. However, abundancy of Tellurium and toxicity of Cadmium are main problems for fabrication and commercialization.

1.1.2.2.3 Copper Indium Gallium Di-Selenide Solar Cell (CIGS)

CIGS is ternary material that acts as a p-type absorber that involves elements copper,

indium, gallium and selenide. Lots of efforts have been done for improvement of efficiency after invention of CIS based thin film solar cells. Alloying with gallium (Ga) is one of the modifications that used for increasing efficiency[11,13]. CIGS solar cells have nearly 19 % efficiency and more cost effective than silicon based solar cells.

1.1.2.3 Third Generation Solar Cell

Third generation of solar cells composed of five main categories: nanocrystal, polymers, perovskite solar cells, dye sensitized and concentrated [10,11]. Although designed systems have not been completely commercialized yet, they are quite promising innovations in the field of third generation solar cells.

1.1.2.3.1 Nanocrystal Solar Cell

Semiconductor substances which mainly chosen from transition metal groups have been used. Nanocrystal solar cell has also named as quantum dots solar cells that came from the fact that size of crystal structures are in nanometer scale[11].

1.1.2.3.2 Concentrated Solar Cell

Basically, in order to collect sunlight energy to small area of solar cell, sunlight rays directed toward surface by mirrors and lenses[11].

1.1.2.3.3 Dye Sensitized Solar Cell

Unlike other third generation organic photovoltaics, no p-n junction takes place in the system. There were four main parts involved; semiconductor electrode, dye sensitizer, redox mediator and counter electrode. DSSC are extremely flexible, cost-effective and transparent. Nevertheless, stability of dye moieties are main problem in the field[14].

1.1.2.3.4 Perovskite Solar Cell

The term perovskites used for the materials which have common formula as ABX_3 where A is larger cation, commonly methylammonium ($CH_3NH^{3+)}$ with R_A = 0.18 nm, B is smaller cation, generally Pb (R_B = 0.119 nm) and X is halogen which is generally iodine. Basic design principle of perovskite solar cell was shown in Figure 1. Moreover, easy fabrication, low cost and also high mobility of free charge carrier are some features. Main obstacles of PSC are stability issues and toxicity of lead[15,16].

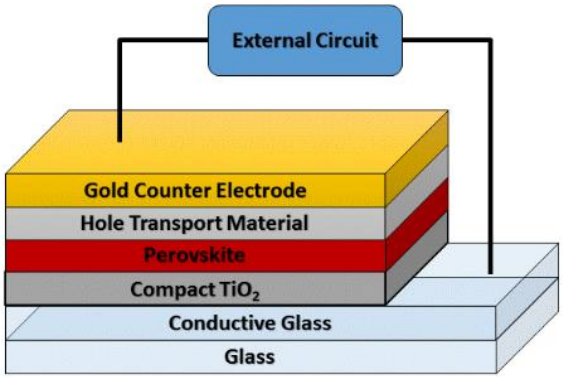

Figure 1 Perovskite Solar Cell Architecture

1.1.2.3.5 Polymer Solar Cell

As the energy demand increases, it is inevitable to find any alternative way to obtain sustainable and clean energy. One of the most encouraging alternative ways for this demand is using photovoltaics (OPV) that combine properties such as flexibility, semi-transparency and solution processing with being cost-effective and environment-friendly[17,18].

In the light of results of recent studies, it is a fact that replacement from silicon cells to organic solar cells is not possible. Therefore, application areas are directed toward recharging surfaces for laptops, phones, small home electronics, packages, clothes and accumulation of power for small portable devices such as cell-phones and tablets.

As a result of possible market opportunities a great deal of research was performed in the field of organic photovoltaics and consequently, important improvements were achieved in power conversion efficiencies.

Based on the nature of materials, fabrication of organic solar cells is much easier than fabrication of silicon based cells. Moreover, organic solar cells are much more compatible with thin film substrates than silicon cells. Organic substances fit best with wide variety of manufacturing methods like solution processes, roll-to-roll

technology and so on. While production performed via those techniques, due to their nature, organic substances enable producers to obtain large thin film surfaces coverage with low costs. Unlike semi-conductive derivatives, it is possible to make production in low temperature with organic materials which is another reason why organic solar cell is cost-effective.

As adjusting properties like altering the length or functional group of corresponding polymer unit, it is possible to change the molecular mass and the band gap. In addition to this advantage, manufacturing of different patterns and obtaining different color are also possible via combining both organic and inorganic units together. Another advantage that obtained at the end is devices produced are lightweight and

flexible which eliminate risks of getting easily damaged and provide convenience in storage, transportation and construction[17].

1.1.3 Basic Working Principle of Polymer Solar Cell

As an illustrated in Figure 2, donor and acceptor units which are active organic substances placed between two electrodes. One of electrode, used as an anode, should be transparent in order to harvest energy that come from sun. Most commonly, indium doped tin oxide (ITO) that supported by glass or plastic used as an electrode. Also, other metal oxides such as fluorine doped tin oxide (FTO), aluminum doped zinc oxide (ZnO/Al) used in construction of device[19] .

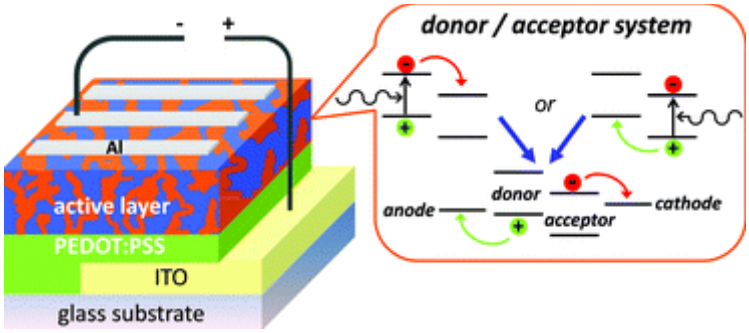

Figure 2 Polymer Solar Cell Architecture

Basically, four main steps were followed in order to create current in photovoltaic system;

Absorption of light or photon passed through transparent electrode results in generation of exciton. Resulting exciton diffuses through donor and acceptor interfaces then electron-hole pair separation takes place to form free charge carriers. Separated electrons were transferred to cathode meanwhile holes were transferred to anode. As a consequence of this phenomenon electrical energy was obtained.[1,20,21]

1.1.4 Characteristic Features of Polymer Solar Cell

Parameters such as fill factor, power conversion efficiency, V_{oc} and I_{sc} essential for stating characteristic behavior and performance of constructed device.[22,23]

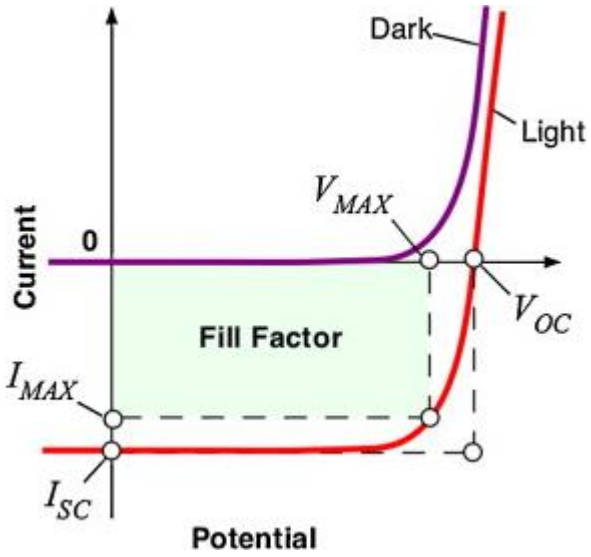

Figure 3 Diagram of JV Curve

Under dark and illuminated cases, specific behaviors of OPVs were characterized by current vs voltage figures as shown in Figure 3, V_{oc} is the open circuit voltage between anode and cathode while no flow of current go through the system and I_{sc} is short circuit current that value obtained from OPV while no external voltage exist. I_{max} and V_{max} are the parameters of current and voltage values that maximum power.

Fill factor is defined by a formula $P_{max}/(V_{oc}.I_{sc})$ or $(V_{max}\cdot I_{max})/(V_{oc}\cdot I_{sc})$

And power conversion efficiency determined by a formula $P_{max}/(E.s)$ where E is incident radiant energy and s is a surface area of corresponding cell[24].

1.1.5 Device Design of Polymer Solar Cell

Due to difference in physical nature of organic semiconductors compared to inorganic semiconductors, design of photovoltaic cell has also show differences. Semiconducting polymers or small organic molecules that used in organic photovoltaic systems are absorb light and initiate the process of transporting the electrical charges from the conduction bands of the donor material to the conduction band of the acceptor material.

There are different types of structures of organic photovoltaic systems are present such as single or multiple active layers where electron donating and electron withdrawing units are placed. In order to get high conversion efficiencies, it is necessary to perform optimizations in the device from aspect of light absorption, charge transfer, separation of counter charges and collection of the charges.

Briefly, at single layer system, Organic semi-conductor material was placed between two terminal electrodes which are ITO and Al, Ca, Mg or Ag that create an electrical field over semi-conductor material to separate hole-electron pair and facilitate transportation of corresponding charges to anode and cathode as illustrated in Figure 4.

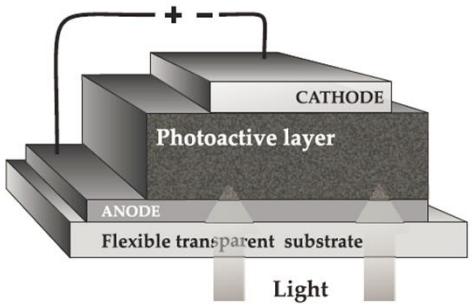

Figure 4 Single Layer Solar Cell Architecture

As a second approach, apart from single layer PSC, at double layer construction, two organic materials which one of them act as a donor and the other as an acceptor were placed between terminal electrodes. Separation of exciton was achieved more successfully. However, transfer of charges was not efficient enough.

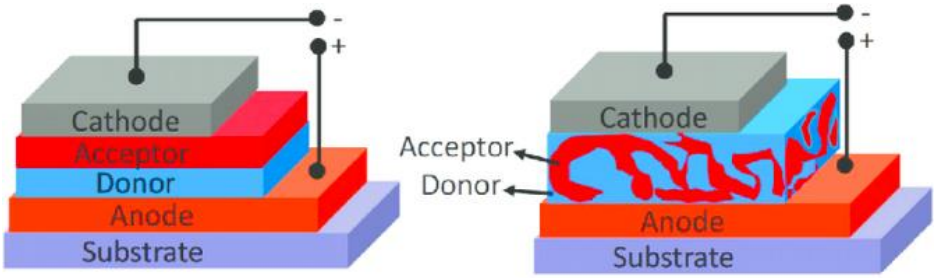

Figure 5 Bilayer and Bulk Heterojunction Architecture

Thirdly, in bulk heterojunction device design, semiconductor donor and acceptor materials were blended as a bulk. Since donor and acceptor were blended, wider interface area was obtained, therefore, more exciton diffusion takes place and consequence of this more electron-hole separation were achieved. This translated into significant increase in efficiency of organic solar cell. Due to those features, bulk-heterojunction architecture is the most commonly preferred device structure[24]. As emphasized in previous parts, there have been a great amount of efforts in the field of organic photovoltaics and efficiency of OPV devices have been increased from 0.1% to nearly 12%. However, the obtained efficiency values are still not high enough to meet needs of industry. Therefore, devices are not being commercialized yet. Most important handicaps that prevent improvements are, firstly, materials used in cell have lack of ability to absorb energy in NIR region but visible region. Consequently, huge amount of energy might came from NIR region were missed. Secondly, even if polymeric materials that ability to absorb energy from NIR used, due to nature of having low band gap leads to diminishing the V_{oc} value of corresponding cell[1].

1.1.5.1 NIR Absorbing Donor-Acceptor Type Polymers

In 1991, a conducting polymer that synthesized from Th (thiophene unit) as a donor and Py (pyrrole unit) as an acceptor showed that interaction between these units caused to intramolecular charge transfer which leads to further stabilization of quinoid architecture, consequently, red shift was observed [25,26].

Since then detail studies related with to these phenomena were performed and numerous new materials with different types of structures, as represented at Figure 6, were realized.

One of the commonly used units in literature is benzothiadiazole, BT. It is used as an acceptor moiety. Recently a copolymer that contains BT unit, namely PffBT4T-2OD (Figure 6, polymer **5**) has reached to 10.8% power conversion efficiency as a single-junction solar cell.

Secondly, diketopyrrolopyrrole, DPP, was another unit that highly employed in polymers for OSC applications and it was stated that PCE value of one of its copolymer DPPTT-T (Figure 6, polymer **9**) was founded as 8.8%.

Another important acceptor core unit used in this area is Thieno[3,4-*b*]thiophene which important developments have been succeeded. PTB7 involved solar cell has 9.15 % efficiency with 0.740 V V_{oc} value while PTB7-Th involved solar cell has 10.28%, 0.815 V respectively[27,28]. In another modification, thiophene units were switched to selenophene (Figure 6, polymer **12)**. Power conversion of synthesized polymer PBDTSe-TT was determined as 9%. Main reason for this increment is explained as higher intermolecular interaction between Se units leads to favorable morphology and therefore higher efficiency was obtained[29].

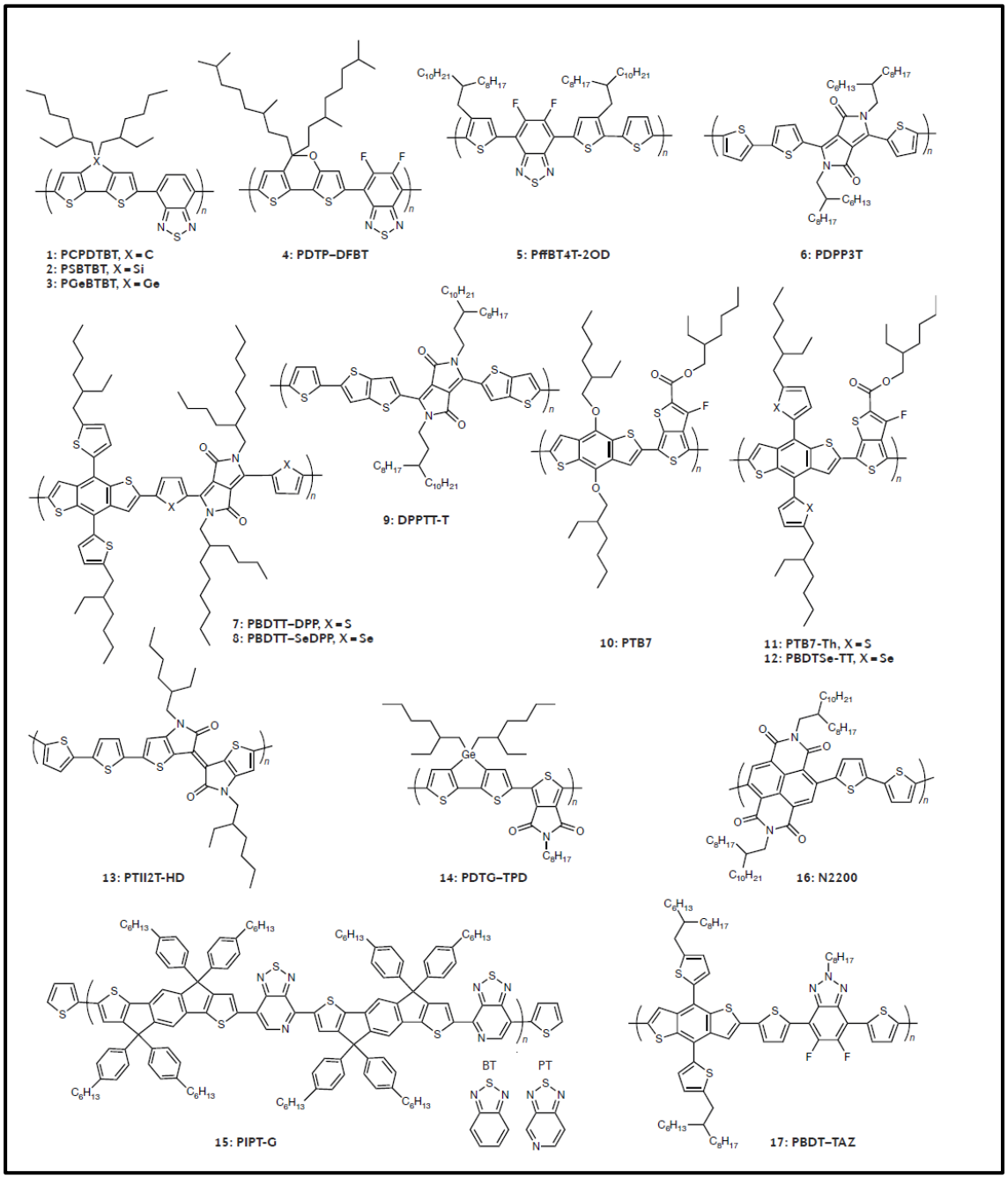

Figure 6 Schematic Representation of NIR Absorbing Polymer Units

1.1.5.3 Tandem Polymer Solar Cells

Innovations related with NIR absorbing donor-acceptor type made on designing organic photovoltaics that with tandem architecture possible, where two or more active layers had involved as in inorganic solar cells to harvest energy that not only

from visible but also from NIR region. Briefly, as an illustration, in double-layer junction, two active layers are used with one wide band gap material to absorb high energy photons and one low band gap material that absorb low energy photons are used.

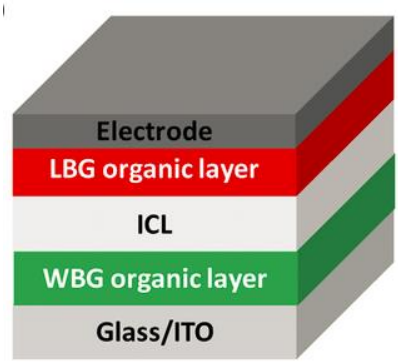

Figure 7 Tandem Polymer Solar Cell Architecture

As stated earlier, effective collection of photon to create more charge carriers is the critical point towards high in power conversion efficiency. Consequently, tandem device architecture is one approach for achieving effective collection of photons. In the literature, It was stated in 2007 that Kim et al. was achieved to brought two effective cells together and obtained 6.50% power conversion efficiency. Another important study was conducted by Yang et al. where 10% efficiency for double tandem cell was achieved. Additionally, with designing triple junction photovoltaic with a different level of band gaps Yang group was able to reach 11.5% PCE value. Zong et al. has reached to 11.62% PCE in double junction photovoltaic by synthesizing new promising low band gap polymer with 1.4 eV optical band gap [30,31].

However, due to the fact that each cell should be design and optimize to cohere I_{sc} of each cell, manufacturing of tandem organic photovoltaics is still costly and tedious.

1.1.5.4 Ternary Polymer Solar Cells

Another alternative method that investigated is ternary architecture. Basically, active layers were composed of three main parts that are Donor: Acceptor and the additional component. Three main mechanism were involved which are energy

transfer mechanism; charge transfer mechanism and parallel like or alloy model. The structures are categorized as D_1:D_2:A and D:A_1:D_2 with respect to the energy levels of the third component. As the third component mainly used for stronger absorption of light, small organic molecules that have advantages such as being easily synthesized and low band gap polymers, nanoparticles like Au, Ag were employed[32].

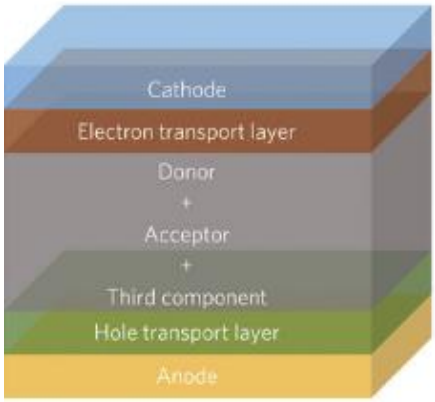

Figure 8 Ternary Polymer Solar Cell Architecture

Stille Coupling

Synthesis of D-A type copolymerization was achieved by transition metal-catalyzed cross-coupling reactions such as Suzuki-Miyaura, Sonogashira or Stille coupling.

Stille Cross coupling reaction is one of the most effective synthetic routes that for formation of C-C bond among aromatic halides and stannanes in the presence of palladium catalyst[33].

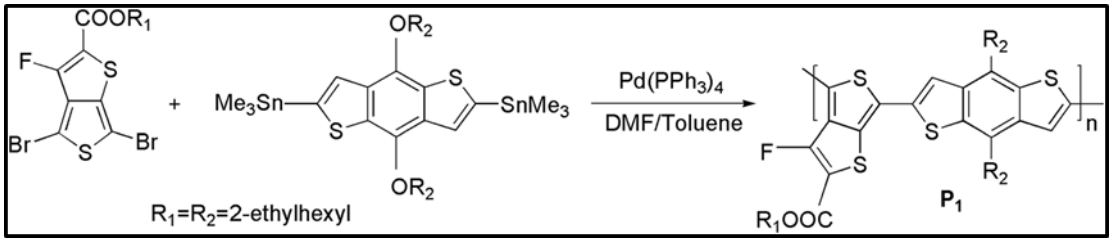

Figure 9 Stille Coupling Reaction

1.1.6 Aim of the Study

Main purpose of this study is to synthesize 2-ethylhexyl 4,6-dibromothieno [3,4-b]thiophene-2-carboxylate (TT), 2-ethylhexyl 4,6-di(selenophene-2-yl)thieno[3,4-b]thiophene-2-carboxylate and fluorinated derivative of corresponding TT unit, namely, 2-ethylhexyl 4,6-dibromo-3-fluorothieno[3,4-b]thiophene-2-carboxylate and perform copolymerization via commercially available 4-(2-ethylhexyl)-2,6-bis(trimethylstannyl)-4H-dithieno[3,2-b:2',3'-d]pyrrole with Stille cross-coupling to obtain materials that can absorb both in visible and near infrared regions. These materials will be used as donors in organic solar cells applications. All polymers that are designed in the context of this theses study are novel. In addition to synthesis and solar cell applications, electrochemical, spectroelectrochemical and kinetic studies of the synthesized polymers will be conducted to investigate properties such as redox behaviors, optical properties and electronic band gaps, HOMO-LUMO levels, percent transmittances and switching times.

1.2 Experimental

1.2.1 Materials

All the chemicals were purchased from Aldrich except 4-(2-ethylhexyl)-2,6-bis(trimethylstannyl)-4H-dithieno[3,2-b:2',3'-d]pyrrole that purchased from Solarmer.

1.2.2 Methods and Equipments

All the reactions were carried out under argon atmosphere unless otherwise mentioned. The same methods were used for synthesis of PTTDTPy that described in the literature. Et_2O, toluene, DMF, THF were dried with sodium and benzophenone or used from Mbraun MBSPS5 solvent drying system. ^{1}H and ^{13}C NMR analyses of poly-2-ethylhexyl4-(4-(2-ethylhexyl)-6-methyl-4H-dithieno[3,2-b:2',3'-d]pyrrol-3-yl)-6-methylthieno[3,4-b]thiophene-2-carboxylate were done via Bruker Spectrospin Avance DPX-400 Spectrometer. $CDCl_3$ and d_6-DMSO were used as a solvent and tetramethylsilane was used as internal reference. Electrochemical analysis was conducted with a three electrode cell system. Platinum wire used as the counter electrode, ITO coated glass slide was the working electrode and silver wire was the reference electrode. Varian Cary 5000 UV-Vis spectrometer was used for spectroelectrochemical study.

1.2.3 Monomer Syntheses

1.2.3.1 Synthetic Route of 2-Ethylhexyl 4,6-dibromothieno [3,4-b]thiophene-2-carboxylate

1.2.3.1.1 Synthesis of Tetrabromothiophene[34]

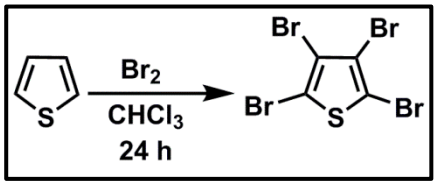

Scheme 2.1 Synthesis of Tetrabromothiophene

To a solution of thiophene (10.0 g, 0.119 mol) in chloroform (10 mL), bromine (37 mL, 0.72 mol) in $CHCl_3$ (40 mL) was added dropwise within 3 hours at 0 °C under argon atmosphere. After warming the reaction mixture to room temperature, further addition of bromine (5.0 mL, 0.097 mol) was performed and the mixture was stirred at reflux temperature for another 3 hours. A saturated aqueous solution of NaOH (150 mL) was added dropwise and stirred for 1 hour in reflux temperature under argon atmosphere. Extraction was performed 3 times with DCM and combined organic phases were dried over anhydrous $MgSO_4$. The solution was filtrated and the solvent was evaporated under reduced pressure. Recrystallization was performed to crude product from 3:1 (v/v) solution of methanol and $CHCl_3$ and white crystals (45.8 g) was obtained with a 96% yield.

^{13}C NMR (400 MHz, $CDCl_3$) δ (ppm) 117.0, 110.3

1.2.3.1.2 Synthesis of 3,4-Dibromothiophene[34]

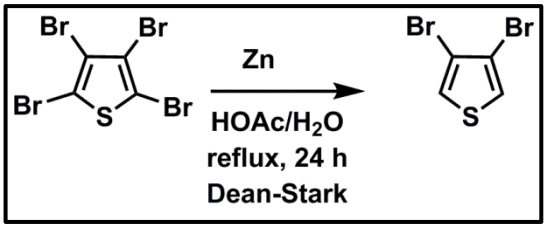

Scheme 2.2 Synthesis of 3,4-Dibromothiophene

To a 100 mL reaction vessel with 20 mL of glacial acetic acid and 40 mL of water, the mixture of tetrabromothiophene (25.0 g, 62.5 mmol) and zinc powder (12.7 g, 194 mmol) was added by portion within 45 min. Then, reaction mixture was stirred at 120 °C under argon atmosphere for 24 hours by using Dean-Stark apparatus. Colorless liquid product that was collected in the apparatus was taken directly. The remaining aqueous layer was extracted with DCM. Organic phases and the first collected organic liquid were combined, dried and the solvent was evaporated to give target compound (13.0 g, 86%).

^{1}H NMR (400 MHz, $CDCl_3$) δ (ppm) 7.22 (s, 2H)

^{13}C NMR (400 MHz, $CDCl_3$) δ (ppm) 123.8, 114.0

1.2.3.1.3 Synthesis of 4-Bromothiophene-4-carbaldehyde[35]

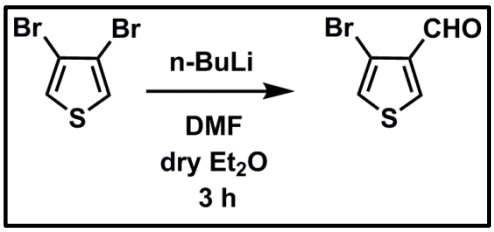

Scheme 2.3 Synthesis of 4-Bromothiophene-4-carbaldehyde

Under argon atmosphere, n-BuLi (5.9 mL, 2.5 M in hexane) was added dropwise to the solution of 3,4 dibromothiophene (4.00 g, 16.5 mmol) in 56 mL of dry Et_2O at -78 °C and stirred for 40 min. Then, dry DMF (1.20 g, 16.5 mmol) was added slowly

and the mixture was stirred for another 2 hours. After bringing the reaction to room temperature, the mixture was poured into a saturated NH_4Cl solution and extraction was performed with Et_2O twice and dried with anhydrous $MgSO_4$, filtered and the solvent was evaporated. Purification was done with silica gel column chromatography (Hexane/EtOAc=10/1) and light yellow oil product was obtained (1.71 g, 54%).

^{1}H NMR (400 MHz, $CDCl_3$) δ (ppm) 9.87 (s, 1H), 8.08 (d, *J* = 3.4 Hz, 1H), 7.30 (d, *J* = 3.5 Hz, 1H).

^{13}C NMR (400 MHz, $CDCl_3$) δ (ppm) 184.7, 137.5, 134.6, 125.1, 111.3.

1.2.3.1.4 Synthesis of Ethyl thieno [3,4-b]thiophene-2-carboxylate[35]

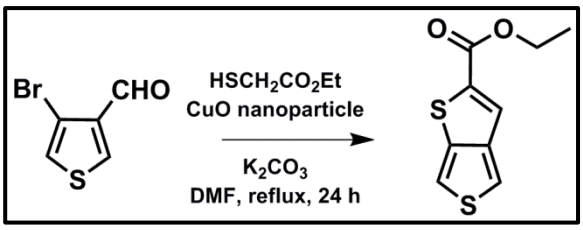

Scheme 2.4 Synthesis of Ethyl thieno [3,4-b]thiophene-2-carboxylate

To a solution of 4- bromothiophene-4-carbaldehyde (1.70 g, 8.89 mL) in dry DMF, CuO nanoparticle (140 mg, 1.70 mmol) and K_2CO_3 (1.85 g, 13.1 mmol) was added. Then, at 60 °C ethyl mercaptoacetate (1.2 g, 1.1 mL, 9.8 mmol) was added dropwise and the reaction mixture was stirred overnight at that temperature under argon atmosphere. After bringing the reaction to room temperature, it was poured into distilled water and the mixture was extracted twice Et_2O. Collected organic layers were washed successively with brine and distilled water. The organic phase was dried (with $MgSO_4$) and the solvent was evaporated. Silica gel column chromatography was performed for purification (Hexane/EtOAc=9/1) and 1.69 g of light yellow solid product was obtained (84%).

^{1}H NMR (400 MHz, $CDCl_3$) δ (ppm) 7.7 (s, 1H), 7.6 (d, *J* = 2.7 Hz, 1H), 7.3 (d, *J* = 2.7 Hz, 1H), 4.4 (q, *J* = 7.1 Hz, 2H), 1.4 (t, *J* = 7.1 Hz, 3H)

^{13}C NMR (400 MHz, $CDCl_3$) δ (ppm) 163.5, 146.3, 140.3, 140.2, 123.8, 116.9, 111.7, 61.9, 14.6

1.2.3.1.5 Synthesis of Ethyl 2,5 -dibromothieno[3,4-b]thiophene-2-carboxylate[36]

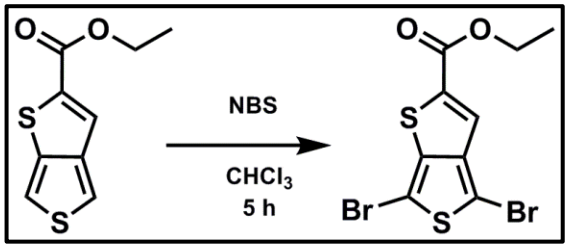

Scheme 2.5 Synthesis of Ethyl 2,5 -dibromothieno[3,4-b]thiophene-2-carboxylate

N-bromosuccinimide (211 mg, 1.17 mmol) was added portionwise to a solution of ethyl thieno [3 4-b] thiophene-2-carboxylate (100 mg, 0.470 mmol) in 20 mL of $CHCl_3$ at 35 °C. The reaction mixture was stirred at that temperature for 3 hours and poured into distilled water and extracted three times with $CHCl_3$. Collected organic phases was washed with distilled water and dried over anhydrous $MgSO_4$ and the solvent was evaporated. The attained brown solid was recrystallized from ethanol and light yellow solid was obtained (120 mg, 68%).

^{1}H NMR (400 MHz, $CDCl_3$) δ (ppm) 7.53 (s, 1H), 4.38 (q, *J* = 7.1 Hz, 2H), 1.40 (t, *J* = 7.1 Hz, 3H)

^{13}C NMR (400 MHz, $CDCl_3$) δ (ppm) 162.3, 145.6, 141.1, 140.4, 123.2, 102.3, 97.1, 62.1, 14.3

1.2.3.1.6 Synthesis of 4,6 -Dibromothieno[3,4-b]thiophene-2-carboxylic acid[35]

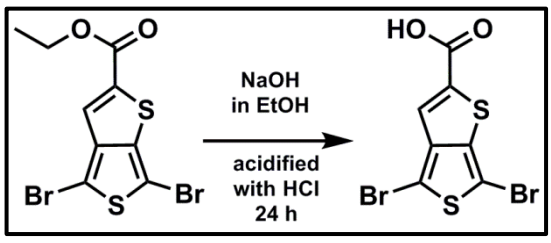

Scheme 2.6 Synthesis of 4,6 -Dibromothieno[3,4-b]thiophene-2-carboxylic acid

To a solution of NaOH (140 mg, 3.58 mmol) in 30 mL of ethanol, ethyl 2,5-dibromothieno [3,4-b]thiophene-2-carboxylate (650 mg, 1.76 mmol) was added and the mixture was stirred overnight at a reflux temperature under argon atmosphere. After bringing reaction to room temperature, mixture was poured into water and extracted twice with hexane. Then, to aqueous phase, concentrated HCl was added dropwise and formed yellow solid was filtered and recrystallized from ethanol (580 mg, 90%).

^{1}H NMR (400 MHz, DMSO) δ (ppm) 7.47 (s, 1H)

^{13}C NMR (400 MHz, DMSO) δ (ppm) 163.0, 145.3, 142.9, 139.5, 122.3, 102.5, 97.4

1.2.3.1.7 Synthesis of 2-Ethylhexyl 4,6-dibromothieno [3,4-b]thiophene-2-carboxylate[37]

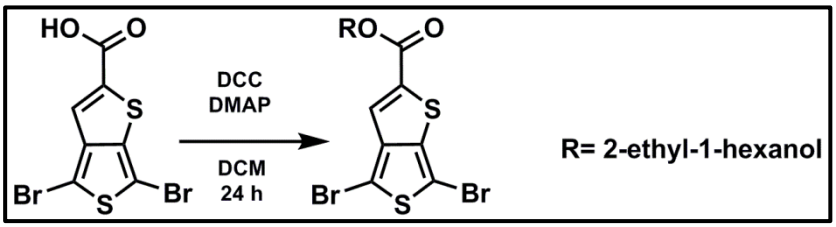

Scheme 2.7 Synthesis of 2-Ethylhexyl 4,6-dibromothieno [3,4-b]thiophene-2-carboxylate

A solution of 4,6 -Dibromothieno[3,4-b]thiophene-2-carboxylic acid (250 mg, 0.731 mmol), DCC (181 mg, 0.877 mmol) and DMAP (30.8 mg, 0.252 mmol) in 30 mL DCM were mixed and 2-ethyl-hexanol (476 mg, 3.65 mmol) was added. After mixing under argon atmosphere at room temperature, solution was poured into distilled water and extracted with DCM. Collected organic phases dried over anhydrous $MgSO_4$, filtered and the reaction solvent was evaporated. For further purification, silica gel column chromatography was performed. (Hexane/DCM=4/1) and dark orange oil was obtained (238 mg, 78%).

^{1}H NMR (400 MHz, $CDCl_3$) δ(ppm) 7.40 (s, 1H), 4.22 (s, 2H), 1.70 – 1.62 (m, 1H), 1.43 – 1.32 (m, 8H), 0.93 – 0.91 (m, 6H)

^{13}C NMR (400 MHz, $CDCl_3$) δ(ppm) 162.2, 145.4, 141.1, 140.4, 122.9, 102.2, 97.1, 68.3, 38.8, 30.5, 29.0, 23.9, 23.0, 14.1, 11.1

1.2.3.2 Synthetic Route of 2-Ethylhexyl 4,6-di(selenophene-2-yl)thieno[3,4-b]thiophene-2-carboxylate

1.2.3.2.1 Synthesis of Tributyl(selenophen-2-yl)stannane[38]

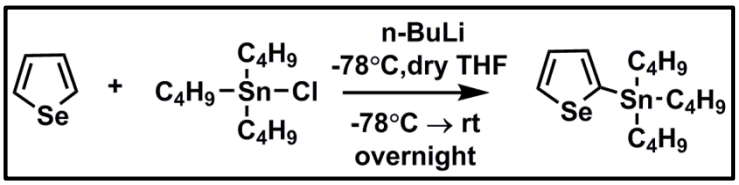

Scheme 2.8 Synthesis of Tributyl(selenophen-2-yl)stannane

To a solution of selenophene (1.00 g, 7.63 mmol) in 25 mL of dry THF, n-BuLi (3.4 mL, 2.5 M in hexane) was added dropwise at -78 °C within 45 minutes under argon atmosphere and the mixture was stirred for 1 hour at that temperature. After addition of tributyltin chloride (2.75 g, 8.84 mmol) to the reaction mixture slowly, temperature was raised to room temperature and the reaction mixture was stirred overnight. Solvent of the reaction was removed and the crude product was dissolved in $CHCl_3$. Solution was washed three times with water, dried over anhydrous $MgSO_4$, filtered. After removal of the solvent, light brown oil was obtained (3.1 g, 97%).

^{1}H NMR (400 MHz, $CDCl_3$) δ(ppm) 8.62 – 8.24 (m, 1H), 7.66 – 7.47 (m, 2H), 1.73 – 1.54 (m, 6H), 1.46 – 1.31 (m, 6H), 1.29 – 1.06 (m, 6H), 0.98 – 0.88 (m, 9H)

^{13}C NMR (100 MHz, $CDCl_3$) δ(ppm) 143.6, 137.9, 135.3, 130.5, 29.0, 27.3, 13.7, 11.1

1.2.3.2.2 Synthesis of 2-Ethylhexyl 4,6-di(selenophene-2-yl)thieno[3,4-b]thiophene-2-carboxylate

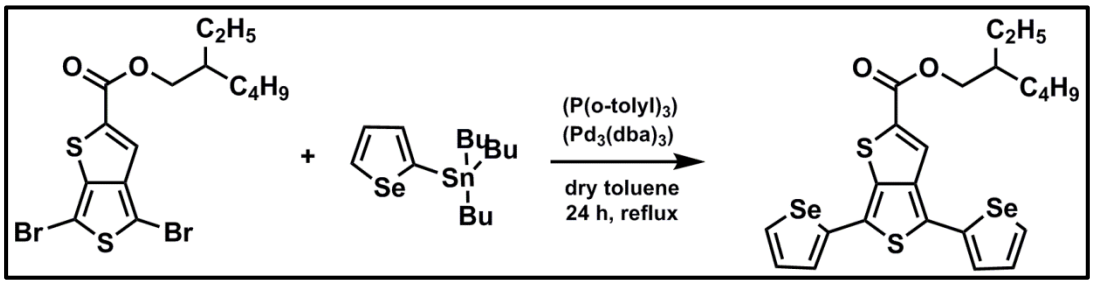

Scheme 2.9 Synthesis of 2-Ethylhexyl 4,6-di(selenophene-2-yl)thieno[3,4-b]thiophene-2-carboxylate

After applying vacuum-argon cycles successively to a 50 mL, 2 neck reaction flask, to a solution of 2-ethylhexyl 4.6-dibromothieno [3,4-b]thiophene-2-carboxylate (100 mg, 0,220 mmol) in 20 ml dry toluene was prepared. To this solution tributyl(selenophen-2-yl)stannane, (277 mg, 0,660 mmol) was added. After addition of tri(o-tolyl)phosphine ($P(o\text{-}tolyl)_3$) (10.1 mg, 0.0332 mmol) and tris(dibenzylideneacetone) dipalladium(0) ($Pd_2(dba)_3$) (10.1 mg, 0.0110 mmol) catalyst, the reaction mixture was stirred at reflux temperature under argon atmosphere for 20 hours. After bringing reaction to room temperature, the reaction solvent was removed. Crude solid was purified with silica gel column chromatography (Hexane/EtOAc=50/1) and orange solid was obtained (70 mg, 58%).

^{1}H NMR (400 MHz, $CDCl_3$) δ (ppm) 8.01 (d, *J* = 5.5 Hz, 2H), 7.88 (s, 1H), 7.39 (d, *J* = 1.9 Hz, 2H), 7.30 (d, *J* = 3.7 Hz, 2H), 4.25 (s, 2H), 1.79 – 1.68 (m, 1H), 1.46 – 1.32 (m, 8H), 0.99 – 0.89 (m, 6H)

^{13}C NMR ($CDCl_3$) δ (ppm) 162.9, 141.8, 140.5, 140.1, 139.9, 136.5, 131.5, 130.9, 130.6, 130.5, 129.8, 127.2, 126.0, 124.3, 124.2, 124.0, 68.4, 38.9, 30.6, 29.1, 24.1, 23.1, 14.2, 11.2

1.2.3.3 Synthetic Route of 2-Ethylhexyl 4,6-dibromo-3-fluorothieno[3,4-b]thiophene-2-carboxylate

1.2.3.3.1 Synthesis of Methyl 2, 3 –Bis (chloromethyl) thiophene-2-carboxylate[39]

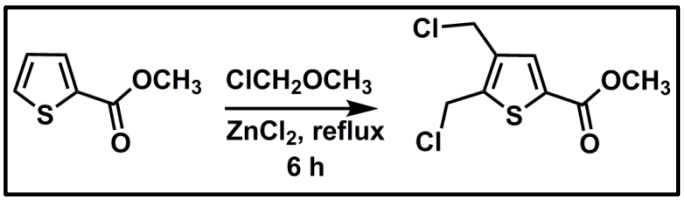

Scheme 2.10 Synthesis of Methyl 2, 3 –bis (chloromethyl) thiophene-2-carboxylate

To a suspension of dry zinc chloride (3.83 g, 28.1 mmol) and 3.32 mL chlorodimethyl ether, a solution of methyl 2-thiophenecarboxylate (4.0 g, 28 mmol) in 33.2 mL chlorodimethyl ether was added dropwise within 15 minutes. The temperature of the reaction was raised to 50 °C and stirred for 6 hours. Then the reaction was cooled to room temperature and it was poured into ice and stirred for additional 1 hour. The mixture was filtered with cold water and formed yellow product was recrystallized from petroleum ether to get 3.32 g white crystals (50% yield).

^{1}H NMR (400 MHz, $CDCl_3$) δ (ppm) 7.70 (s, 1H), 4.77 (s, 2H), 4.58 (s, 2H), 3.87 (s, 3H)

^{13}C NMR (400 MHz, CDCl3) δ(ppm) 161.8, 143.8, 137.1, 134.8, 132.9, 52.4, 37.4, 37.1

1.2.3.3.2 Synthesis of Methyl 4, 6-Dihydrothieno[3,4-b]thiophene-2-carboxylate[39]

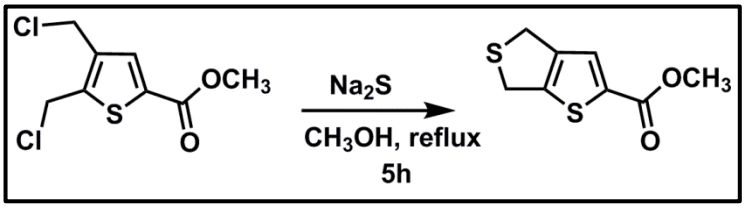

Scheme 2.11 Synthesis of Methyl 4, 6-dihydrothieno[3,4-b]thiophene-2-carboxylate

A solution of 2,3-Bis(chloromethyl)thiophene-2-carboxylate (200 mg, 0.836 mmol) in 10 mL of methanol heated until boiling and Na_2S (221 mg, 0.920 mmol) in 7 mL of methanol was added dropwise to this solution and stirred for 5 hours. After bringing the reaction mixture to room temperature, formed solid particles were filtered and dissolved in methanol. The solution was washed with distilled water three times and collected organic phases were dried over $MgSO_4$, filtered and the solvent was evaporated. Crude product was purified with silica gel column chromatography. (DCM/Hexane=2/1) (30 mg, 18%).

^{1}H NMR (400 MHz, $CDCl_3$) δ (ppm) 7.46 (s, 1H), 4.18 – 4.17 (m, 2H), 4.05 – 4.03 (m, 2H), 3.86 (s, 3H)

^{13}C NMR (400 MHz, $CDCl_3$) δ (ppm) 162.2, 146.6, 143.9, 137.0, 127.8, 52.1, 33.5, 33.1

1.2.3.3.3 Synthesis of 4,6-Dihydro[3,4-b]thiophene-2-carboxylic acid [39]

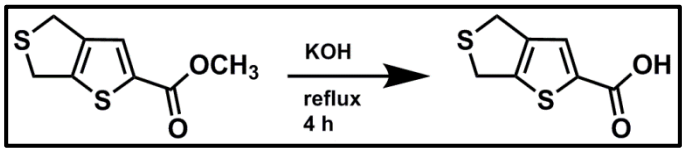

Scheme 2.12 Synthesis of 4,6-Dihydro[3,4-b]thiophene-2-carboxylic acid

To methyl 4,6-dihydrothieno[3,4-b]thiophene-2-carboxylate (300 mg, 1.50 mmol), 1 M NaOH in methanol was added and the mixture was stirred overnight at reflux temperature under argon atmosphere. After cooling the reaction to room temperature, the mixture was poured into distilled water and extracted twice with petroleum ether. Then, concentrated HCl was added to aqueous phase and solid particles that were formed was filtered and dried. For purification, crude product was filtered through plug of silica (DCM/Methanol, 10%) and 215 mg white solid was obtained (77%).

^{1}H NMR (400 MHz, DMSO-d_6) δ(ppm) 7.54 (s, 1H), 4.26 (t, 2H), 4.09 (t, 2H)

^{13}C NMR (400 MHz, DMSO-d_6) δ(ppm) 162.8, 145.9, 143.9, 138.3, 127.8, 32.7, 32.4

1.2.3.4 Polymer Syntheses

1.2.3.4.1 Synthesis of Poly- 2-Ethylhexyl 4-(4-(2-ethylhexyl)-6-methyl-4H-dithieno[3,2-b:2',3'-d]pyrrol-3-yl)-6-methylthieno[3,4-b]thiophene-2-carboxylate

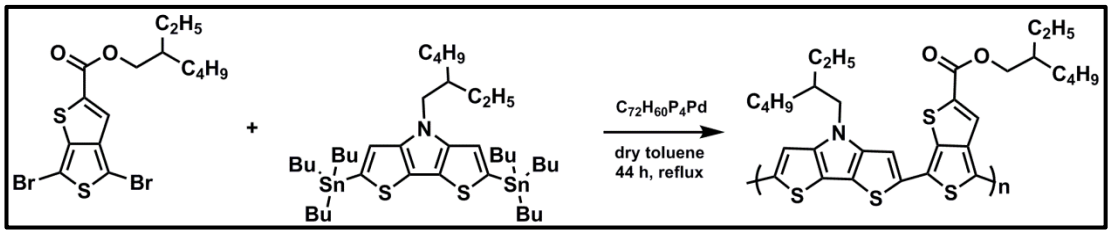

Scheme 2.13 Synthesis of Poly- 2-Ethylhexyl 4-(4-(2-ethylhexyl)-6-methyl-4H-dithieno[3,2-b:2',3'-d]pyrrol-3-yl)-6-methylthieno[3,4-b]thiophene-2-carboxylate

After three cycle of vacuum-argon, a solution of 2-ethylhexyl 4,6-dibromothieno [3,4-b]thiophene-2-carboxylate (100 mg, 0.220 mmol) in 10 mL of dry toluene was prepared and 4-(2-ethylhexyl)-2,6-bis(trimethylstannyl)-4H-dithieno[3,2-b:2',3'-d]pyrrole (136 mg, 0.220 mmol) was added. After, bubbling argon through reaction mixture for 20 minutes, tetrakis(triphenylphosphine)palladium(0) (10.2 mg, 0.00833 mmol) was added and reaction mixture was stirred under argon atmosphere. The polymerization was carried out at reflux temperature for 44 hours.

At the end of the 29th and 40th hours, additional amounts of tetrakis(triphenylphosphine)palladium(0) (5.09 mg) were added. The end groups were capped by refluxing the reaction mixture with tributyl(thiophen-2-yl)stannane (1.1 eq) for 4 hours and then with 2-bromothiophene (1.1 eq) for another 4 hours. Then, crude product was precipitated into methanol and collected by filtration. The filtrate was washed successively with hexane, acetone and chloroform for 24 hours in a soxhlet apparatus. After being dried in vacuum oven, TT-DTPy was obtained as a black solid (89 mg, 70%).

1.3 Results and Disscussion

1.3.1 Monomer Syntheses

1.3.1.1 Synthesis of 2-Ethylhexyl 4,6-dibromothieno [3,4-b]thiophene-2-carboxylate

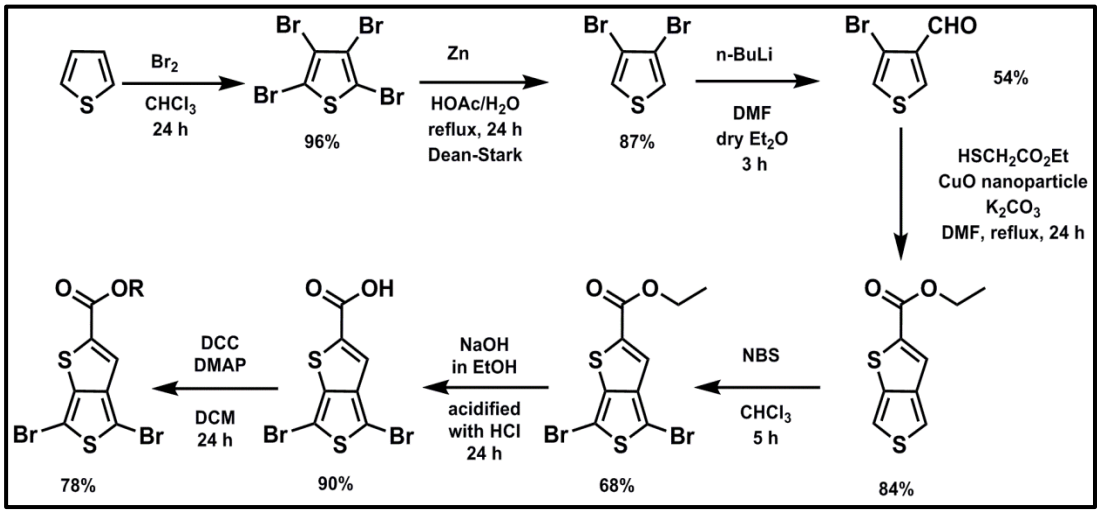

Scheme 3.1 Synthetic Pathway of 2-Ethylhexyl 4,6-dibromothieno [3,4-b]thiophene-2-carboxylate

Synthetic pathway as shown in scheme 3.1 was followed for monomer, 2-ethylhexyl 4,6-dibromothieno [3,4-b]thiophene-2-carboxylate, in an accordance to literature. For synthesis of final product, Steiglich esterification was performed. Although first preference for alkyl chain was 1-dodecanol, the product was extremely unstable. Therefore, as a second attempt, 2-ethyl-1-hexanol was used and the final product was successfully isolated with 78% yield.

1.3.1.2 Synthesis of 2-Ethylhexyl 4,6-di(selenophene-2-yl)thieno[3,4-b]thiophene-2-carboxylate

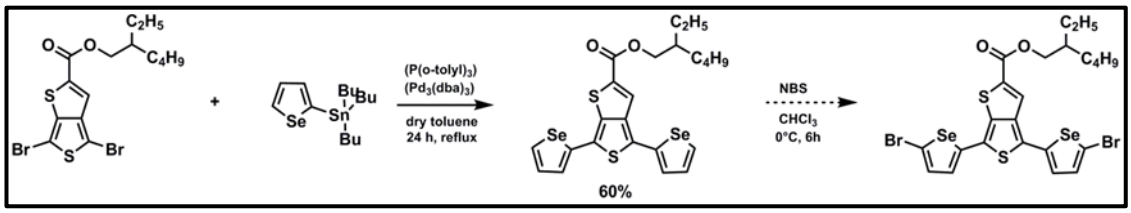

Scheme 3.2 Synthetic Pathway of 2-Ethylhexyl 4, 6-di(selenophene-2-yl)thieno[3,4-b]thiophene-2-carboxylate

After stannylation of selenophene, Stille coupling was performed with previously obtained monomer with tetrakis(triphenylphosphine)palladium(0) $Pd[P(C_6H_5)_3]_4$ as shown in scheme 3.2. However, due to presence of high amount of mono-coupled product and other impurities in crude product, purification was not achieved efficiently via silica gel column chromatography. Therefore, catalyst was changed to 15% tri(o-tolyl)phosphine ($P(o\text{-}tolyl)_3$) and 5% tris(dibenzylideneacetone) dipalladium(0) ($Pd_2(dba)_3$). Consequently, amount of mono-coupled product and other impurities were decreased and purification of di-coupled product was achieved. For dibromination, NBS was used as a brominating agent. However, separation of dibrominated product from mono has been achieved yet. Our studies on purification of the dibrominated species is still ongoing After isolation, copolymerization of synthesized monomer with donors BDTTh and DTPy via Stille coupling will be performed as shown in Scheme 3.3.

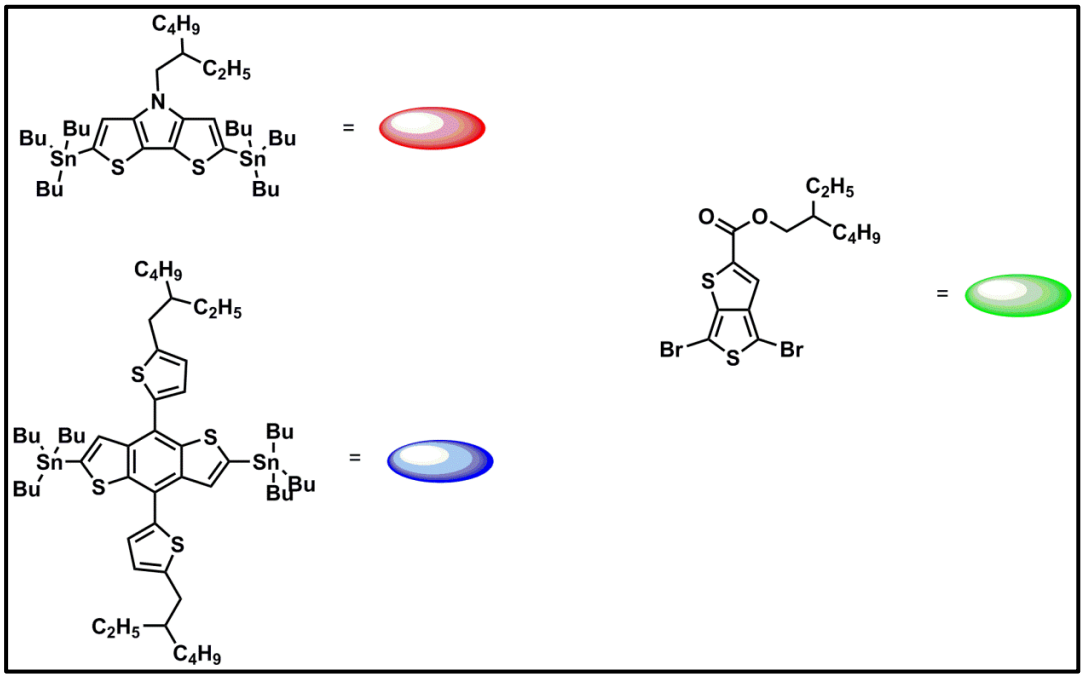

Scheme 3.3.a Representation of BDTTh/DTPy/TT-Se-Br Monomers

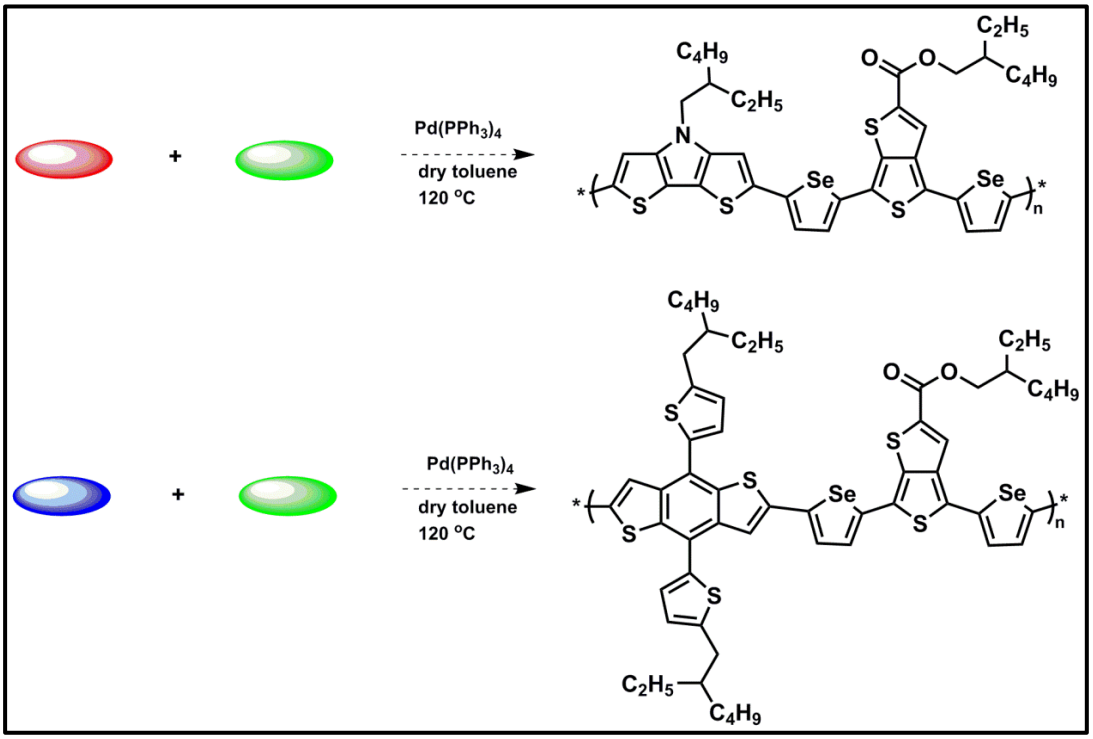

Scheme 3.3.b Synthesis of PTTSeBDTTh/PTTSeDTPy

1.3.1.3 Synthesis of 2-Ethylhexyl 4,6-dibromo-3-fluorothieno[3,4-b]thiophene-2-carboxylate

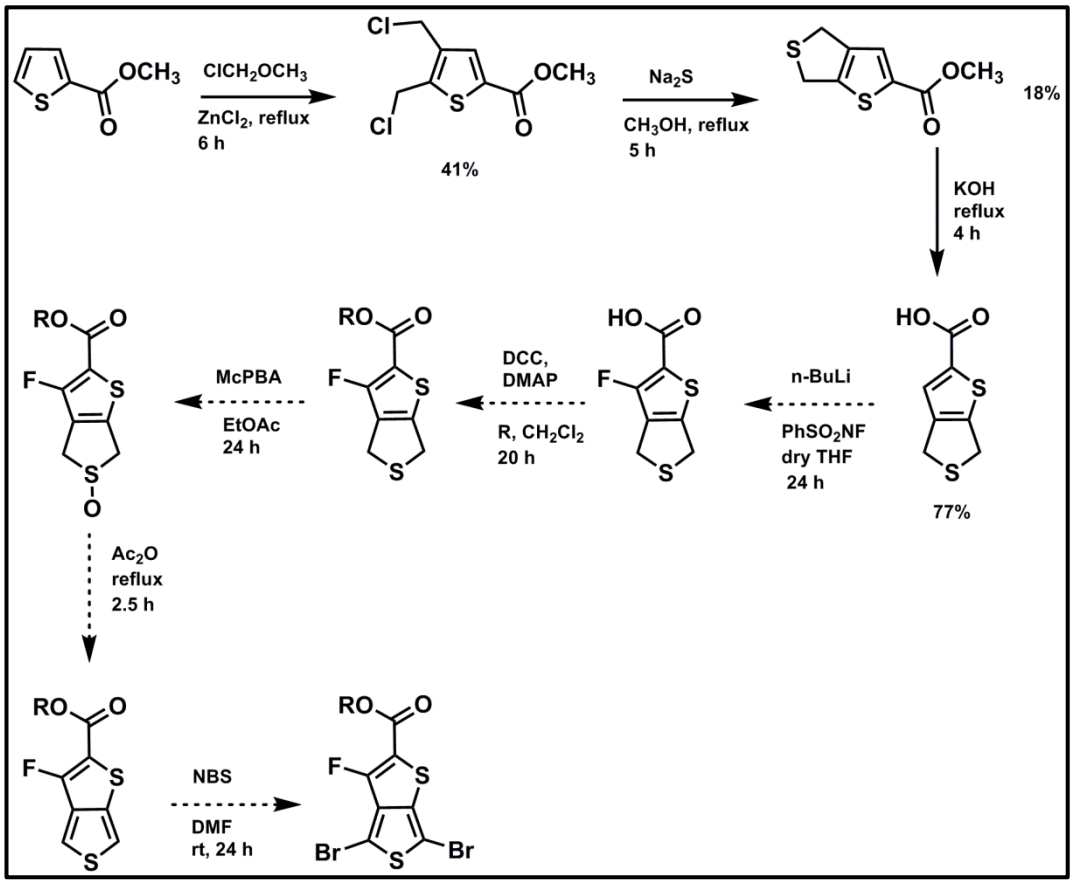

Scheme 3.4 Synthetic Pathway of 2-Ethylhexyl 4,6-dibromo-3-fluorothieno[3,4-b]thiophene-2-carboxylate

After synthesizing methyl 2, 3 –bis (chloromethyl) thiophene-2-carboxylate in the presence of chlorodimethyl ether and the catalyst zinc chloride, cyclization of bischloromethyl was attempted with sodium sulfide nonahydrate ($Na_2S.9H_2O$). However, desired product was obtained with an extremely low yield (18%). In order to eliminate this situation, vacuum distillation was applied to sodium sulfide nonahydrate to decrease the amount of water in structure and reaction was repeated. However, no notable increment was obtained.

1.3.2 Synthesis of Poly-2-ethylhexyl 4-(4-(2-ethylhexyl)-6-methyl-4H-dithieno[3,2-b:2',3'-d]pyrrol-3-yl)-6-methylthieno[3,4-b]thiophene-2-carboxylate

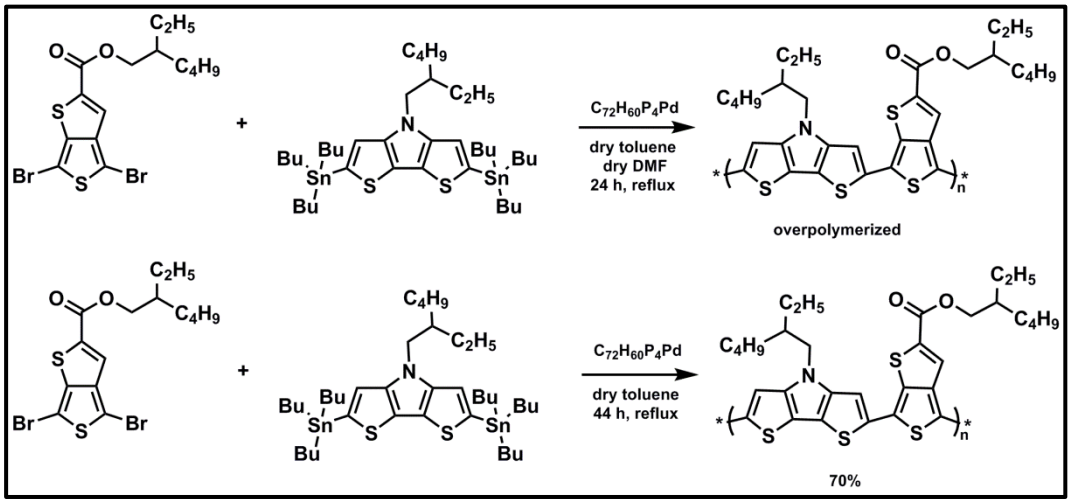

Scheme 3.5 Synthesis of Poly- 2-Ethylhexyl 4-(4-(2-ethylhexyl)-6-methyl-4H-dithieno[3,2-b:2',3'-d]pyrrol-3-yl)-6-methylthieno[3,4-b]thiophene-2-carboxylate

After synthesis of 2-ethylhexyl 4,6-dibromothieno [3,4-b]thiophene-2-carboxylate, coupling reaction with 4-(2-ethylhexyl)-2,6-bis(trimethylstannyl)-4H-dithieno[3,2-b:2',3'-d]pyrrole was carried out with Stille coupling method in the presence of tetrakis(triphenylphosphine)palladium(0) catalyst and dry toluene and dry DMF solvents. However, final product was dissolve neither in chloroform or chlorobenzene. There is too much growth in polymer chain might be a possible reason for this solubility problem. As a second attempt, reaction was run under the same conditions but except, this time, dry DMF was not used. It was observed that product was soluble in chloroform. Characterization of the polymer was done with NMR spectroscopy (Figure 10).

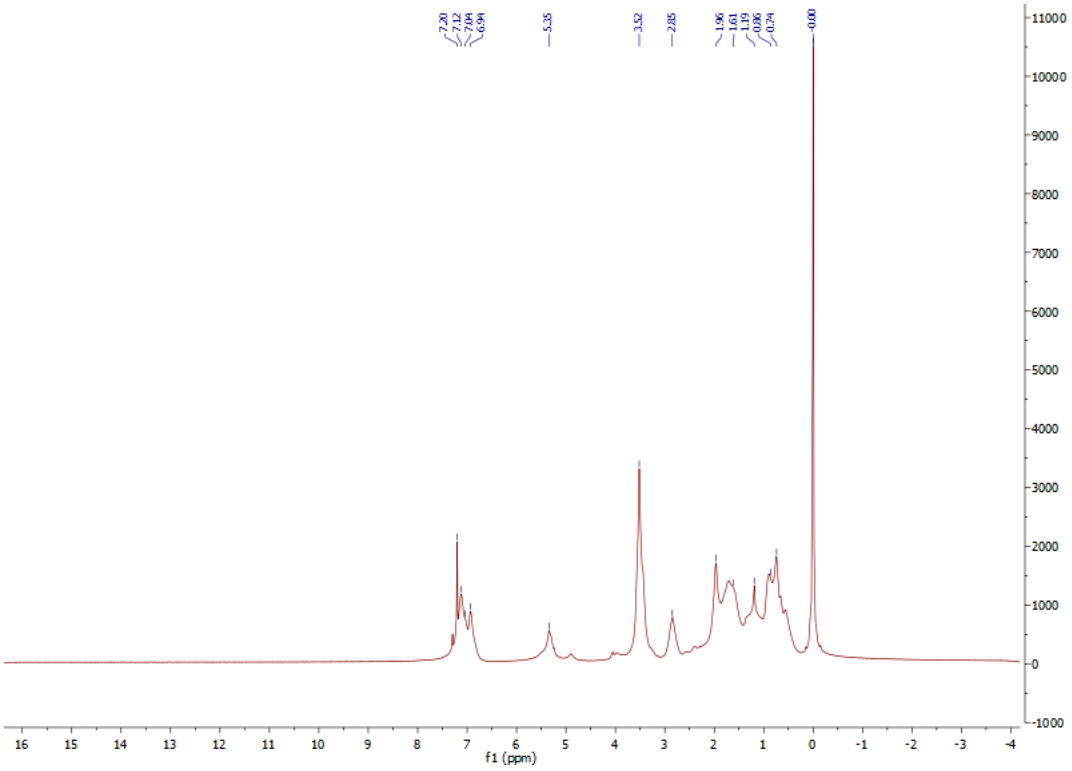

Figure 10 ^{1}H NMR of PTTDTPy

1.3.3 Electrochemical and Electrochromic Properties of Polymers

1.3.3.1 Electrochemical Studies of Polymers

Cyclic voltammogram was used for determining redox behaviors and HOMO/ LUMO levels with a three electrode system.

Polymer film was spray coated on ITO surface that referred as working electrode. As a counter electrode, platinum (Pt) wire was used. Moreover, Silver (Ag) wire was used as a reference electrode.

1.3.3.1.1 Electrochemical Studies of Poly- 2-ethylhexyl 4-(4-(2-ethylhexyl)-6-methyl-4H-dithieno[3,2-b:2',3'-d]pyrrol-3-yl)-6-methylthieno[3,4-b]thiophene-2-carboxylate

2-ethylhexyl 4,6-dibromothieno [3,4-b]thiophene-2-carboxylate was polymerized with 4-(2-ethylhexyl)-2,6-bis(trimethylstannyl)-4H-dithieno[3,2-b:2',3'-d]pyrrole via

Stille coupling and obtained polymer in 4 mg/mL in chloroform was spray coated on ITO coated glass slide and its electrochemical behaviors were studied at monomer free 0.1 M ACN/$TBAPF_6$ solvent/electrolyte solution. Oxidation potentials of the polymer were monitored at 0.25 V and 0.81 V for p-doping and 0.08 V and 0.52 V for p-dedoping(Figure 10).

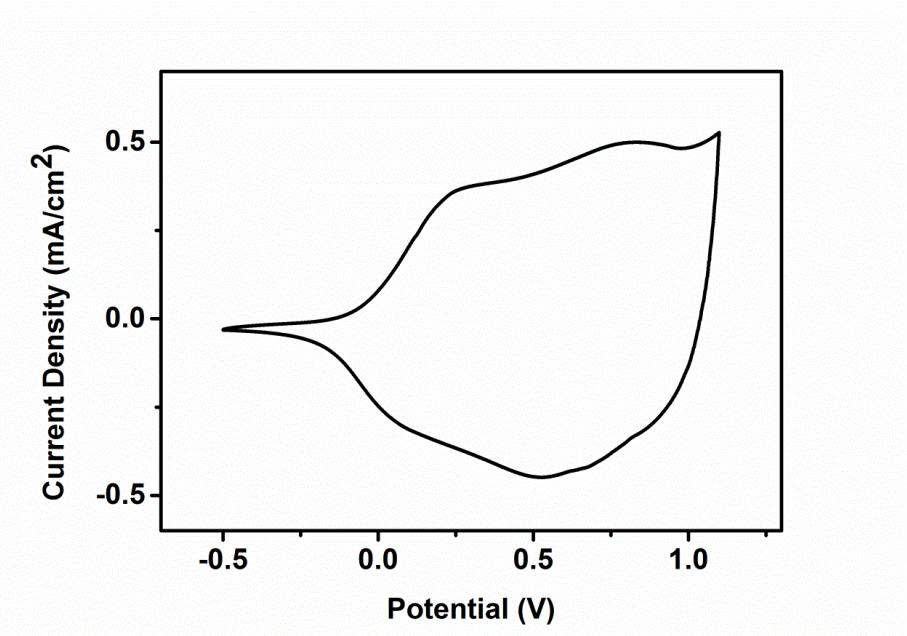

Figure 11 Single Scan Cyclic Voltammetry of PTTDTPy

1.3.3.2 Spectroelectrochemical Studies of Polymers

Spectroelectrochemical studies were conducted for examining optical properties and taking information about mechanism that followed while p-doped. More briefly, these studies give information about formation of polaron and bipolaron bands. Upon determined λ_{max} value, $\lambda_{onset,}$ the point that no absorption was occurred, was founded and optical band gap of corresponding polymer was founded by following equation:

$$E_g^{optical} = \frac{1241}{\lambda \boldsymbol{onset}(\boldsymbol{nm})} eV$$

1.3.3.2.1 Spectroelectrochemical Studies of Poly- 2-ethylhexyl 4-(4-(2-ethylhexyl)-6-methyl-4H-dithieno[3,2-b:2',3'-d]pyrrol-3-yl)-6-methylthieno[3,4-b]thiophene-2-carboxylate

Potential values were applied stepwise between 0 V to 1 V to spray coated monomer free PTTDTPy polymeric films on ITO surface in order to obtain the UV-vis-NIR spectra. From this spectrum, as summarized in table 1, value of λ_{max} determined as 728 nm from neutral state and optical band gap was calculated as 1.2 eV. This clearly shows that a strong NIR absorbing polymer was successfully synthesized.

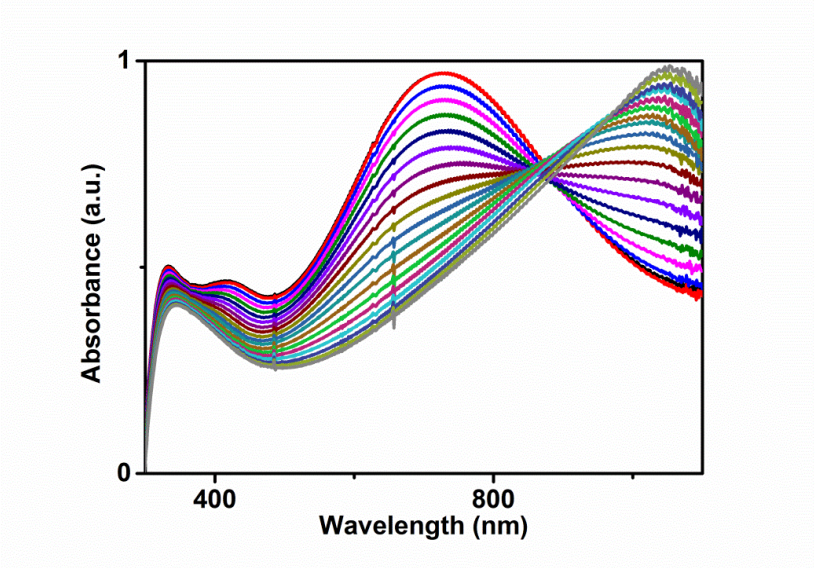

Figure 12 Absorption Spectrum of PTTDTPy

Upon applied positive potentials, color of PTTDTPy varied from blue to gray as shown in Figure below**.**

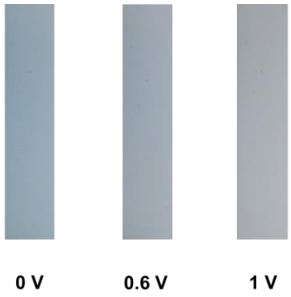

Figure 13 Color Changes Upon Oxidation

HOMO and LUMO level of material were calculated as -4.68 eV (from CV studies) and -3.48 eV (from optical band gap), respectively. From those energy level values, electronic band gap of PTTDTPy was calculated in accordance to equations that mentioned above and founded as 1.2 eV.

Table 1 Summary of Electrochemical and Spectroelectrochemical Properties of PTTDTPy

	$E_{p\text{-doping}}$(V)	$E_{p\text{-dedoping}}$(V)	HOMO(eV)	LUMO (eV)	λ_{max}(nm)	E_g^{op}(eV)
P1	0.25/0.81	0.08/0.52	-4.68	-3.48	728	1.2

1.3.3.3 Kinetic Studies of Polymers

Characteristic features such as percent transmittance and switching times were measured through changing potential values between neutral to oxidative state repeatedly;

1.3.3.3.1 Kinetic Studies of Poly- 2-ethylhexyl 4-(4-(2-ethylhexyl)-6-methyl-4H-dithieno[3,2-b:2',3'-d]pyrrol-3-yl)-6-methylthieno[3,4-b]thiophene-2-carboxylate

As summarized in Table 2, the optical contrast data of PTTDTPy was found as 14 % at 1055 nm and 17% at 720 nm from altering applied potential between neutral state to oxidation state in 30 cycle. Switching times of polymer were also determined from spray coated polymeric films. The values were calculated to be 1.43 s at 1055 nm and 0.9 s at 720 nm.

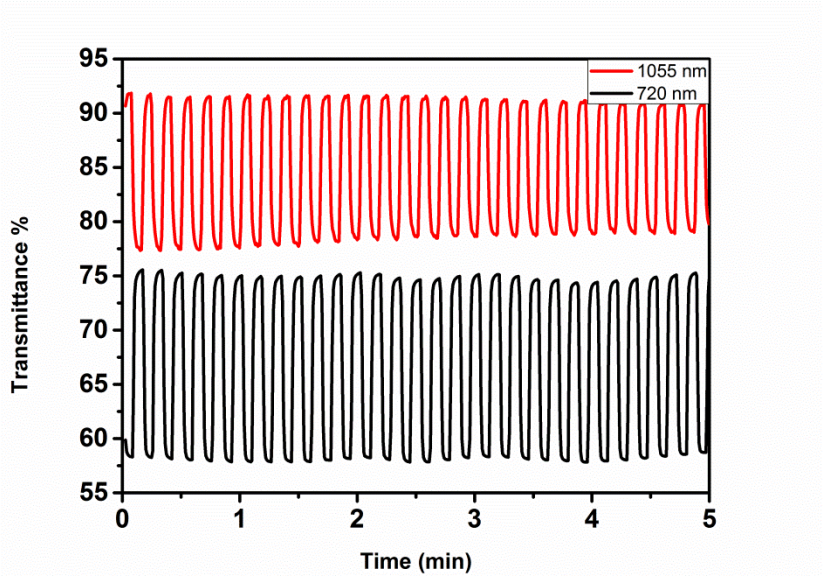

Figure 14 Percent Transmittance of PTTDTPy

Table 2 Summary of Kinetic Properties of PTTDTPy

	Optical contrast (ΔT %)		Switching times (s)
P1	14	1055 nm	1.43
	17	720 nm	0.9

1.3.3.4 Organic Solar Cell Studies of Poly- 2-ethylhexyl 4-(4-(2-ethylhexyl)-6-methyl-4H-dithieno[3,2-b:2',3'-d]pyrrol-3-yl)-6-methylthieno[3,4-b]thiophene-2-carboxylate

The polymer synthesis and purification was performed successfully. As a future study the polymer will be characterized in detail and solar cell studies will be performed.

1.4 Conclusion

After successful synthesis of di-brominated moiety, 2-ethylhexyl 4,6-dibromothieno [3,4-b]thiophene-2-carboxylate as an acceptor, unique donor-acceptor-donor type polymer was synthesized chemically via using Stille Coupling methodology from with commercially available donor 4-(2-ethylhexyl)-2,6-bis(trimethylstannyl)-4H-dithieno[3,2-b:2',3'-d]pyrrole, DTPy. Meanwhile, synthesis of other two acceptor units, 2-ethylhexyl 4,6-di(selenophene-2-yl)thieno[3,4-b]thiophene-2-carboxylate and fluorinated derivative of corresponding TT unit, namely, 2-ethylhexyl 4,6-dibromo-3-fluorothieno[3,4-b]thiophene-2-carboxylate have been pursued.

Each product of every step was characterized by Nuclear Magnetic Resonance (NMR) Spectroscopy and novel PTTDTPy will also characterized by Gel Permeation Chromatography (GPC) for determination of molecular weight.

In electrochemistry studies, oxidation potentials of the polymer were founded as 0.25 V/ 0.81 V for p-doping and 0.08 V/ 0.52 V for p-de-doping. Moreover, spectroelectrochemical studies were and λ_{max} value appeared as 728 nm from neutral state. From spectroelectrochemical and kinetic studies, optical and electronic band gap were calculated as 1.2 eV. Kinetic studies also show optical contrast of PTTDTPy is 14 % at 1055 nm and 17% at 720 nm with 1.43 at 1055 nm and 0.9 at 720 nm switching times. From spectroelectrochemistry studies it is clear that a strong NIR absorbing polymer was successfully synthesized. Organic solar cell application of this promising material is currently being under investigation.

2. SYNTHESIS OF NOVEL BUILDING BLOCKS: PROSOT AND PDIEDOT

2.1 Introduction

2.1.1 Conducting Polymers

From the discovery of first conducting polymer, namely, poly(acetylene) in 1977 with a 10^3 S/cm conductivity[40, 41], interest to this new area increased rapidly due to availability of materials to combine electrical conductivity with main characteristic features of polymers such as flexibility, easy and low cost production[42].

However, properties that compulsory for manufacturing process are easy processing, high stability and conductivity should be involved.

First intrinsically CP, poly(acetylene), was not stable under ambient conditions[43]. Therefore, commercialization is not possible. While investigations related with CP were proceeds, significant candidates were obtained to overcome stability problems which are poly(pyrrole), poly(thiophene), poly(aniline), poly(furan), poly(3,4-ethylenedioxythiophene) (Figure 15)

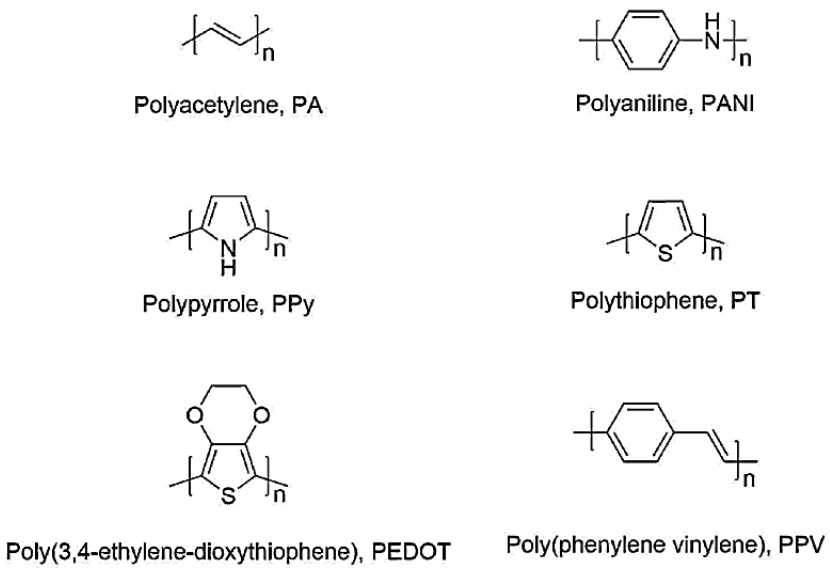

Figure 15 First Conducting Polymers

2.1.1.1 Band Theory

In accordance to theory, when moieties interact with each to form polymer, energy band was formed. Maximum energy band that completely occupied with electrons, HOMO, called as a valance band and minimum energy level that unoccupied, LUMO, called as a conduction band. Energy separation between HOMO and LUMO level named as band gap and amount of this distance gave idea about conduction nature of investigated material. When the band gap of given material is high enough, it is called as insulator with a conductivity value as $\sigma \sim 10^{-7}$ S/cm while for semiconductors are ranging from $\sigma \sim 10^{-7}$ to 10^{2} S/cm and metals are as $\sigma > 10^{2}$ S/cm.

Since energy separation between HOMO and LUMO levels of organic polymeric material is large and no mobility of charge carriers are allowed, generally these materials are called as an insulator. However, by applying suitable voltage and performing oxidation or reduction partially with a suitable dopant, it is possible to generate free charge carries in polymer backbone and conductivity was provided with a value ranging between 10^{-3}–10^{3} S/cm.

It is a fact that HOMO-LUMO energies of given material is crucial in the aspect of transfer of charge carriers, therefore it is essential to emphasize effect of molecular architecture on band gap and parameters like resonance and inter-chain effects, donor-acceptor effect, planarity and bond length alternation. By selecting appropriate donor-acceptor units, a spectrum of absorption is broadened due to intramolecular charge transfer which diminishes the band gap. Substitution of electron donating groups that raise HOMO level or electron-withdrawing group that lower LUMO level lead also to decrease in band gap[44].

2.1.1.1.1 Conduction Mechanism in Conducting Polymers

Either chemical or electrochemical methods were employed in polymerization. Although chemical methods have been widely used, electrochemical polymerization might be preferable if main intention for use of polymeric material is as thin films[45].

Upon redox reactions, solitons, polarons and bipolarons are formed. Soliton is the π-electron that transferred through a conjugated system and if neutral soliton was oxidized positive soliton, if reduced then negative soliton was obtained. As represented in Figure 16, if conjugated polymer was oxidized positive polaron and if reduced, then negative polaron can form. When two positive or two negative polarons are combined respectively, bipolarons were formed on backbone of conjugated polymer.

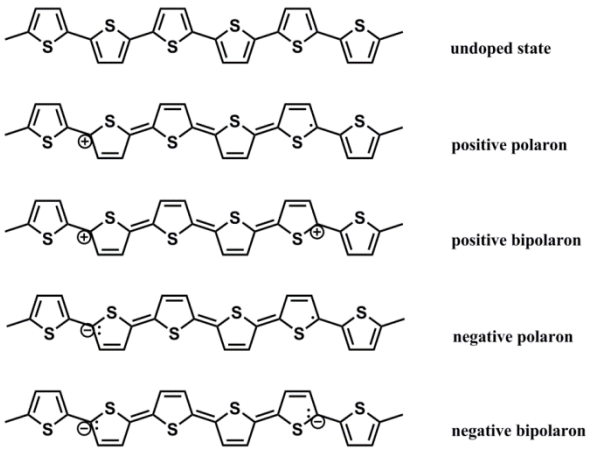

Figure 16 The Charged States Formed Upon Oxidation of Polythiophene

2.1.1.2 General Features of PEDOT

It was stated in the literature that in the case of poly(thiophene) and poly(pyrrole), increased stability originates from the fact that positive charges in the backbone stabilized by nitrogen and sulfur. Other important phenomena to obtain more stable conducting polymer is diminishing steric effect to reach best orientation of polymeric backbone. In other words, there is only two possible sites in monomer for coupling in polymerization that has a linear structure with no β defects[46]. Poly(alkylenedioxythiophene) based polymeric units are one of the best candidate that fits best to achieve this goal[47]. After being synthesized in 1988, more investigations have been conducting related with this family due to being stable to air and having high conductivity (500 S/cm)[48]. Transparent film with a low oxidation potential[49] could be obtained with these materials. One of the first application area for PEDOT was in photographic films as an antistatic layer. Since then, under the light of developments and modifications, different applications of this material and its derivatives have been presented such as counter electrode in polymer capacitors[50], hole injection layer or electrode as ITO in OLEDs[51,52] , hole transport layer in OSC[53,54], biosensor applications[55,56] and nanofibers.[57] Among all of those significant properties, PEDOT has dark blue color that allows efficient absorption in reduced state and has quite transmissive light blue color in oxidized state with a fast switching time and high optical contrast which make it suitable candidate for electrochromic applications[58,59].

As any other conducting polymers, it is also possible to enhance properties such as planarity, conductivity, rigidity or mobility by altering backbone of polymer, perihepral ring composition, introduction of functional groups and changing dopant. Therefore, tremendous effort have focused to develop different sulfur based[60,61], selenium based[62] derivatives (Figure 17).

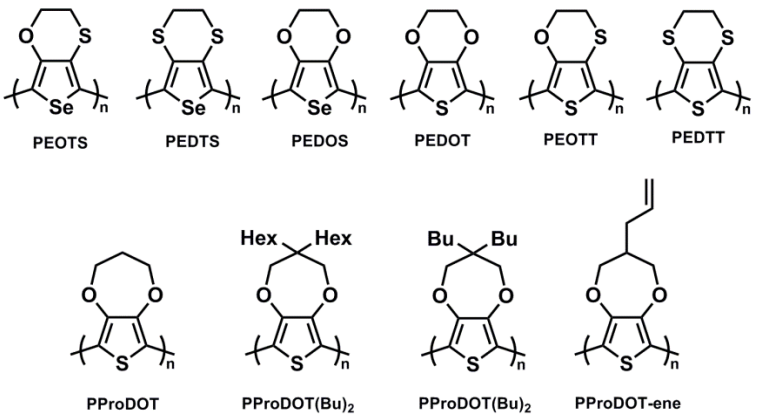

Figure 17 Structures of Some Derivatives of Poly(Alkylenedioxythiophene)

2.1.1.2.1 Synthesis of Monomers

As represented in Figure 18, four main basic steps were involved for synthesis of different variety of alkylenedioxythiophene derivatives[65-67] .

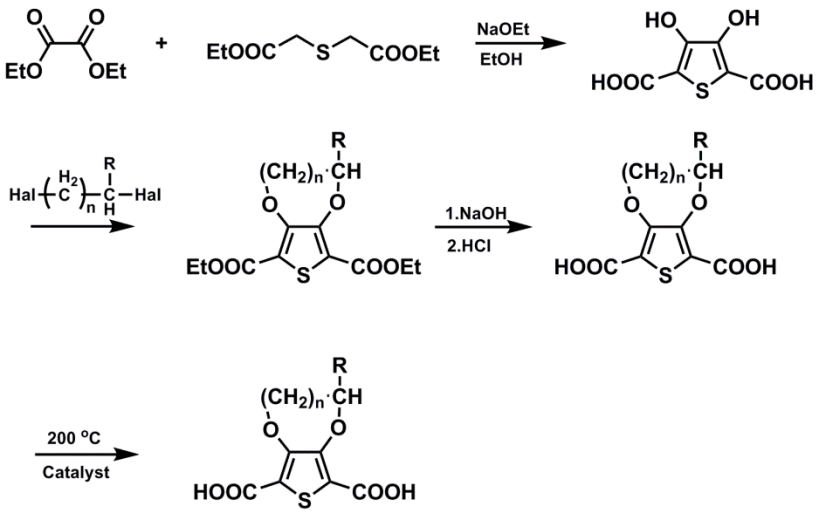

Figure 18 Basic Steps that Used in Synthesis of Alkylenedioxythiophene Monomer

In order to obtain polymer, three methods were developed.1) oxidative chemical polymerization 2) electrochemical polymerization which polymerization process of alkylenedioxythiophene species could be achieved electrochemically which conducted in aqueous electrolytes with satisfying conductivities. Moreover, it was shown that conductivity of obtained polymeric films was stable at 120 °C within 1000 h under storage.[47] 3) From di-halogen unit of EDOT and derivatives, transition metal-mediated coupling reaction such as Stille, Suzuki-Miyaura, Sonogashira etc.

2.1.1.2.2 Main Polymerization Processes of Alkylenedioxythiophene Species

Main mechanism of oxidative chemical polymerization process which followed ECE mechanism (electro-chemical-electro) was illustrated in Figure 18. First, initiation of reaction was achieved by formation of radical cation and from formed radical cation, dimers, trimers, tetramers and finally neutral oligomer/polymer has obtained. Secondly, p-doping was occurred to form conductive cation of the polymer. Stability of resulting conductive polymers was provided by counter ions. In the case of PEDOT, PSS was commonly chosen which also provide dispersion of segments of polymer in aqueous medium and resulting material is highly conductive and transparent.[68]

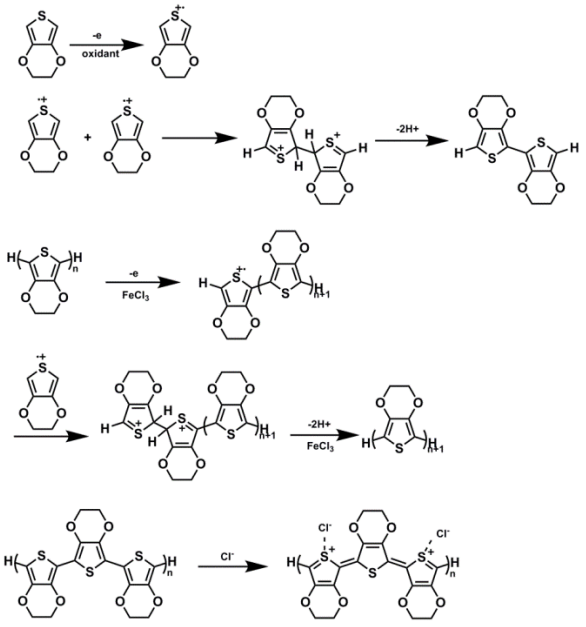

Figure 19 Oxidative Chemical Polymerization of EDOT

2.1.2 Aim of the Study

The aim of this study is to synthesize two unknown derivative of alkylenedioxythiophenes that have a lot of promising potential in the field of organic electronics. One of these derivatives is a symmetric bifunctional dithieno[3,4-b:3',4'-e][1,4]dioxine (DiEDOT), and the other one is oxygen-sulfur containing propylene analogue, 3,4-dihydro-2H-thieno[3,4-b][1,4]oxathiepine (ProSOT).

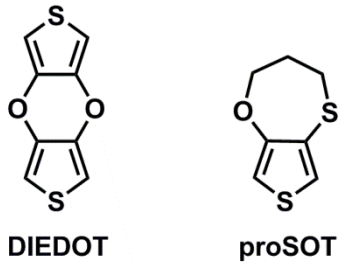

Figure 20 Molecular Structures of Dithieno[3,4-b:3',4'-e][1,4]dioxine and 3,4-Dihydro-2H-thieno[3,4-b][1,4]oxathiepine

PDiEDOT, corresponding homopolymer of EDOT, have the potential to be an outstanding electrochromic material and promising p-type polymer in general. Moreover, although oxygen-sulfur containing (EOTS) and sulfur-sulfur containing (EDTS) analogues of EDOT were realized in the literature, ProSOT has not been realized yet. Therefore, we aimed the synthesis of ProSOT, its electrochemical polymerization and investigation of electrochemical and electrochromic properties of the resulting polymer.

2.2 Experimental

2.2.1 Materials

All the chemicals were purchased from Aldrich.

2.2.2 Methods and Equipment

All the reactions were carried under argon atmosphere unless otherwise mentioned. Synthetic pathways that described in literature were used for synthesis of monomers. Dry THF and dry toluene were distilled over sodium and benzophenone or directly used from Mbraun MBSPS5 solvent drying system.

^{1}H and ^{13}C NMR analysis were conducted via Bruker Spectrospin Avance DPX-400 Spectrometer and d_6-DMSO and $CDCl_3$ solvents were used. TMS was used as an internal reference. Further structural analysis of novel units were conducted by high resolution mass spectroscopy methodology that Waters Synapt MS System was used. For electrochemical analysis, three electrode system cells was used where Platinum wire used as the counter electrode, ITO coated glass slide was the working electrode and silver wire was the reference electrode. Varian Cary 5000 UV-Vis spectrometer was used for spectroelectrochemical study.

2.2.3 Monomer Syntheses

2.2.3.1 Synthetic Route of 6,8-Bis(2,3-dihydrothieno[3,4-b][1,4]dioxin-5-yl)-3,4-dihydro-2H-thieno[3,4-b][1,4]oxathiepine

2.2.3.1.1 Synthesis of 3,4-Dihydro-2H-thieno[3,4-b][1,4]oxathiepine[69]

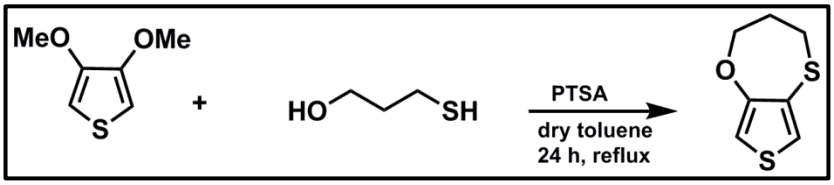

Scheme 2.1 Synthesis of 3,4-Dihydro-2H-thieno[3,4-b][1,4]oxathiepine

To a solution of 3,4 dimethoxythiophene (1.00 g, 6.94 mmol) in 30 mL of dry toluene, 1 mercapto 1 propanol (2.56 g, 27.7 mmol) and p-toluenesulfonic acid(59.5 mg, 346 mmol) was added and the mixture was stirred for 72 hours at reflux temperature under argon atmosphere. After bringing reaction to room temperature, the solution was extracted three times with Et_2O. Combined organic phases were washed successively with dilute $NaHCO_3$ and brine. The organic layer was dried over anhydrous $MgSO_4$, filtered and the solvent was evaporated. For purification, silica gel column chromatography was performed (Hexane/DCM=1/2) and white solid was obtained (603 mg, 50%).

^{1}H NMR (400 MHz, $CDCl_3$) δ (ppm) 6.99 (d, *J*=3.2 Hz, 1 H), 6.59 (d, *J*=3.5 Hz, 1H), 4.02 (t, 2H), 2.79-2.70 (m, 2H), 2.28-2.15 (m, 2H)

^{13}C NMR (400 MHz, $CDCl_3$) δ (ppm) 159.2, 127.2, 122.6, 108.8, 73.0, 35.1, 32.0

2.2.3.1.2 Synthesis of 6,8–Dibromo-3,4-dihydro-2H-thieno[3,4b][1,4] oxathiephine[69]

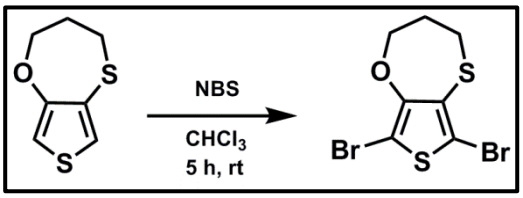

Scheme 2.2 Synthesis of 6,8–Dibromo-3,4-dihydro-2H-thieno[3,4b][1,4] oxathiephine

Through the solution of 3,4-dihydro-2H-thieno[3,4-b][1,4]oxathiepine (603 mg, 3.50 mmol) in 30 mL of $CHCl_3$ argon was bubbled for 20 minutes. Then N-bromosuccinimide (1.87 g, 10.5 mmol) was added portionwise at 0 °C. The mixture was poured into water and extracted three times with $CHCl_3$. Combined organic phases were dried over anhydrous $MgSO_4$, filtered and the solvent was evaporated. For purification, silica gel column chromatography was performed (DCM/Hexane=2/1) and white solid was obtained (884 mg, 76%).

^{1}H NMR (400 MHz, $CDCl_3$) δ (ppm) 4.24 (t, *J*= 5.1 Hz, 1H), 2.95 (t, *J*= 5.9 Hz, 1H), 2.34 (p, *J*= 5.9, 5.7, 4.6 Hz, 1H).

^{13}C NMR (400 MHz, $CDCl_3$) δ (ppm) 154.6, 128.8, 107.7, 94.8, 72.5, 34.0, 31.2

2.2.3.1.3 Synthesis of Tributyl(2,3-dihydrothieno[3,4-b][1,4]dioxin-5-yl)stannane

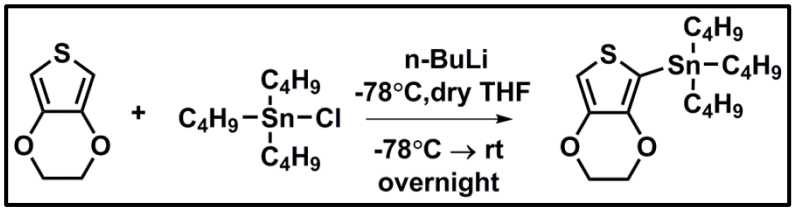

Scheme 2.3 Synthesis of Tributyl(2,3-dihydrothieno[3,4-b][1,4]dioxin-5-yl)stannane

To a solution of 3,4-ethylenedioxythiophene (100 mg, 0.703 mmol) in 10 mL of dry THF, n-BuLi (0.30 mL, 2.5 M in hexane) was added dropwise within 30 minutes at -78 °C under argon atmosphere and stirred for 1 hour at that temperature. After addition of tributyltin chloride (275 mg, 0.884 mmol) to the reaction mixture slowly, temperature was raised to room temperature and reaction mixture was stirred overnight. Solvent of the reaction was removed and crude product was dissolved in $CHCl_3$. Solution was washed three times with water, dried over anhydrous $MgSO_4$, filtered and the solvent was evaporated to yield light brown oil (300 mg, 99%).

^{1}H NMR (400 MHz, $CDCl_3$) δ (ppm) 6.59 (m, 1H), 4.24 – 4.04 (m, 4H), 1.59 (m, 6H), 1.44 – 1.30 (m, 6H), 1.23 – 1.07 (m, 6H), 0.92 (m, 9H)

^{13}C NMR (400 MHz, $CDCl_3$) δ(ppm) 147.7, 142.5, 108.9, 105.8, 64.7, 64.6, 29.0, 27.2, 13.7, 10.5

2.2.3.1.4 Synthesis of 6,8-Bis(2,3-dihydrothieno[3,4-b][1,4]dioxin-5-yl)-3,4-dihydro-2H-thieno[3,4-b][1,4]oxathiepine

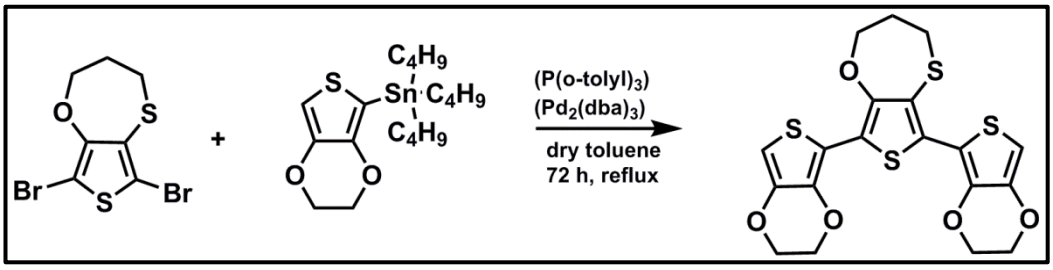

Scheme 2.4 Synthesis of 6,8-Bis(2,3-dihydrothieno[3,4-b][1,4]dioxin-5-yl)-3,4-dihydro-2H-thieno[3,4-b][1,4]oxathiepine

To a solution of 6,8–dibromo-3,4-dihydro-2H-thieno[3,4b][1,4] oxathiephine (100 mg, 0.303 mmol) and tributyl(2,3-dihydrothieno[3,4-b][1,4]dioxin-5-yl)stannane (405 mg, 0.939 mmol) in 50 mL of dry toluene, tris(dibenzylideneacetone)dipalladium(0) (13.9 mg, 0.0152 mmol) and tri(o-tolyl)phosphine (13.8 mg, 0.0453 mmol) catalysts were added successively. The mixture was stirred for 72 hours at reflux temperature under argon atmosphere. For

purification, silica gel column chromatography was performed (DCM/Hexane=1/1) and yellow solid was obtained (69 mg, 50%).

^{1}H NMR (400 MHz, $CDCl_3$) δ(ppm) 6.34 (s, 1H), 6.26 (s, 1H), 4.35-4.32 (m, 8H), 4.18 – 4.11 (m, 2H), 2.87 – 2.81 (m, 2H), 2.41 – 2.31 (m, 2H)
^{13}C NMR (400 MHz, $CDCl_3$) δ(ppm) 153.6, 141.3, 141.2, 138.9, 137.3, 127.1, 123.5, 117.5, 111.2, 109.9, 99.6, 98.3, 72.6, 65.2, 65.1, 64.6, 64.5, 34.7, 32.60.

2.2.3.2 Synthetic Route of Selenopheno[3,4-b]thieno[3,4-e][1,4]dioxine&dithieno[3,4-b:3',4'-e][1,4]dioxine

2.2.3.2.1 Synthesis of L(+)-Diethyl L-tartrate[70]

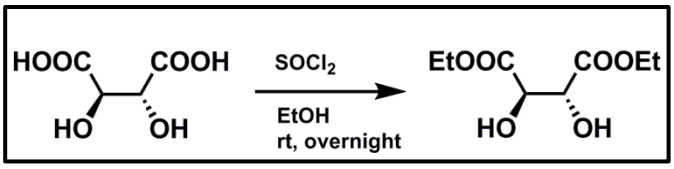

Scheme 2.6 Synthesis of L(+)-Diethyl L-tartrate

To a solution of D-tartaric acid (5.00 g, 33.3 mmol) in 300 mL EtOH, $SOCl_2$ (5.00 mL, 73.3 mmol) was added dropwise and the mixture was stirred overnight at room temperature. After concentrating the solution, DCM was added and the mixture was washed successively with saturated $NaHCO_3$ and brine. Combined organic phases were dried over anhydrous $MgSO_4$, filtered, concentrated and light yellow oil was obtained (5.15 g, 75%).

^{1}H NMR (400 MHz, $CDCl_3$) δ 4.53 (d, *J*=7.6 Hz, 2H), 4.32 (q, *J*=7.2 Hz, 4H), 3.22 (d, *J*=6. Hz, 2H), 1.32 (t, *J*= 7.1 Hz, 6 H)

^{13}C NMR (400 MHz, $CDCl_3$) δ 171.5, 72.1, 62.4, 14.1.

2.2.3.3.2 Synthesis of Diethyl 2-phenyl-1,3-dioxolane-4,5-dicarboxylate[71]

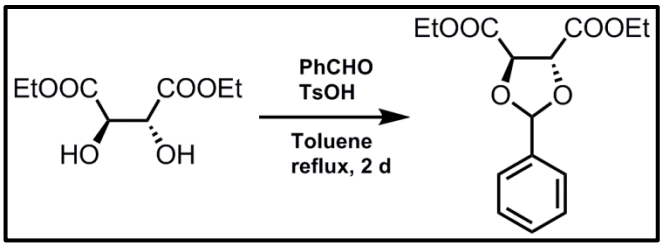

Scheme 2.7 Synthesis of Diethyl 2-phenyl-1,3-dioxolane-4,5-dicarboxylate

To a solution of diethyl tartrate (5.0 g, 24 mmol) in 63 mL toluene, benzaldehyde (2.47 mL, 24.3 mmol) and p-toluenesulfonic acid (208 mg, 1.21 mmol) were added successively and reaction mixture was stirred at reflux temperature by using Dean-Stark apparatus for 48 hours. After cooling down the reaction mixture to room temperature, $NaHCO_3$ was added for neutralization. The solvent was evaporated and extraction was performed three times with Et_2O. Combined organic phases were dried over anhydrous $MgSO_4$, filtered and concentrated. Remaining benzaldehyde was distilled off at 60 °C and white solid was obtained (3.14 g, 44%).

^{1}H NMR (400 MHz, $CDCl_3$) δ 7.60-7.58 (m, 3H), 7.42-7.39 (m, 2H), 6.16 (s,1H), 4.95 (d, *J*=4.0 Hz, 1H), 4.83 (d, *J*= 4.0 Hz, 1H), 4.30 (m, 4H), 1.33 (dt, *J*=18.7, 7.1 Hz, 6H)

^{13}C NMR (400 MHz, $CDCl_3$) δ 169.7, 169.1, 135.5, 129.9, 128.4, 127.2, 106.7, 77.6, 62.1, 14.1

2.2.3.3.3 Synthesis of (2-phenyl-1,3-dioxolane-4,5-diyl)dimethanol[72]

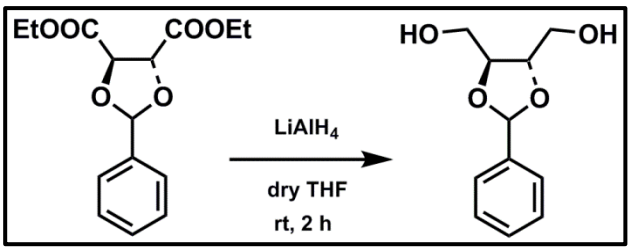

Scheme 2.8 Synthesis of (2-phenyl-1,3-dioxolane-4,5-diyl)dimethanol

To a suspension of $LiAlH_4$ (542 mg, 14.2 mmol) in 8 mL of dry THF , solution of diethyl 2-phenyl-1,3-dioxolane-4,5-dicarboxylate (2.0 g, 6.8 mmol) in 6 mL of dry THF was added dropwise at 0 °C, reaction mixture was warmed up to room temperature and stirred for 3 hours under argon atmosphere. Et_2O was added at 0 °C for dilution, 0.5 mL of water was added slowly. Then, 0.5 mL of 15% aqueous NaOH solution was added and 1.5 mL of water added again. After stirring for 15 minutes and warming up to room temperature, the reaction mixture was dried over anhydrous $MgSO_4$ and filtered through celite pad.

For further purification, silica gel column chromatography was performed (EtOAc/Hexane=3/1) and white solid was obtained (900 mg, 63%).

^{1}H NMR (400 MHz, $CDCl_3$) δ 7.48 (dd, *J*=6.4, 3.2 Hz, 2H), 7.43-7.36 (m, 3H), 5.97 (s, 1H), 4.16 (dd, *J*= 4.9, 2.5 Hz, 2H), 3.93-3.73 (m, 4H), 2.34 (m, 2H)

^{13}C NMR (400 MHz, $CDCl_3$) δ 137.2, 129.6, 128.5, 126.5, 103.9, 79.4, 78.5, 62.4, 62.3

2.2.3.3.4 Synthesis of 4,5-Bis(bromomethyl)-2-phenyl-1,3-dioxolane[73]

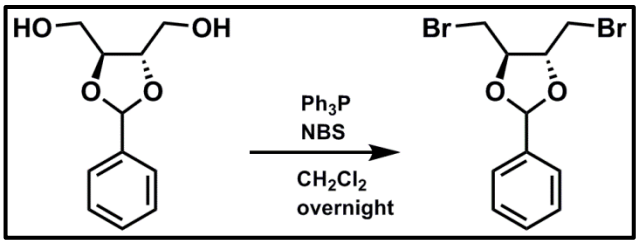

Scheme 2.9 Synthesis of 4,5-Bis(bromomethyl)-2-phenyl-1,3-dioxolane

To a solution of N-bromosuccimide (10.3 g, 56.4 mmol) in 75 mL of DCM, triphenylphosphine (14.8 g, 56.4 mmol) and (2-phenyl-1,3-dioxolane-4,5-diyl)dimethanol (3.95 g, 18.8 mmol) was added successively at -78 °C. The reaction mixture was stirred overnight in the dark at room temperature. For purification, silica gel column chromatography was performed (Hexane/EtOAc= 2/1) and yellow oil was obtained (3.37g, 53%).

^{1}H NMR (400 MHz, $CDCl_3$) δ 7.53 (m, *J*=6.8, 2.8 Hz, 2H), 7.46-7.37 (m, 3H), 6.07 (s, 1H), 4.38 (m, 2H), 3.62 (m, *J*=5.6 Hz, 4H)

^{13}C NMR (400 MHz, $CDCl_3$) δ 136.6, 129.8, 128.5, 126.7, 104.4, 80.0, 79.1, 32.5, 32.0.

2.2.3.3.5 Synthesis of 1,4-Dibromobutane-2,3-diol[72]

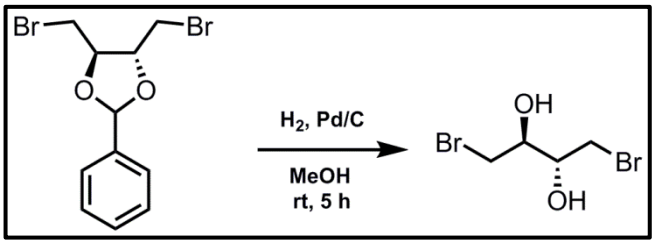

Scheme 2.10 Synthesis of 1,4-Dibromobutane-2,3-diol

To solution of 4,5-bis(bromomethyl)-2-phenyl-1,3-dioxolane (3.00 g, 8.93 mmol) in 150 mL of methanol, palladium on carbon (10%, 90 mg) and several drops of hydrochloric acid were added. Suspension was stirred for 3 hours under H_2 atmosphere. Then, the reaction mixture was filtered through celite pad and the solvent was evaporated. For purification, silica gel column chromatography was performed (Hexane/EtOAc=2/1) and white solid was obtained (1.20 g, 54%).

^{1}H NMR (400 MHz, $CDCl_3$) δ 3.99 (m, 2H), 3.57-3.48 (m, 4H), 2.65 (d, *J*=5.7 Hz, 2H)

^{13}C NMR (400 MHz, $CDCl_3$) δ 71.4, 34.7

2.2.3.3.6 Synthesis of 3,4 Dimethoxythiophene[48]

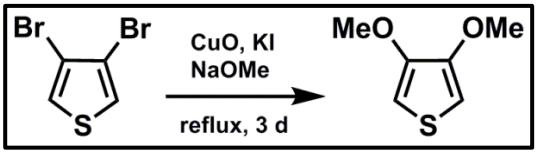

Scheme 2.11 Synthesis of 3,4 Dimethoxythiophene

Sodium (3.99 g, 173 mmol) was dissolved in 50 mL of methanol. Prepared sodium methoxide was added to a mixture of 3,4 dibromothiophene (7.0 g, 29 mmol), copper(II)oxide (2.29 g, 28.9 mmol) and potassium iodide (240 mg, 1.45 mmol). Then reaction was stirred at reflux temperature for 48 hours. Additional amount of sodium methoxide (669 mg Na in 8 mL of methanol) was added to this mixture and the reaction was refluxed for another 24 hours. After cooling to room temperature, solvent was evaporated and crude product was purified with silica gel column chromatography (Hexane/DCM=5/1) (1.59 g, 90%).

^{1}H NMR (400 MHz, $CDCl_3$): δ (ppm) 6.19 (s, 1H), 3.86 (s,3H)

^{13}C NMR (400 MHz, $CDCl_3$): δ (ppm) 147.8, 96.3, 57.6

2.2.3.3.7 Synthesis of 2,3-Bis(bromomethyl)-2,3-dihydrothieno[3,4-b][1,4]dioxine[69]

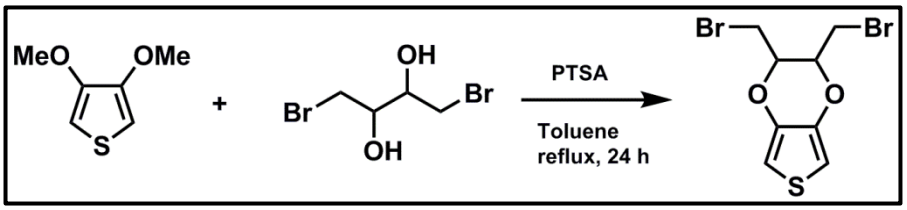

Scheme 2.12 Synthesis of 2,3-Bis(bromomethyl)-2,3-dihydrothieno[3,4-b][1,4]dioxine

To a solution of 1,4-dibromobutane-2,3-diol (3.62 g, 14.6 mmol) in 22 mL of dry toluene, 3,4-dimethoxythiophene (1.0 g, 6.9 mmol) and p-toluenesulfonic acid(65.9 mg, 346 mmol) was added and the reaction mixture was stirred at reflux temperature under argon atmosphere for 4 days. After concentrating the solution, DCM was added and the mixture was washed with saturated $NaHCO_3$. Combined organic phases were dried over anhydrous $MgSO_4$, filtered, concentrated. Silica gel column chromatography was performed for further purification to yield light yellow solid. (DCM/Hexane=1/2) (600 mg, 26%)

^{1}H NMR (400 MHz, $CDCl_3$) δ (ppm) 6.40 (s, 1H), 4.45 (t, 1 H), 3.61 (m, 2H)

^{13}C NMR (400 MHz, $CDCl_3$) δ (ppm) 139.4, 100.9, 73.0, 25.5

2.3 Results and Disscussion

2.3.1 Monomer Syntheses

2.3.1.1 Synthesis of 6,8-Bis(2,3-dihydrothieno[3,4-b][1,4]dioxin-5-yl)-3,4-dihydro-2H-thieno[3,4-b][1,4]oxathiepine

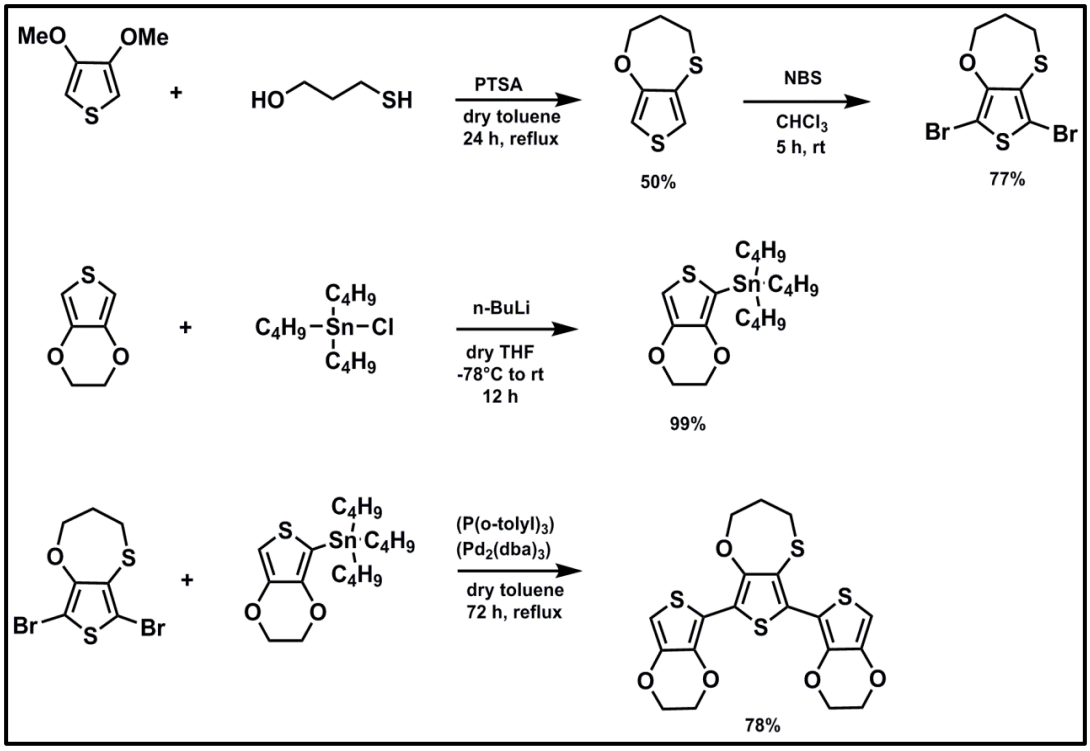

Scheme 3.1 Synthetic Pathway of 6,8-Bis(2,3-dihydrothieno[3,4-b][1,4]dioxin-5-yl)-3,4-dihydro-2H-thieno[3,4-b][1,4]oxathiepine

As in the transetherification procedure that applied for synthesis of other derivatives e.g ProDOT, p-toluenesulfonic acid,as a catalyst, and dry toluene ,as a solvent, were used for obtaining central unit. After performing dibromination to ProSOT, 3,4-Ethylenedioxythiophene, EDOT, was stannylated.

Then two units were brought together with Stille coupling in the presence of tetrakis(triphenylphosphine)palladium(0) , $Pd[P(C_6H_5)_3]_4$ as a catalyst,

In order to decrease ratio of mono-product, reaction was repeated with 15% tri(o-tolyl)phosphine ($P(o\text{-tolyl})_3$) and 5% tris(dibenzylideneacetone) dipalladium(0) ($Pd_2(dba)_3$) catalyst. Consequently, change in the preference of catalyst leads to ratio of di-product over mono-product was increased and purification with silica gel column chromatography was successful.

2.3.1.2 Synthesis of Selenopheno[3,4-b]thieno[3,4-e][1,4]dioxine&dithieno[3,4-b:3',4'-e][1,4]dioxine

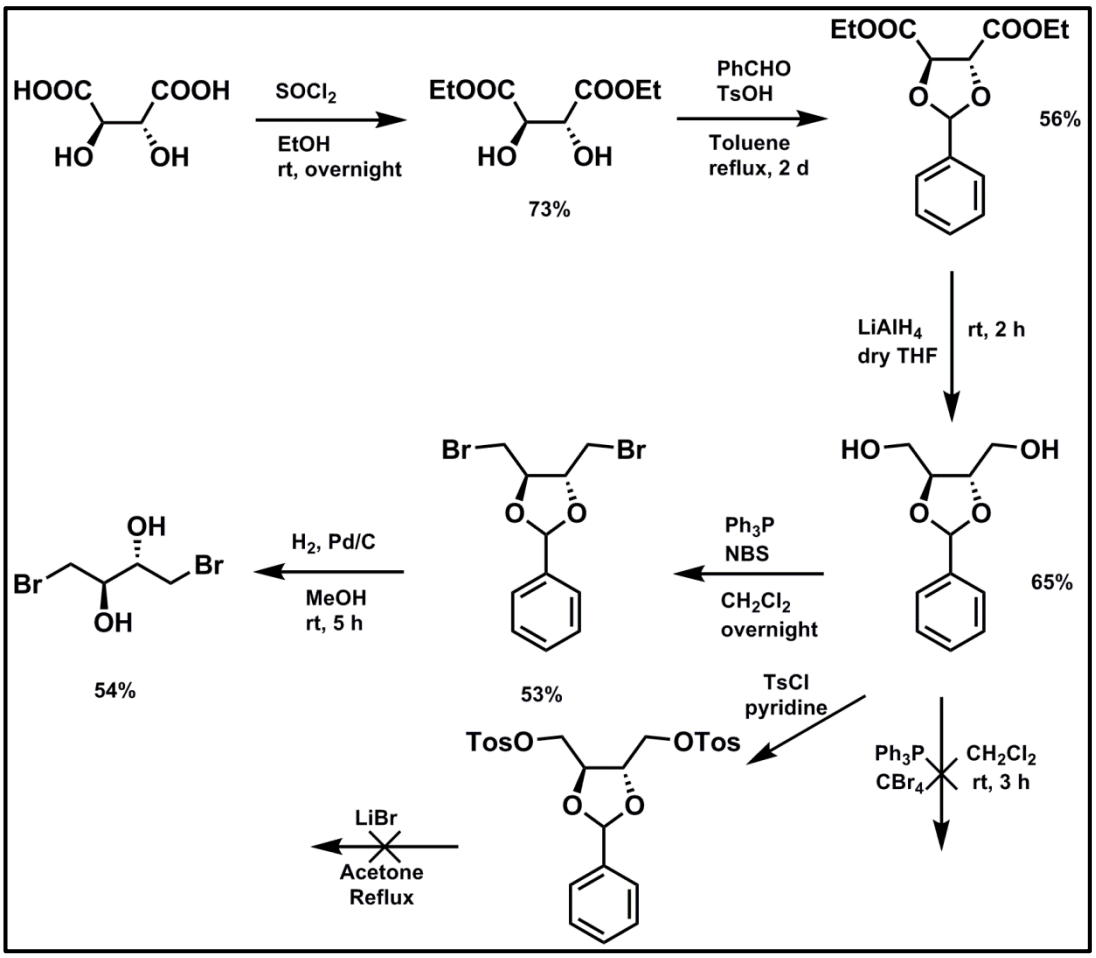

Scheme 3.3 Synthetic Pathway of (2*R*,3*R*)-1,4-Dibromobutane-2,3-diol

Tartaric acid was esterified in ethanol with the presence of thionyl chloride, protection of ester groups via benzaldehyde was performed. Then the resulting diol was protected via benzaldehyde. However, due to problem in separation of desired product from benzaldehyde using silica gel column chromatography, after evaporation of the solvent of the reaction, the temperature of the bath was increased to 60 °C and excess benzaldehyde was removed. Then, reduction reaction was performed with $LiAlH_4$ and for bromination, CBr_4 and Ph_3P were used.

However, target dibromo molecule was not able to produced. As a second attempt, alcohol was tosylated with TsCl in the presence of pyridine then for bromine substitution, LiBr in acetone were utilized. However, significant amount of side products were observed, therefore yield of the desired product was quite low. In the third attempt, NBS and Ph_3P were used at –78 °C in the presence of DCM and target molecule was successfully synthesized. Then, second reduction reaction was performed with Pd/C (10%) in the presence of H_2 atmosphere to obtain the targeted starting material.

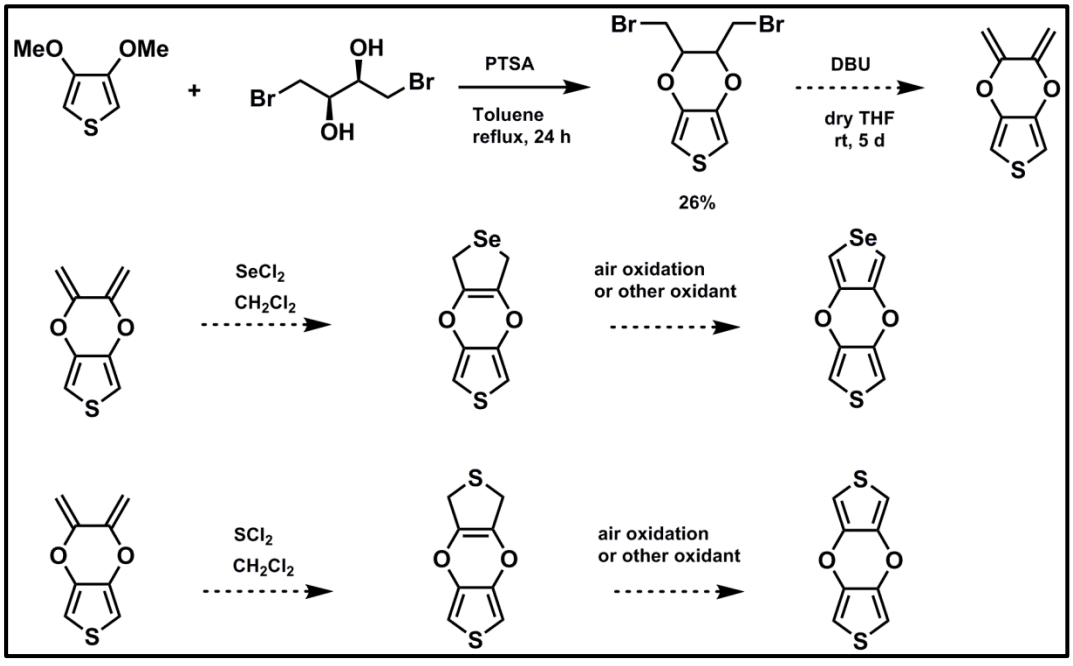

Scheme 3.4 Synthetic Pathway of Selenopheno[3,4-b]thieno[3,4-e][1,4]dioxine&dithieno[3,4-b:3',4'-e][1,4]dioxine

After bromination of thiophene via bromine within 16 hours, tetrabromothiophene was obtained. Then, in presence of Zn powder and acetic acid/water (1/2) and using Dean-Stark apparatus, 3,4-dibromothiophene was formed in accordance with the literature. Starting material, 3,4-dimethoxythiophene was synthesized with using NaOMe, CuO, and KI.

For purification, since crude product has a bulky nature and amount of solvent that used was high, instead of performing extraction, silica gel column chromatography was performed.

From previously synthesized starting materials, diol and 3,4-dimethoxythiophene, transetherification reaction was performed via PTSA as a catalyst in the presence of dry toluene. Then for synthesis of eliminated product, as a first attempt, t-BuOK used as a base in the presence of dry THF. However, target product was not obtained. As a second attempt, mild base, DBU, was used. Although desired product was formed, isolation of eliminated product was not achieved yet. This marks a very important advance in the field because the synthesis of DiEDOT was long pursued and several groups attempted the synthesis of this molecule. Successful synthesis of this intermediate (the diene derivative, Scheme 3.4) almost guarantees the synthesis of the DiEDOT derivative.

2.3.2 Electrochemical and Electrochromic Properties of Polymers

2.3.2.1 Synthesis of Poly- 3,4-dihydro-2H-thieno[3,4-b][1,4]oxathiepine

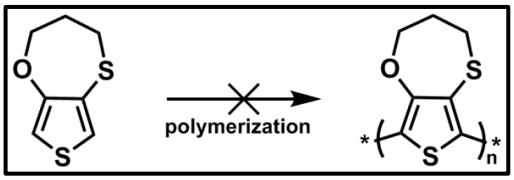

Scheme 3.5 Sythetic Pathway of Poly- 3,4-Dihydro-2H-thieno[3,4-b][1,4]oxathiepine

We were quite happy that the synthesis of ProSOT was successfully achieved. The related EDOT derivative where one of the oxygens was exchanged with sulfur resulted in very interesting electrochromic properties.

However, unfortunately, homopolymer of 3,4-dihydro-2H-thieno[3,4-b][1,4]oxathiepine was not able to be synthesized by electrochemical methods even though a number of conditions were applied**.**

2.3.2.2 Synthesis of Poly-6,8-bis(2,3-dihydrothieno[3,4-b][1,4]dioxin-5-yl)-3,4-dihydro-2H-thieno[3,4-b][1,4]oxathiepine

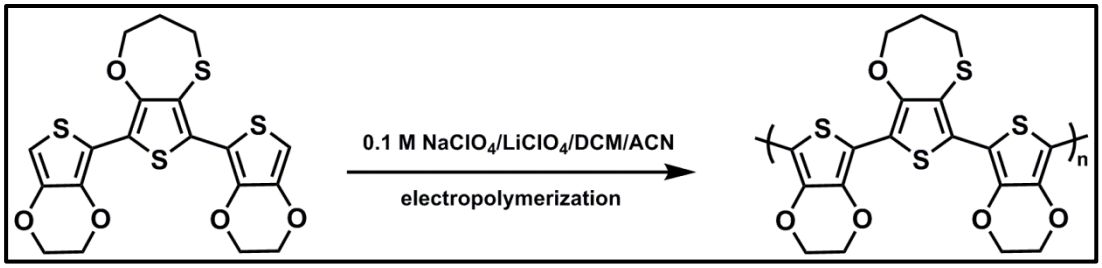

Scheme 3.6 Synthetic Pathway of Poly-6,8-Bis(2,3-dihydrothieno[3,4-b][1,4]dioxin-5-yl)-3,4-dihydro-2H-thieno[3,4-b][1,4]oxathiepine

Even though homopolymer of ProSOT could not be synthesized we thought that polymers bearing this unit will still possess good electrochromic properties. For this aim we successfully synthesized the EDOT coupled monomer. We were pleased to see that electrochemical polymerization of this material was successful and an electrochromic polymer film was successfully deposited on ITO electrodes. Details are given below.

2.3.2.2.1 Electropolymerization of 6,8-Bis(2,3-dihydrothieno[3,4-b][1,4]dioxin-5-yl)-3,4-dihydro-2H-thieno[3,4-b][1,4]oxathiepine

Electrochemical polymerization was conducted from a DCM/ACN (5/95, v/v) solvent system with 0.01 M 6,8-bis(2,3-dihydrothieno[3,4-b][1,4]dioxin-5-yl)-3,4-dihydro-2H-thieno[3,4-b][1,4]oxathiepine monomer concentration. Sodium

perchlorate/lithium perchlorate ($NaClO_4/LiClO_4$) (in 1/1 ratio) was used as supporting electrolyte and a scan rate of 100 mV/s was applied (Figure 21).

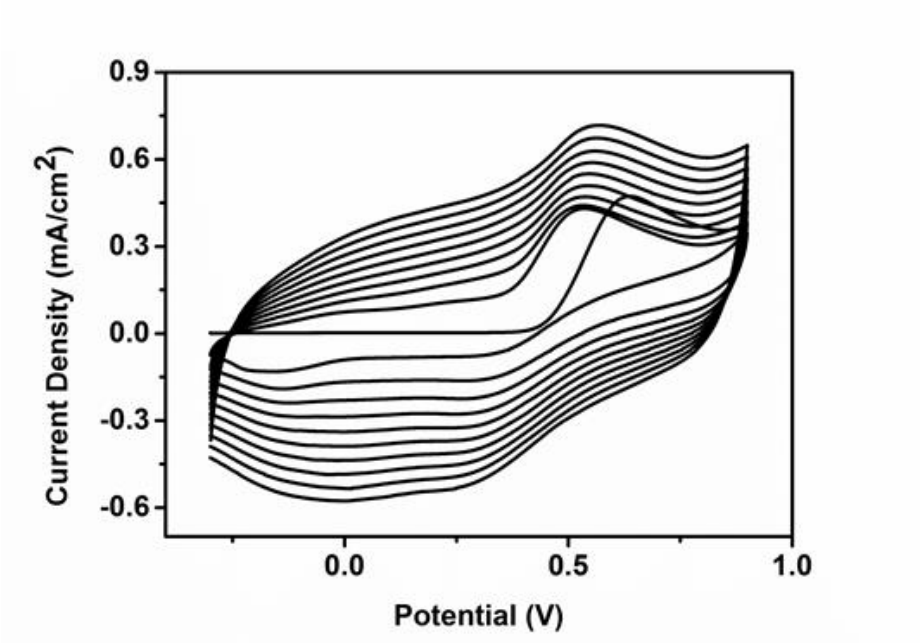

Figure 21 Repeated Scan Polymerization of ProSOT

2.3.2.2.2 Electrochemical Studies of Poly-6,8-bis(2,3-dihydrothieno[3,4-b][1,4]dioxin-5-yl)-3,4-dihydro-2H-thieno[3,4-b][1,4]oxathiepine

6,8-bis(2,3-dihydrothieno[3,4-b][1,4]dioxin-5-yl)-3,4-dihydro-2H-thieno[3,4-b][1,4]oxathiepine was polymerized via CV as described above and then CV was recorded in monomer free 0.1 M solution of $TBAPF_6$ in ACN. Oxidation potentials of the polymer were detected at 0.26 V for p-doping and 0.04 V for p-dedoping (Figure 22).

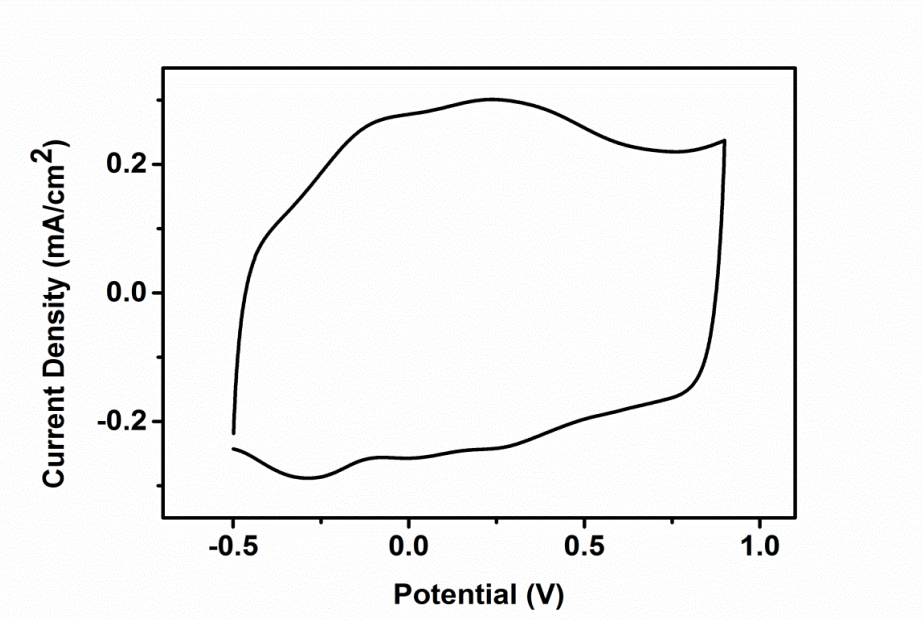

Figure 22 Single Scan Cyclic Voltammetry of ProSOT

Dependency of polymerization to scan rate was determined as shown in Figure 23. Then, scan rate vs current density graph was plotted from obtained data which showed a linear relation. This means that the polymer film is well adhered to the electrode surface and the redox process are non-diffusion controlled.

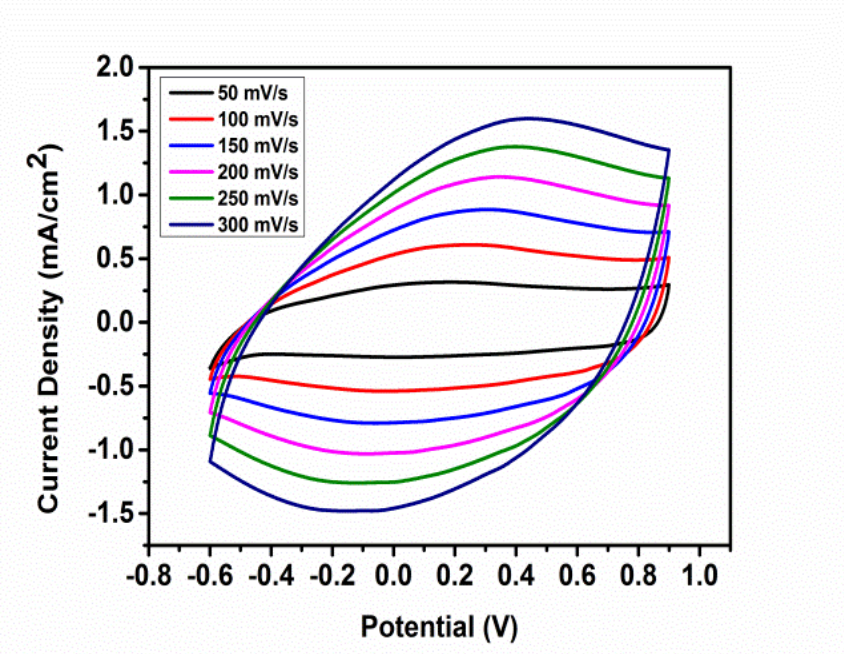

Figure 23 Cyclic Voltammogram of ProSOT at Different Scan Rates

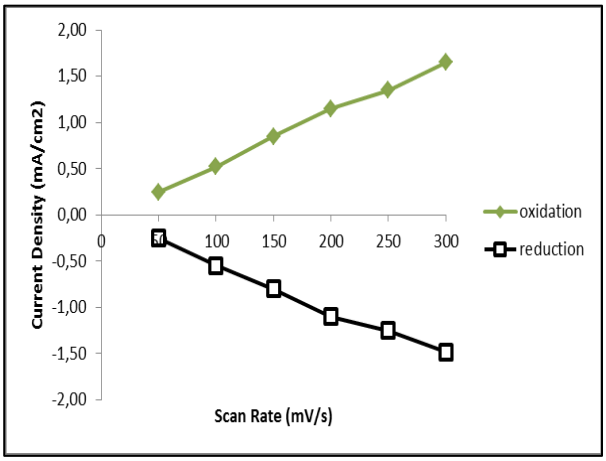

Figure 24 Scan Rate vs Current Density Plot of ProSOT

2.2.3.2 Spectroelectrochemical Studies of Polymers

2.2.3.2.3 Spectroelectrochemical Studies of Poly-6,8-bis(2,3-dihydrothieno[3,4-b][1,4]dioxin-5-yl)-3,4-dihydro-2H-thieno[3,4-b][1,4]oxathiepine

Potential between -0.6 V to 0.6 V was applied in a stepwise manner to electrochemically polymerized films on ITO coated glass slide, UV-vis-NIR spectrum were recorded at each step. Two absorption maxima, λ_{max}, were appeared at 515 nm and 555 nm. Optical band gap of corresponding polymer was calculated as 1.60 eV. Moreover, upon applied potential changes, color of ProSOT changes from purple to transparent light blue.

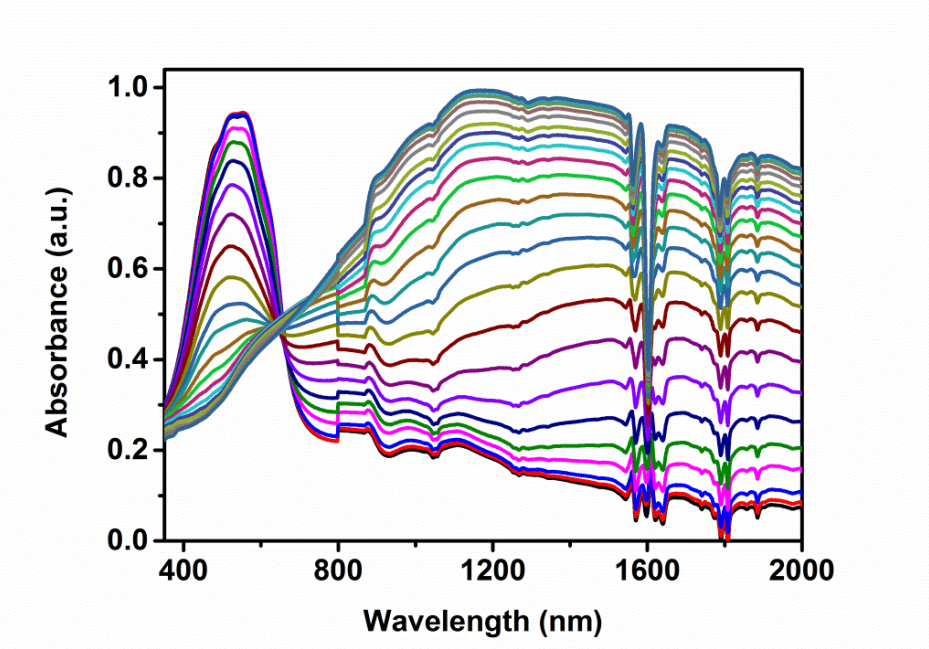

Figure 25 Spectroelectrochemical Study of ProSOT

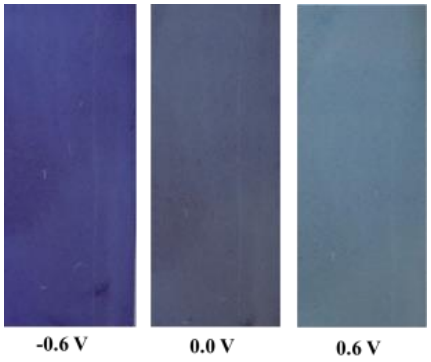

Figure 26 Color Changes Upon Oxidation

As summarized in Table 3, HOMO and LUMO (from optical band gap) level of material were calculated as -4.22 eV and -2.62 eV respectively.

Table 3 Summary of Electrochemical and Spectroelectrochemical Properties of ProSOT

	$E_{p\text{-doping}}$ (V)	$E_{p\text{-dedoping}}$ (V)	HOMO (eV)	LUMO (eV)	λ_{max}(nm)	E_g^{op} (eV)
P1	0.26	0.04	-4.22	-2.62	555/515	1.60

2.2.3.3 Kinetic Studies of Polymers

2.2.3.3.3 Kinetic Studies of Poly-6,8-bis(2,3-dihydrothieno[3,4-b][1,4]dioxin-5-yl)-3,4-dihydro-2H-thieno[3,4-b][1,4]oxathiepine

Time vs % transmittance plot was obtained from switching the polymer between neutral and oxidation states repeatedly upon applied potentials at 515 nm for 25 cycles. As a result, optical contrast of corresponding polymer was founded as 49% with 0.8 sec fast switching time.

These switching characteristics are better than the homopolymer of PEDOT (44% optical contrast with 2.2s switching time)[74]. This promising result suggests that ProSOT unit is promising building block for development of novel high performance electrochromic materials.

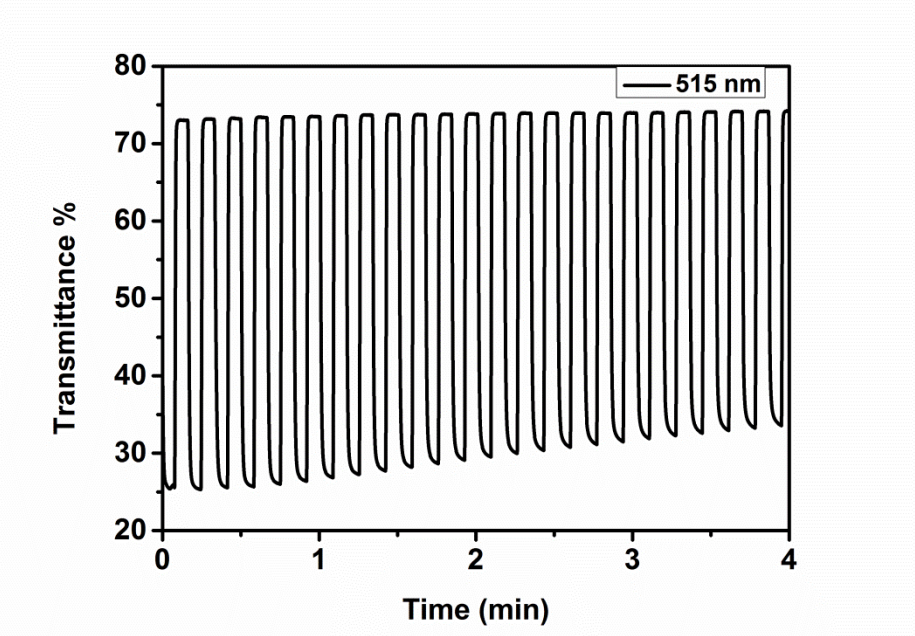

Figure 27 Percent Transmittance of ProSOT

Table 4 Summary of Kinetic Properties of ProSOT

	Optical contrast (ΔT %)		Switching times (s)
P1	49	515 nm	0.8

2.4 Conclusion

A novel analogue of EDOT, 3,4-dihydro-2H-thieno[3,4-b][1,4]oxathiepine was synthesized successfully. All intermediate steps and final product were characterized with NMR and HRMS.

For polymerization, cyclic voltammogram was used. Nevertheless, it was observed that polymerization was not proceeding electrochemically.

Furthermore, di-brominated product of the core unit was coupled with 3,4-ethylenedioxythiophene and polymerized electrochemically. As a result, oxidation potentials of the polymer for doping/de-doping were founded as -0.07 V/0.26 V and -0.29 V /0.04. There is two λ_{max} values were appeared at absorption spectra are 515 nm and 555 nm and optical band gap of ProSOT was calculated as 1.60 eV. Moreover, at 515 nm, optical contrast was founded as 49% with 0.8 sec fast switching time. These switching characteristics are better than the homopolymer of PEDOT (44% optical contrast with 2.2s switching time). This promising result suggests that ProSOT unit is promising building block for development of novel high performance electrochromic materials.

Synthesis of selenopheno[3,4-b]thieno[3,4-e][1,4]dioxine and dithieno[3,4-b:3',4'-e][1,4]dioxine are still proceeding. Once their syntheses were accomplished, electrochemical polymerization and investigation of electrochromic properties will be investigated. Then these units will be coupled with with benzothiodiazole, quinoxaline or pyrrole based acceptors and after their polymerization, electrochemical/electrochromic properties will be investigated.

REFERENCES

(1) Gupta, A.; Sharma, S.; Up, B. **2013**, *4* (2231), 16.

(2) Burke, D. J.; Lipomi, D. J. *Energy Environ. Sci.* **2013**, *6* (7), 2053.

(3) Dincer, I. *Renew. Sustain. Energy Rev.* **2000**, *4* (2), 157.

(4) Kesters, J.; Verstappen, P.; Kelchtermans, M.; Lutsen, L.; Vanderzande, D.; Maes, W. *Adv. Energy Mater.* **2015**, *5* (13), 1.

(5) Yadav, A.; Kumar, P. *Int. J. Technol. Res. Eng.* **2015**, *2* (11), 2347.

(6) Kallmann, H.; Pope, M. *J. Chem. Phys.* **1959**, *30* (2), 585.

(7) Tang, C. W. *Appl. Phys. Lett.* **1986**, *48* (2), 183.

(8) B.Srinivas, S.Balaji, M. N. B. Y. S. R. *Int. J. Eng. Res. Online* **2015**, *3*, 178.

(9) Goetzberger, A.; Hebling, C.; Schock, H.-W. *Mater. Sci. Eng. R Reports* **2003**, *40* (1), 1.

(10) Kibria, M. T.; Ahammed, A.; Sony, S. M.; Hossain, F. *Int. Conf. Environ. Asp. Bangladesh* **2014**, 51.

(11) Sharma, S.; Jain, K. K.; Sharma, A. *Mater. Sci. Appl.* **2015**, *6* (December), 1145.

(12) Chopra, K. L.; Paulson, P. D.; Dutta, V. *Prog. Photovoltaics Res. Appl.* **2004**, *12* (23), 69.

(13) Ramanujam, J.; Singh, U. P.; Tomassini, M.; Barreau, N.; Steijvers, H.; Berkumd, J. van; Vroon, Z.; Zeman, M.; Zimmermann, U.; Cunha, A. F. da; Edoff, M.; Nishiwaki, S.; Romanyuk, Y. E.; Bilger, G.; Tiwari, A. N.; Bjorkman, C. P.; Spiering, S.; Tiwari, A. N.; Torndahl, T.; Cirlin, G. E. *Energy Environ. Sci.* **2017**, *361/362*, 540.

(14) Arjunan, T. V; Senthil, T. S. *Mater. Technol.* **2013**, *28* (1–2), 9.

(15) Green, M. A.; Ho-Baillie, A.; Snaith, H. J.; J., S. H.; J, S. H. *Nat. Photonics* **2014**, *8* (7), 506.

(16) Liu, M.; Johnston, M. B.; Snaith, H. J. *Nature* **20139**, *501* (7467), 395.

(17) Bagher, A. M. *Sustain. Energy* **2014**, *2* (3), 85.

(18) Son, H. J.; Wang, W.; Xu, T.; Liang, Y.; Wu, Y.; Li, G.; Yu, L. *J. Am. Chem. Soc.* **2011**, *133* (6), 1885.

(19) Salinas, J. F.; Yip, H. L.; Chueh, C. C.; Li, C. Z.; Maldonado, J. L.; Jen, A. K. Y. *Adv. Mater.* **2012**, *24* (47), 6362.

(20) Brabec, C. J.; Sariciftci, N. S.; Hummelen, J. C. *Adv. Funtional Mater.* **2001**, *11* (1), 15.

(21) Yeh, N.; Yeh, P. *Renew. Sustain. Energy Rev.* **2013**, *21*, 421.

(22) Li, M.; Gao, K.; Wan, X.; Zhang, Q.; Kan, B.; Xia, R.; Liu, F.; Yang, X.; Feng, H.; Ni, W.; Wang, Y.; Peng, J.; Zhang, H.; Liang, Z.; Yip, H.-L.; Peng, X.; Cao, Y.; Chen, Y. *Nat. Photonics* **2017**, *11* (February), 85.

(23) Qi, B.; Wang, J. *Phys. Chem. Chem. Phys.* **2013**, *15*, 8972.

(24) Kaur, N.; Singh, M.; Pathak, D.; Wagner, T.; Nunzi, J. M. *Synth. Met.* **2014**, *190*, 20.

(25) Zhou, Z.-H.; Maruyama, T.; Kanbara, T.; Ikeda, T.; Ichimura, K.; Yamamoto, T.; Tokuda, K. *J. Chem. Soc. Chem. Commun.* **1991**, *1460* (1210), 1210.

(26) Li, G.; Chang, W.-H.; Yang, Y. *Nat. Rev. Mater.* **2017**, *2* (8), 17043.

(27) He, Z.; Xiao, B.; Liu, F.; Wu, H.; Yang, Y.; Xiao, S.; Wang, C.; Russell, T. P.; Cao, Y. *Nat. Photonics* **2015**, *9* (3), 174.

(28) He, Z.; Zhong, C.; Su, S.; Xu, M.; Wu, H.; Cao, Y. *Nat. Photonics* **2012**, *6* (9), 591.

(29) van Franeker, J. J.; Turbiez, M.; Li, W.; Wienk, M. M.; Janssen, R. A. J. *Nat. Commun.* **2015**, *6*, 6229.

(30) Zheng, Z.; Zhang, S.; Zhang, J.; Qin, Y.; Li, W.; Yu, R.; Wei, Z.; Hou, J. *Adv. Mater.* **2016**, 5133.

(31) Chen, C. C.; Chang, W. H.; Yoshimura, K.; Ohya, K.; You, J.; Gao, J.; Hong, Z.; Yang, Y. *Adv. Mater.* **2014**, *26* (32), 5670.

(32) Ameri, T.; Khoram, P.; Min, J.; Brabec, C. J. *Adv. Mater.* **2013**, *25* (31), 4245.

(33) Raj, M. R.; Kim, M.; Kim, H. Il; Lee, G.-Y.; Park, C. W.; Park, T. *J. Phys. Chem. A* **2017**, *5*, 3330.

(34) Chen, X.; Liu, B.; Zou, Y.; Tang, W.; Li, Y.; Xiao, D. *RSC Adv.* **2012**, *2* (19), 7439.

(35) Zhu, D.; Sun, L.; Bao, X.; Wen, S.; Han, L.; Gu, C.; Guo, J.; Yang, R. *RSC Adv.* **2015**, *5* (77), 62336.

(36) Baek, M. J.; Lee, S. H.; Zong, K.; Lee, Y. S. *Synth. Met.* **2010**, *160* (11–12), 1197.

(37) Chen, X.; Chen, L.; Chen, Y. *J. Polym. Sci. Part A Polym. Chem.* **2013**, *51* (19), 4156.

(38) Kim, B.; Yeom, H. R.; Yun, M. H.; Kim, J. Y.; Yang, C. **2012**.

(39) Zwanenburg, D.J.;Haan, H. De Wynberg, H. **1966**, *31*, 3363.

(40) Shirakawa, H. *Curr. Appl. Phys.* **2001**, *1* (4–5), 281.

(41) Chiang, C. K.; Gau, S. C.; Fincher, C. R.; Park, Y. W.; MacDiarmid, A. G.; Heeger, A. J. *Appl. Phys. Lett.* **1978**, *33* (1), 18.

(42) Lövenich, W. *Polym. Sci. Ser. C* **2014**, *56* (1), 135.

(43) Kirchmeyer, S.; Reuter, K. *J. Mater. Chem.* **2005**, *15* (21), 2077.

(44) Li, Y. *Org. Optoelectron. Mater.* **2015**, 27.

(45) Inzelt, G. *Conducting Polymers*; Springer: Berlin, **2008**; p. 123.

(46) Roncali, J.; Blanchard, P.; Frère, P. *J. Mater. Chem.* **2005**, *15* (16), 1589.

(47) Heywang, G.; Jonas, F. *Adv. Mater.* **1992**, *4* (2), 116.

(48) Wang, Z.; Mo, D.; Chen, S.; Xu, J.; Lu, B.; Jiang, Q.; Feng, Z.; Xiong, J.; Zhen, S. *J. Polym. Sci. Part A Polym. Chem.* **2015**, *53* (19), 2285.

(49) Sahoo, R.; Mishra, S. P.; Kumar, A.; Sindhu, S.; Narasimha Rao, K.; Gopal, E. S. R. *Opt. Mater. (Amst).* **2007**, *30* (1), 143.

(50) Kudoh, Y.; Akami, K.; Matsuya, Y. *Synth. Met.* **1999**, *102* (1–3), 973.

(51) Benor, A.; Takizawa, S. ya; Pérez-Bolívar, C.; Anzenbacher, P. *Org. Electron. physics, Mater. Appl.* **2010**, *11* (5), 938.

(52) Chen, S.; Jiang, X.; So, F. *Org. Electron.* **2013**, *14* (10), 2518.

(53) Tait, J. G.; Worfolk, B. J.; Maloney, S. A.; Hauger, T. C.; Elias, A. L.; Buriak, J. M.; Harris, K. D. *Sol. Energy Mater. Sol. Cells* **2013**, *110*, 98.

(54) Emmott, C. J. M.; Urbina, A.; Nelson, J. *Sol. Energy Mater. Sol. Cells* **2012**, *97*, 14.

(55) Zhang, L.; Wen, Y.; Yao, Y.; Xu, J.; Duan, X.; Zhang, G. *Electrochim. Acta* **2014**, *116*, 343.

(56) Cheng, Y. H.; Kung, C. W.; Chou, L. Y.; Vittal, R.; Ho, K. C. *Sensors Actuators, B Chem.* **2014**, *192*, 762.

(57) Nanodots, P.; Electropolymerization, T. **2012**, No. 4, 3018.

(58) Sankaran, B.; Reynolds, J. R. *Macromolecules* **1997**, *30* (9), 2582.

(59) Welsh, D. M.; Kumar, A.; Meijer, E. W.; Reynolds, J. R. *Adv. Mater.* **1999**, *11* (16), 1379.

(60) Spencer, H. J.; Skabara, P. J.; Giles, M.; McCulloch, I.; Coles, S. J.; Hursthouse, M. B. *J. Mater. Chem.* **2005**, *15* (45), 4783.

(61) Welsh, D. M.; Kloeppner, L. J.; Madrigal, L.; Pinto, M. R.; Thompson, B. C.; Schanze, K. S.; Abboud, K. A.; Powell, D.; Reynolds, J. R. *Macromolecules* **2002**, *35* (17), 6517.

(62) Lu, B.; Zhen, S.; Zhang, S.; Xu, J.; Zhao, G. *Polym. Chem.* **2014**, *5* (17), 4896.

(63) Sönmez, G.; Schwendeman, I.; Schottland, P.; Zong, K.; Reynolds, J. R. *Macromolecules* **2003**, *36* (3), 639.

(64) Schottland, P.; Zong, K.; Gaupp, C. L.; Thompson, B. C.; Thomas, C. A.; Giurgiu, I.; Hickman, R.; Abboud, K. A.; Reynolds, J. R. *Macromolecules* **2000**, *33* (19), 7051.

(65) Von Kieseritzky, F.; Allared, F.; Dahlstedt, E.; Hellberg, J. *Tetrahedron Lett.* **2004**, *45* (31), 6049.

(66) Merz, A.; Rehm, C. *J. für Prakt. Chem.* **1996**, *338*, 672.

(67) Halfpenny, J.; Rooney, P. B.; Sloman, Z. S. *J. Chem. Soc. Perkin Trans. 1* **2001**, No. 20, 2595.

(68) Aasmundtveit, K. E.; Samuelsent, E. J.; Pettersson, L. a a; Johansson, T.; Feidenhans, R. *Synth. Met.* **1999**, *101* (379), 561.

(69) Reeves, B. D.; Grenier, C. R. G.; Argun, A. A.; Cirpan, A.; McCarley, T. D.; Reynolds, J. R. *Macromolecules* **2004**, *37* (20), 7559.

(70) Zhou, X.; Liu, W. J.; Ye, J. L.; Huang, P. Q. *Tetrahedron* **2007**, *63* (27), 6346.

(71) Martinková, M.; Mezeiová, E.; Fabišíková, M.; Gonda, J.; Pilátová, M.; Mojžiš, J. *Carbohydr. Res.* **2015**, *402*, 6.

(72) Suzuki, Y.; Wakatsuki, J.; Tsubaki, M.; Sato, M. *Tetrahedron* **2013**, *69* (46), 9690.

(73) Zhao, S.; Wu, Y.; Sun, Q.; Cheng, T. M.; Li, R. T. *Synth.* **2015**, *47* (8), 1154.

(74) Balan, A.; Gunbas, G.; Durmus, A.; Toppare, L. *Chem. Mater.* **2008**, *20* (6), 7510.

APPENDICES

A. NMR SPECTRAS OF SYNTHESIZED MONOMERS

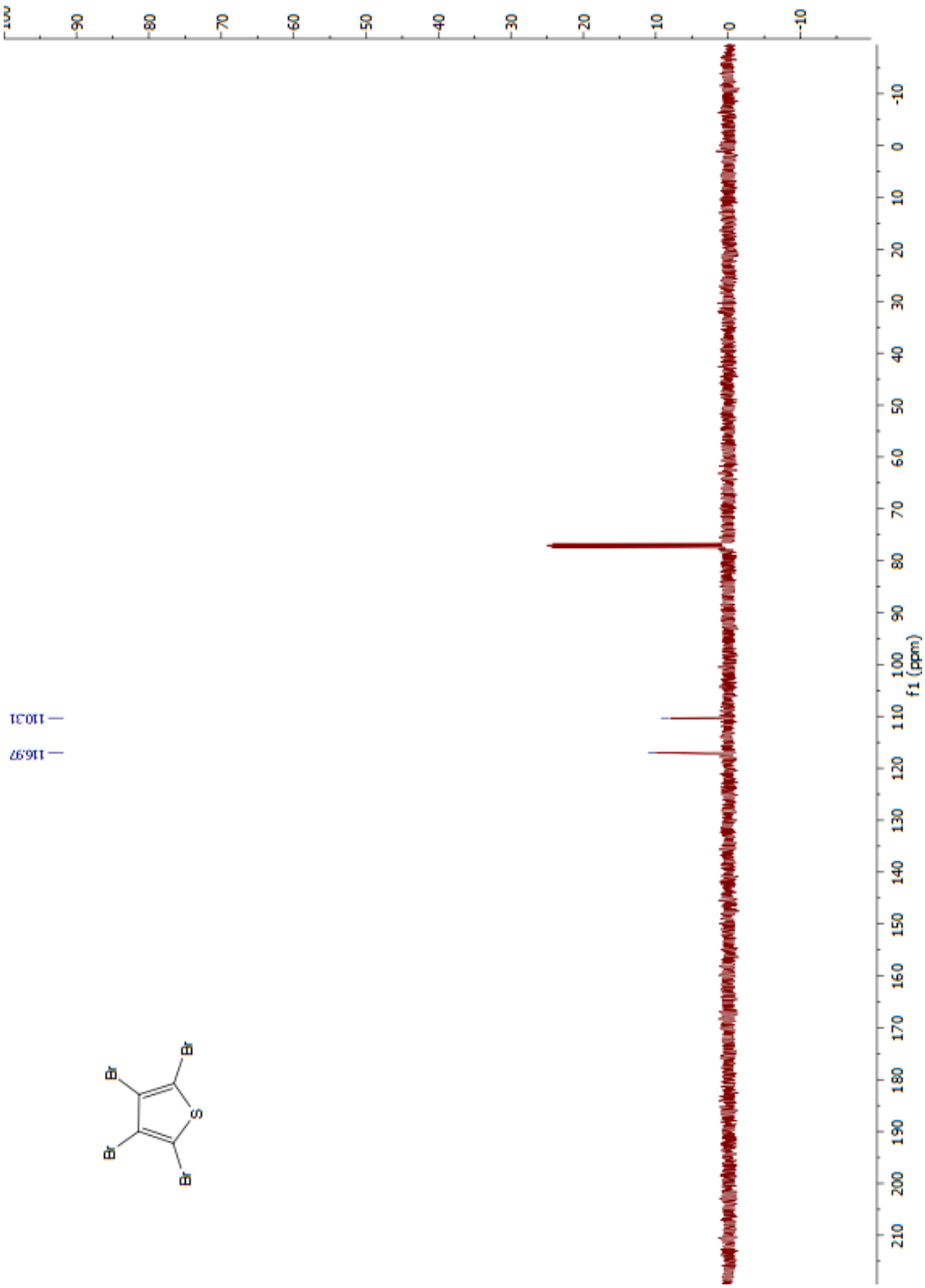

Figure A.1 ^{13}C NMR Spectrum of Tetrabromothiophene

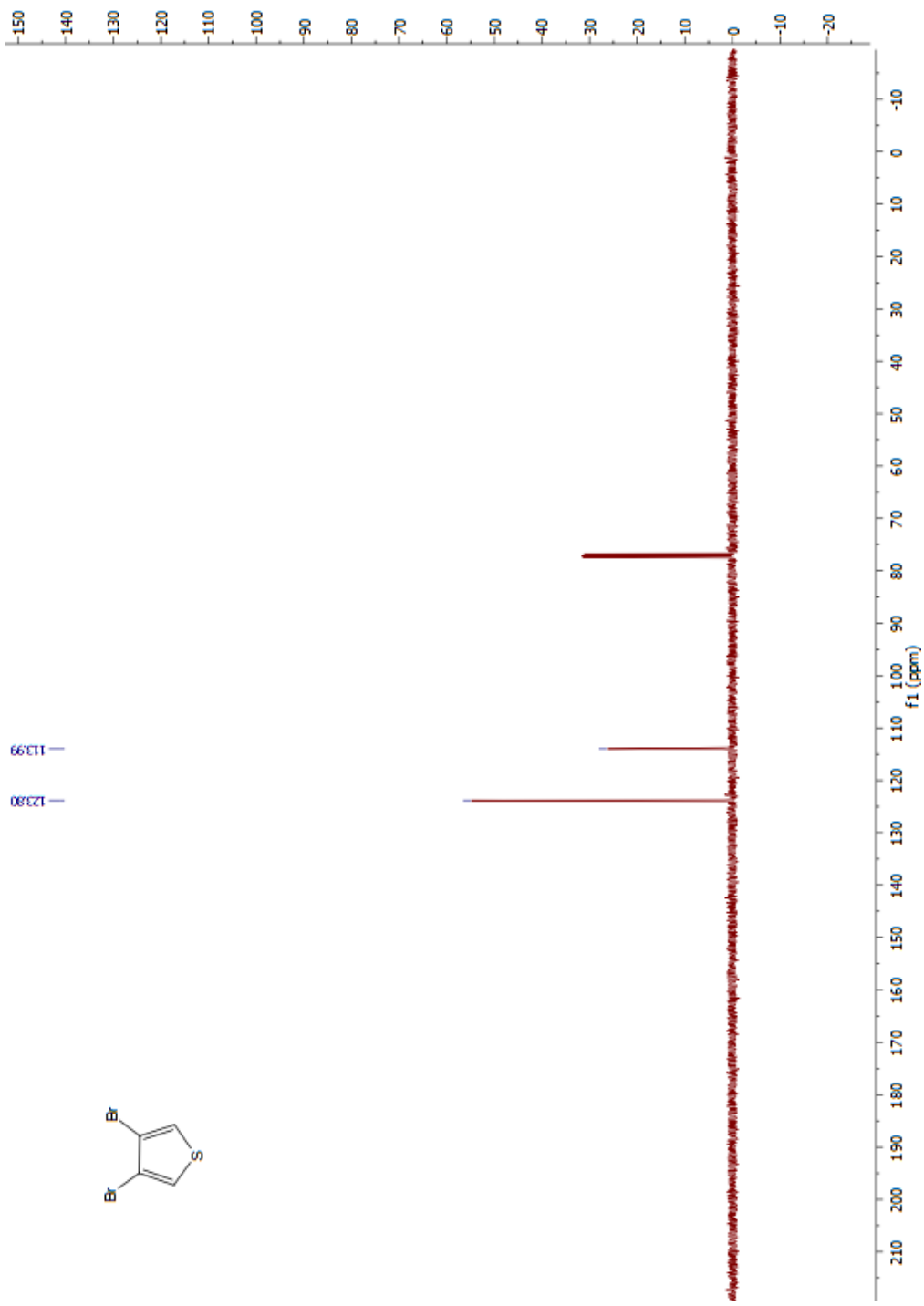

Figure A.2 ^{13}C NMR Spectrum of 3,4-Dibromothiophene

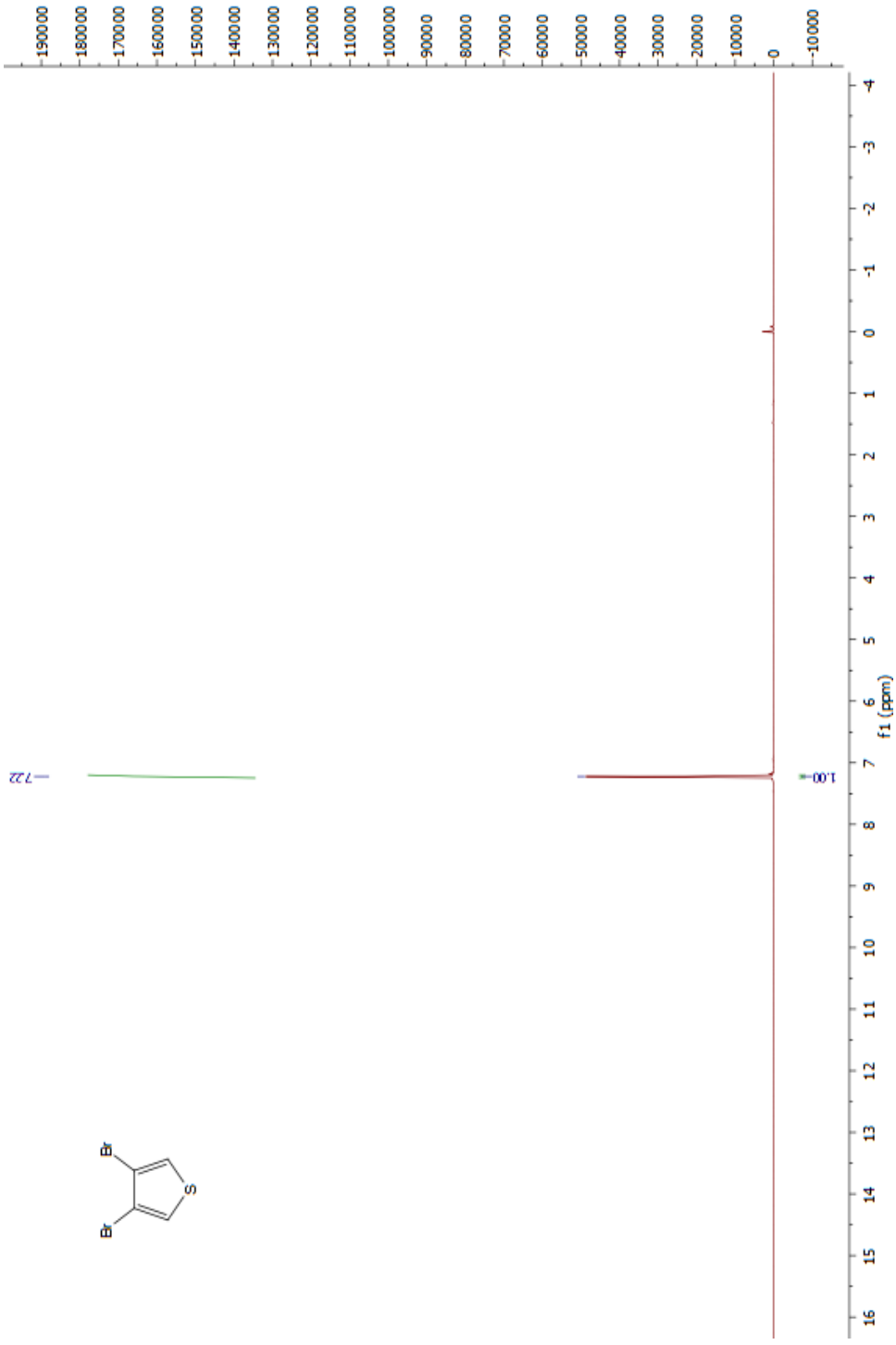

Figure A.3 ^{1}H NMR Spectrum of 3,4-Dibromothiophene

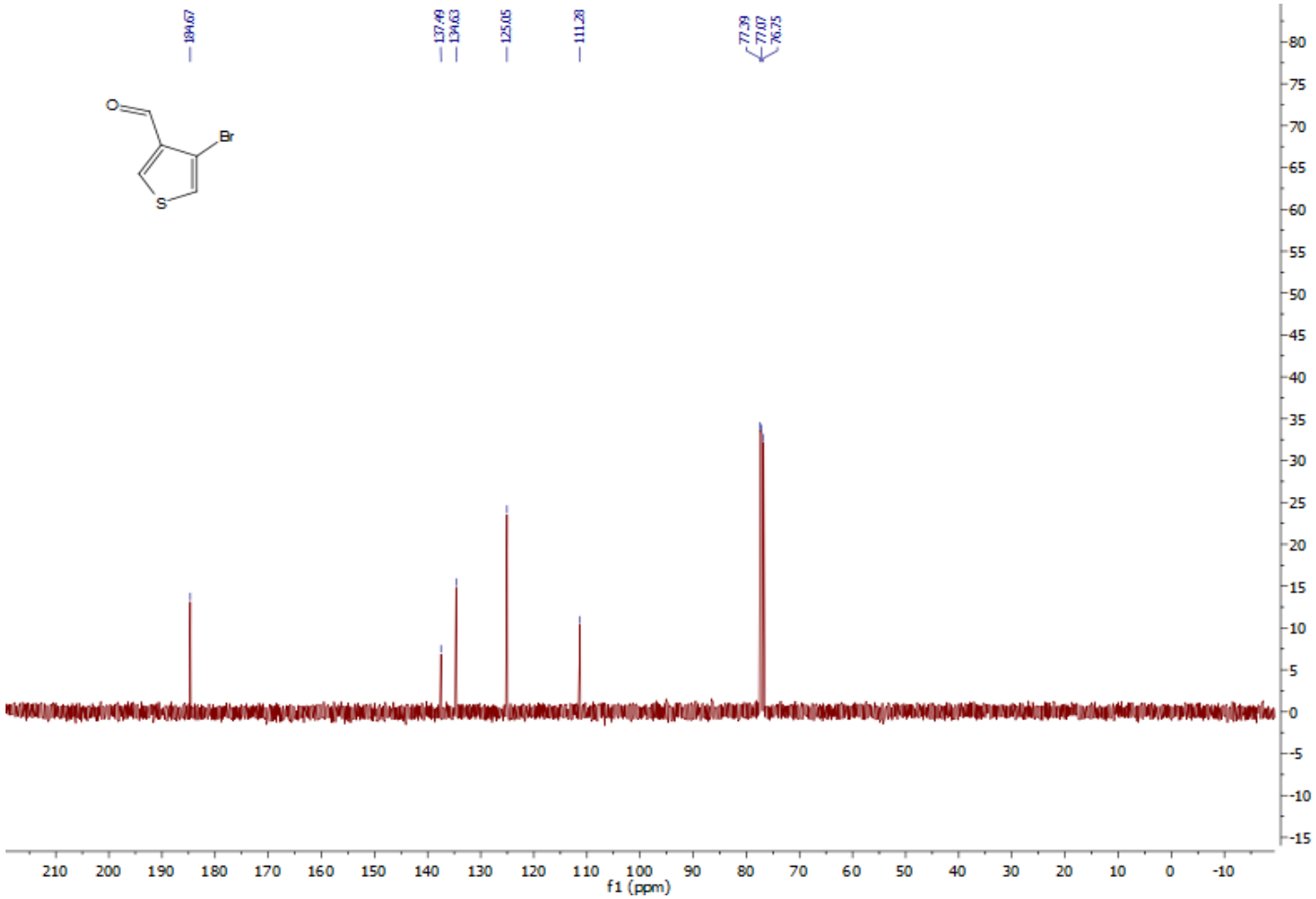

Figure A.4 ^{13}C NMR Spectrum of 4-Bromothiophene-4-carbaldehyde

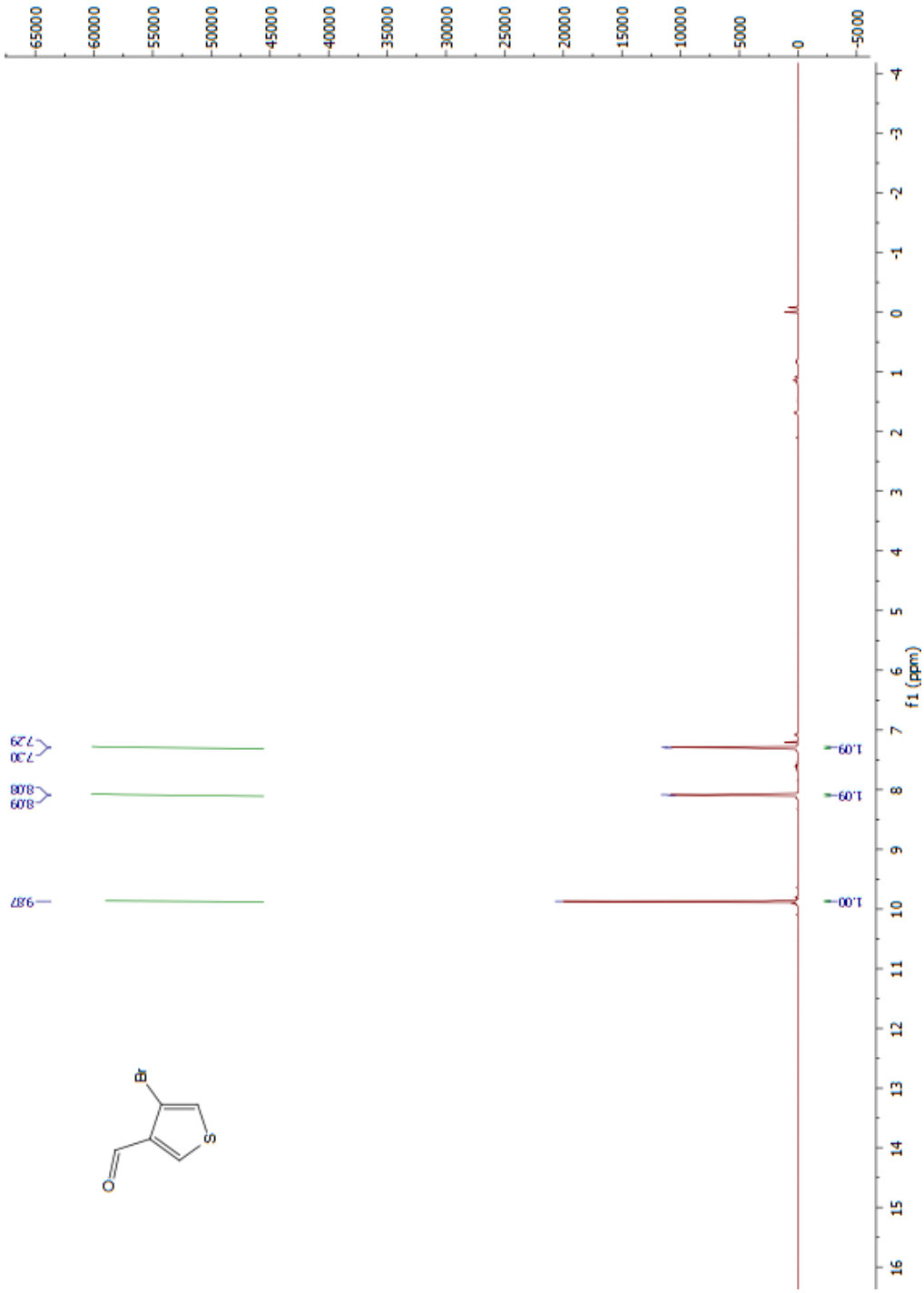

Figure A.5 ^{1}H NMR Spectrum of 4-Bromothiophene-4-carbaldehyde

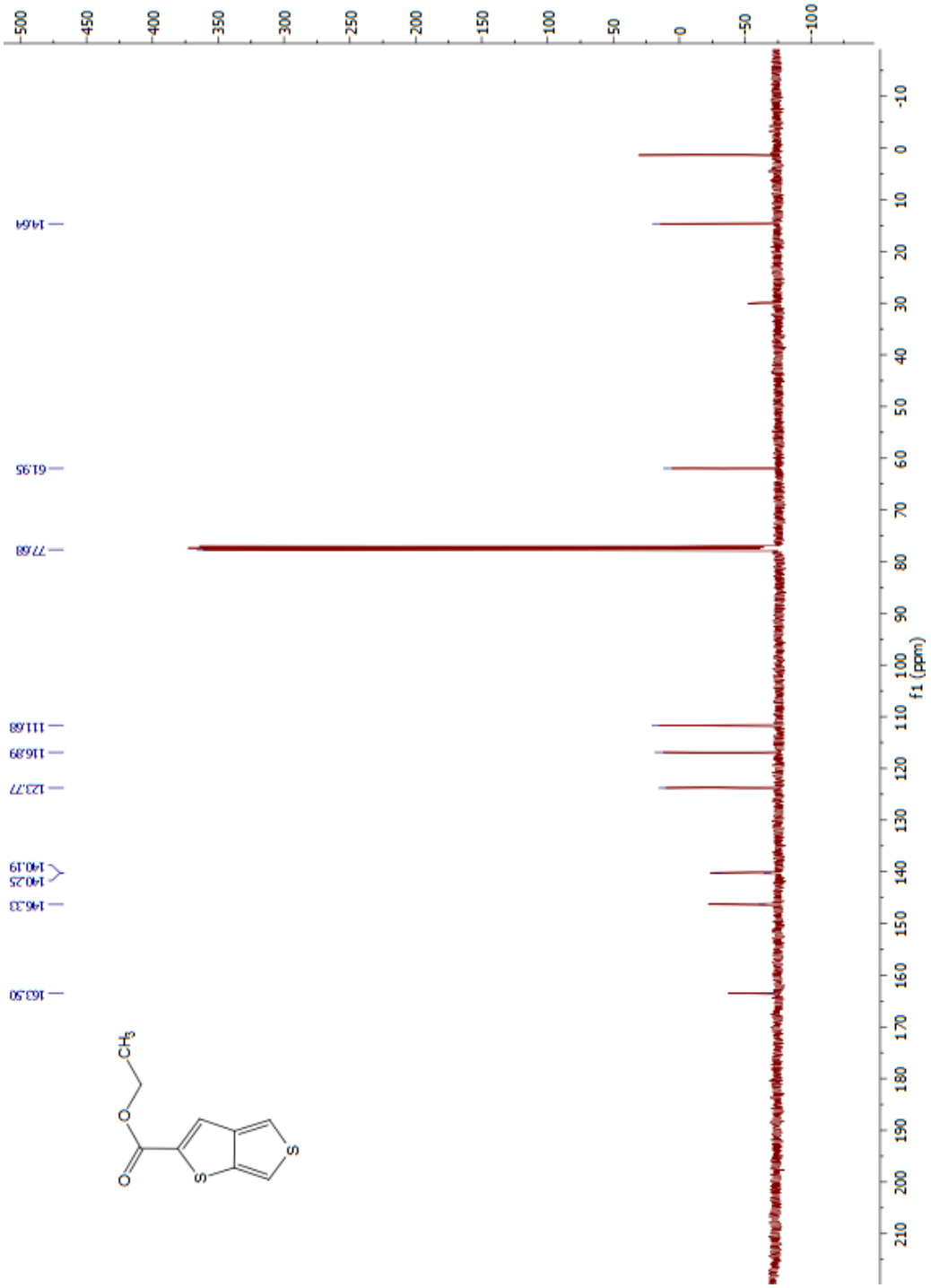

Figure A.6 ^{13}C NMR Spectrum of Ethyl thieno [3,4-b]thiophene-2-carboxylate

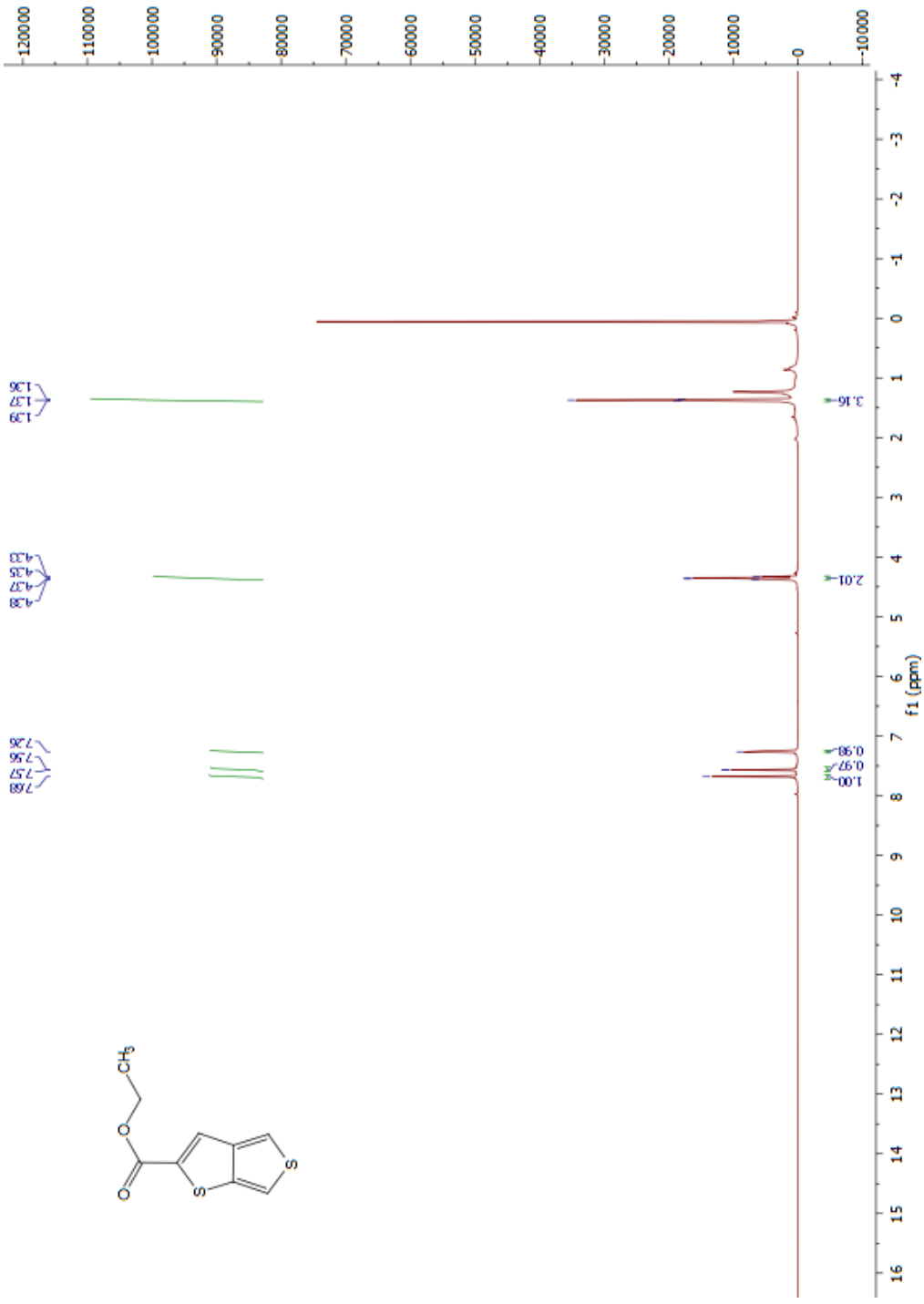

Figure A.7 ^{1}H NMR Spectrum of Ethyl thieno [3,4-b]thiophene-2-carboxylate

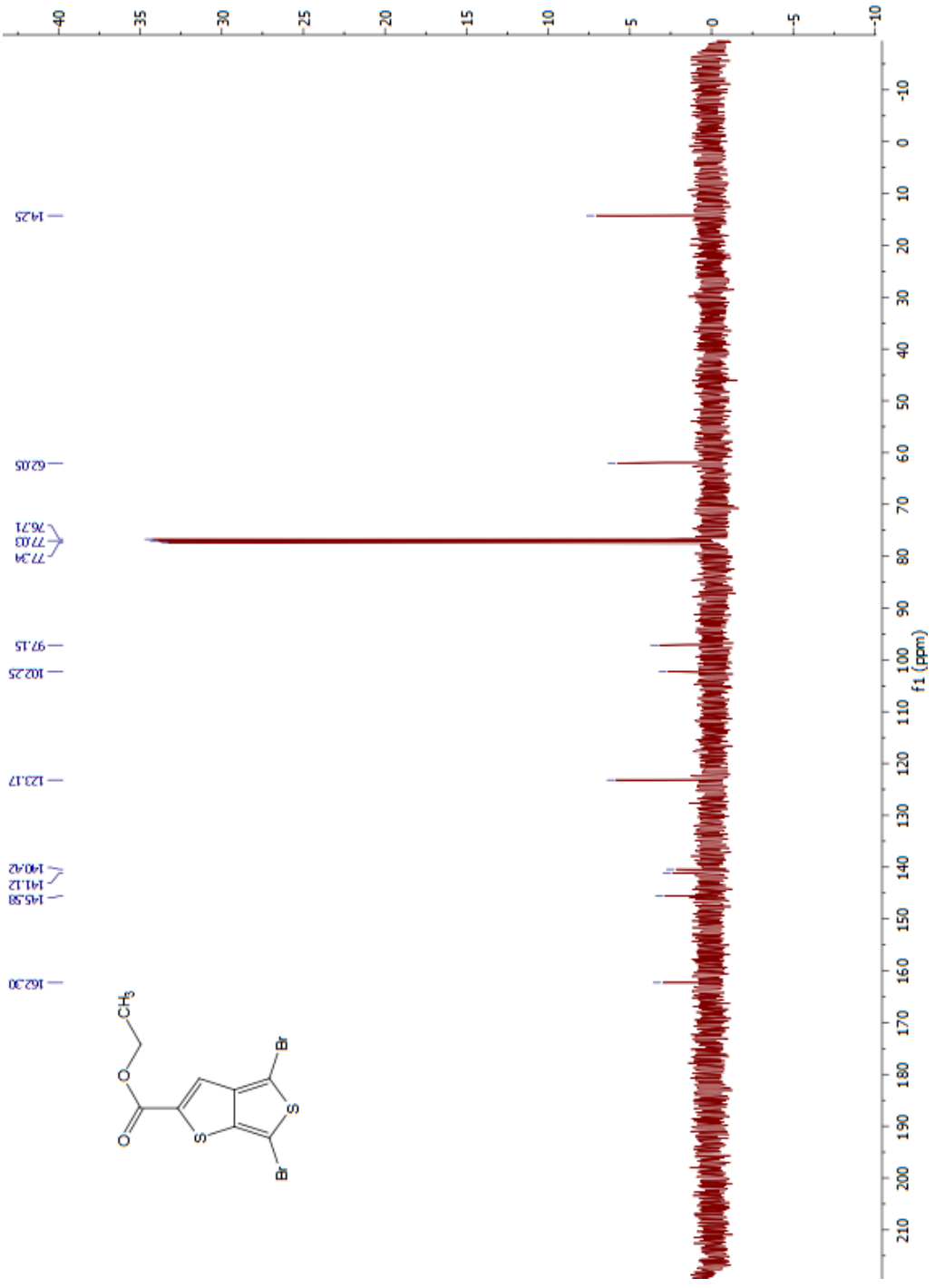

Figure A.8 ^{13}C NMR Spectrum of Ethyl 2,5-dibromothieno [3,4-b]thiophene-2-carboxylate

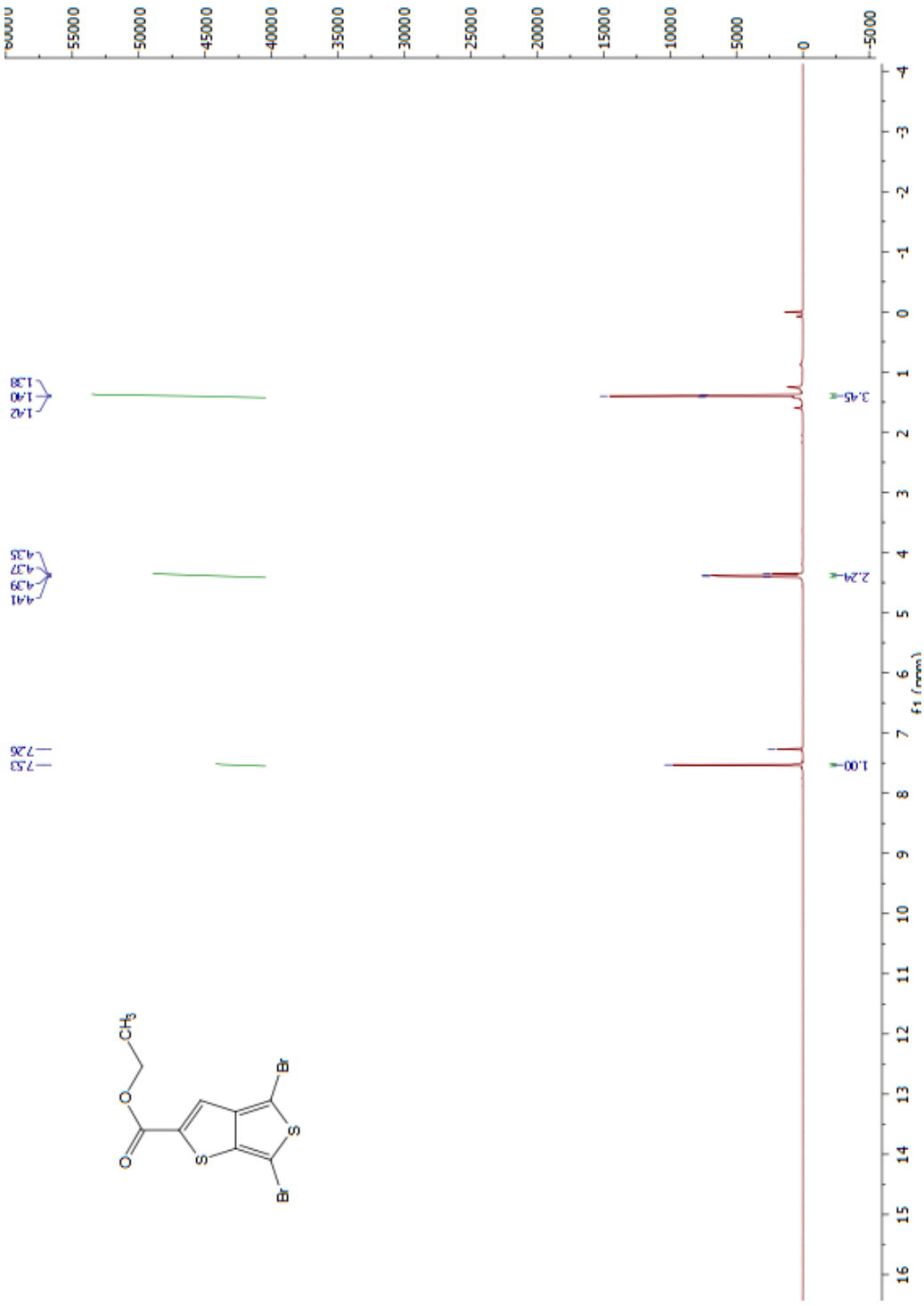

Figure A.7 ^{13}H NMR Spectrum of Ethyl 2,5-dibromothieno [3,4-b]thiophene-2-carboxylate

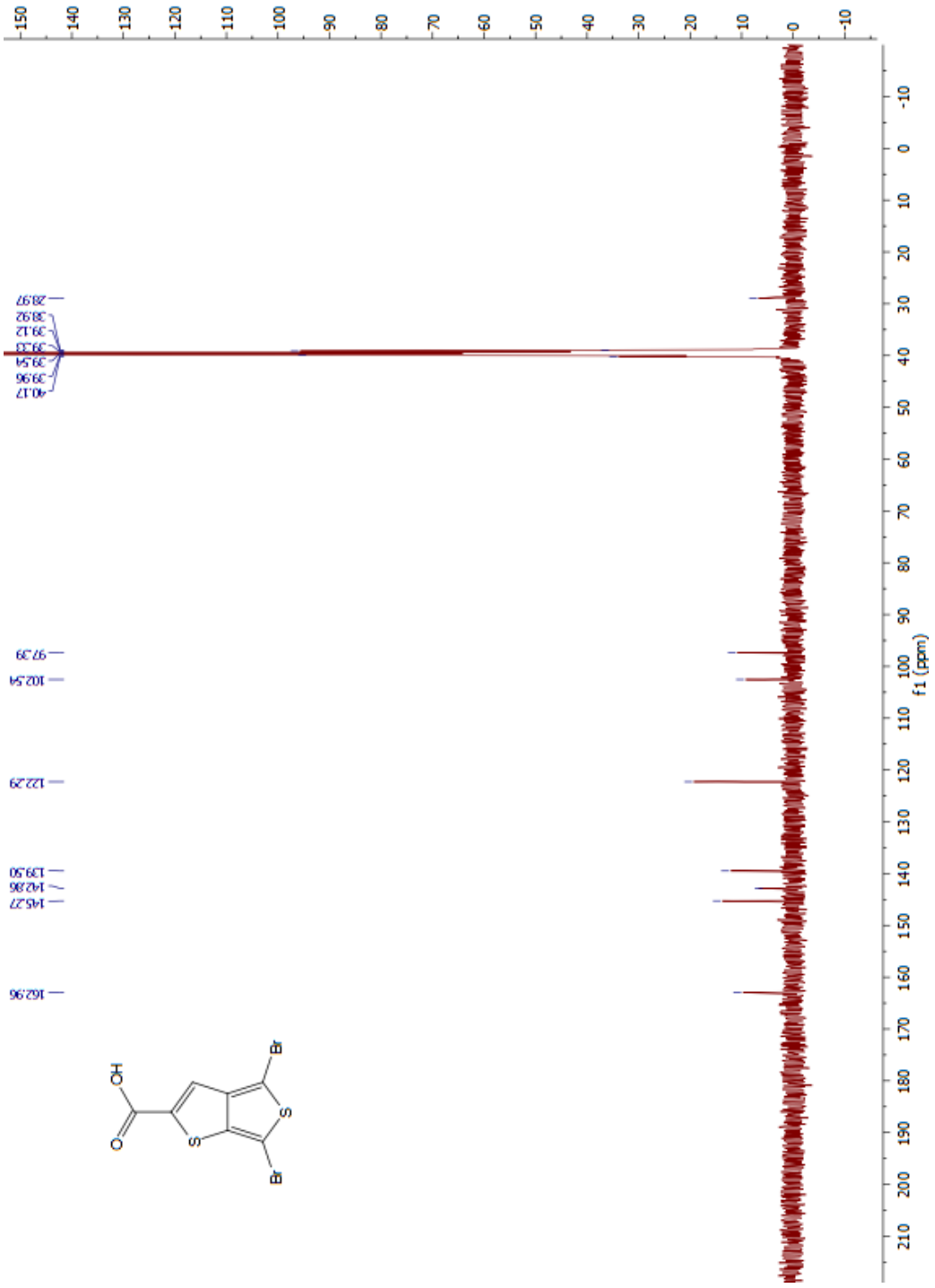

Figure A.10 ^{13}C NMR Spectrum of 4,6 -Dibromothieno[3,4-b]thiophene-2-carboxylic acid

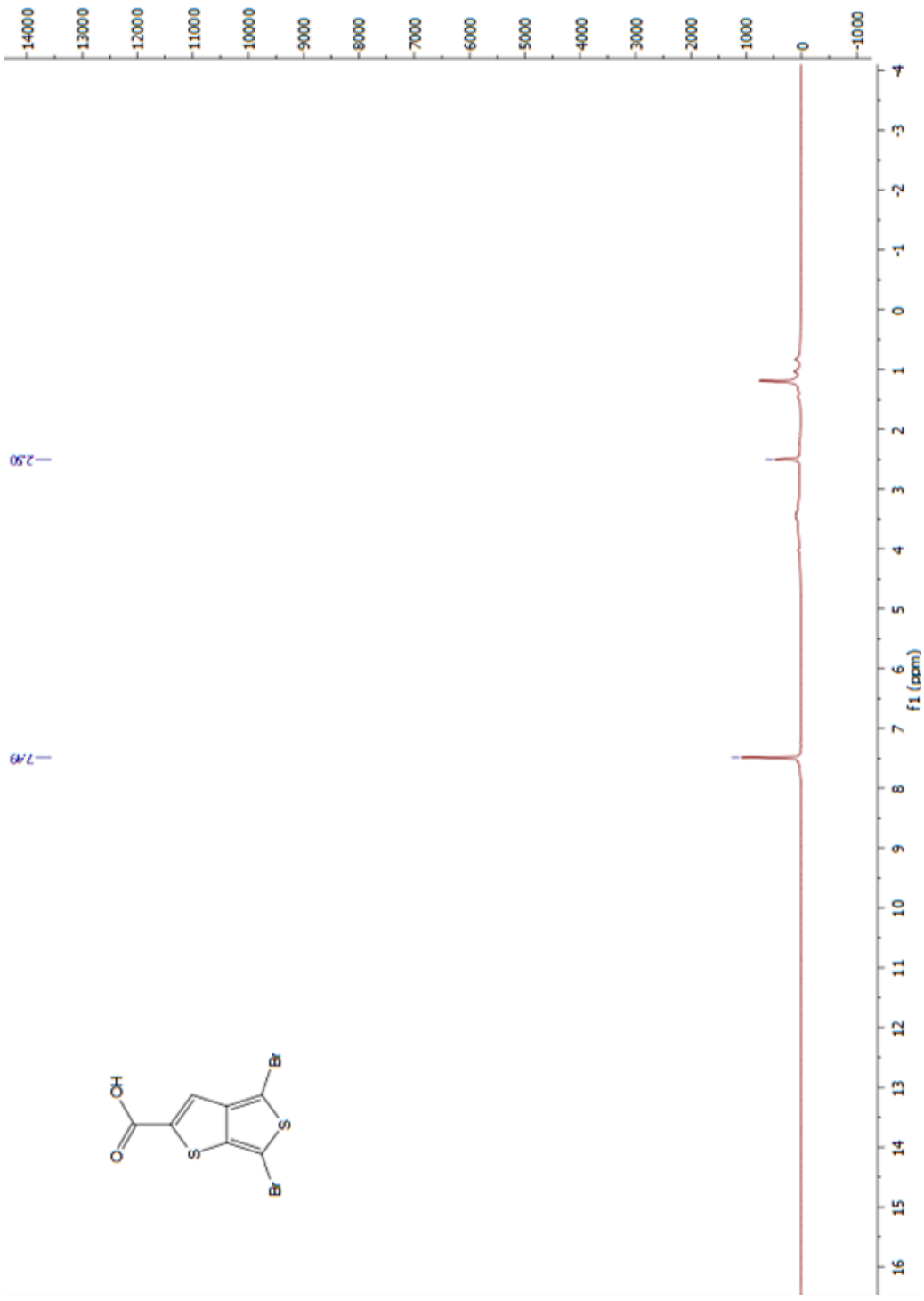

Figure A.8 ^{1}H NMR Spectrum of 4,6 -Dibromothieno[3,4-b]thiophene-2-carboxylic acid

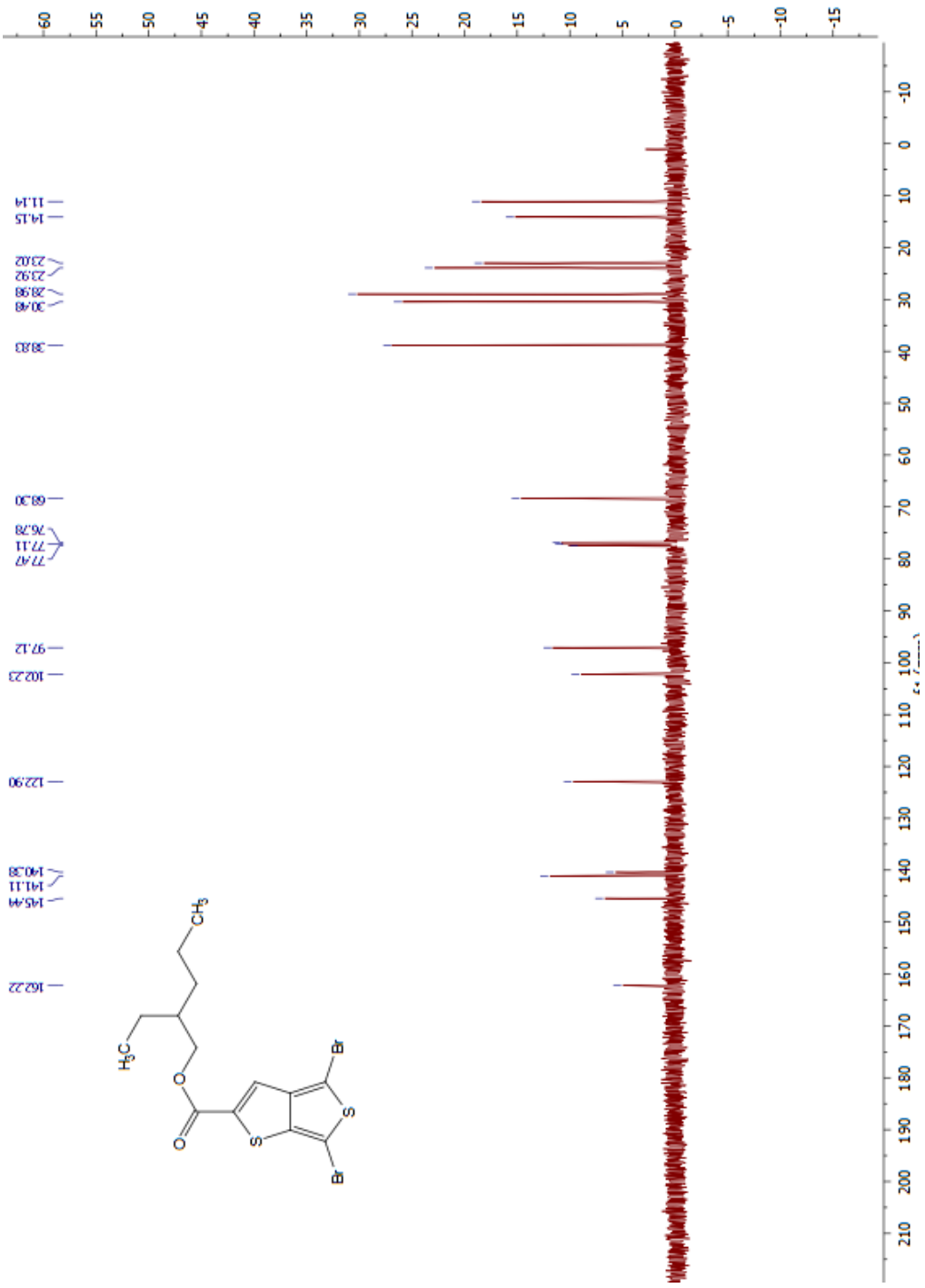

Figure A.12 ^{13}C NMR Spectrum of 2-Ethylhexyl 4,6-dibromothieno [3,4-b]thiophene-2-carboxylate

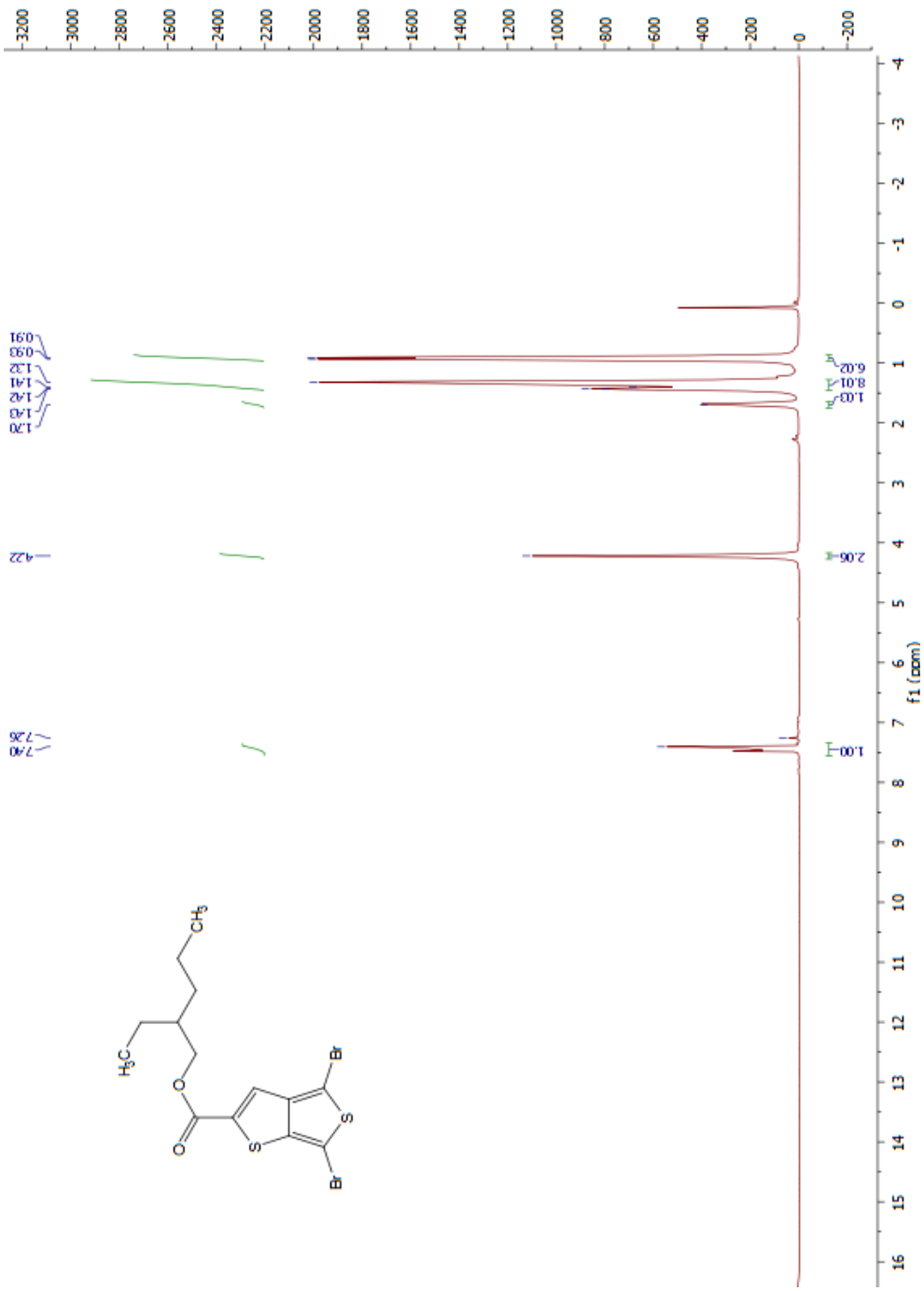

Figure A.13 ^{1}H NMR Spectrum of 2-Ethylhexyl 4,6-dibromothieno [3,4-b]thiophene-2-carboxylate

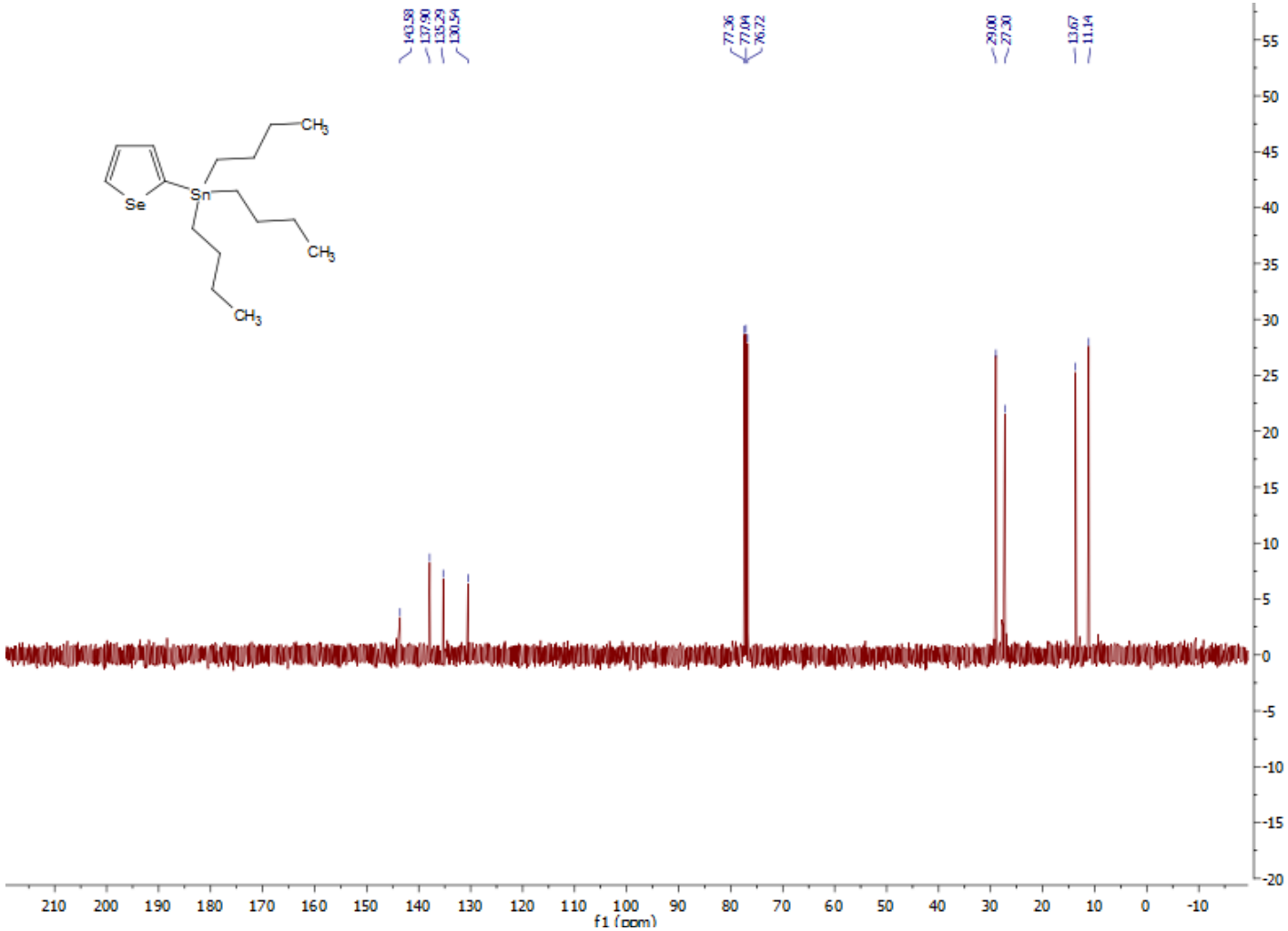

Figure A.14 ^{13}C NMR Spectrum of Tributyl(selenophen-2-yl)stannane

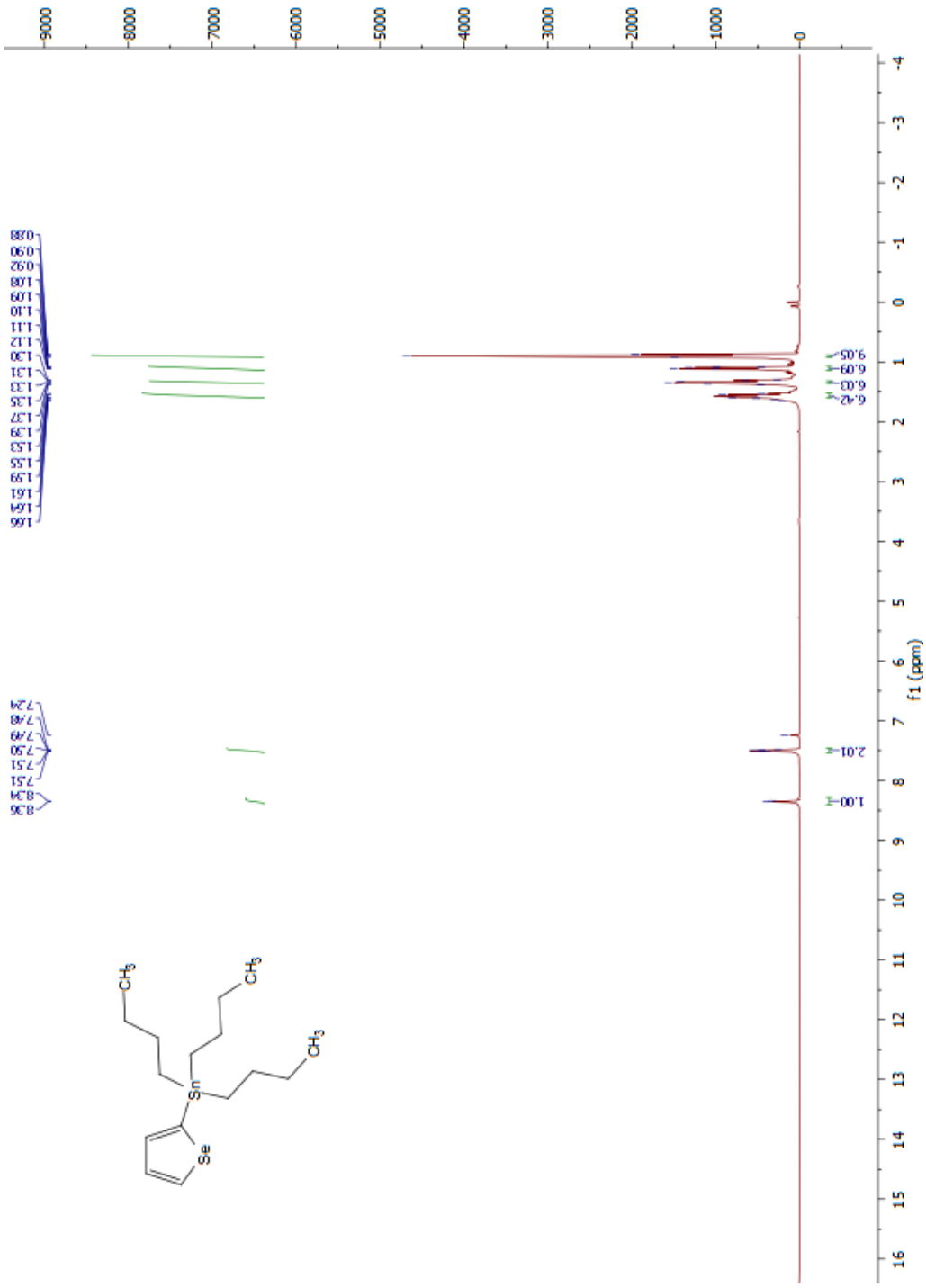

Figure A.15 ^{1}H NMR Spectrum of Tributyl(selenophen-2-yl)stannane

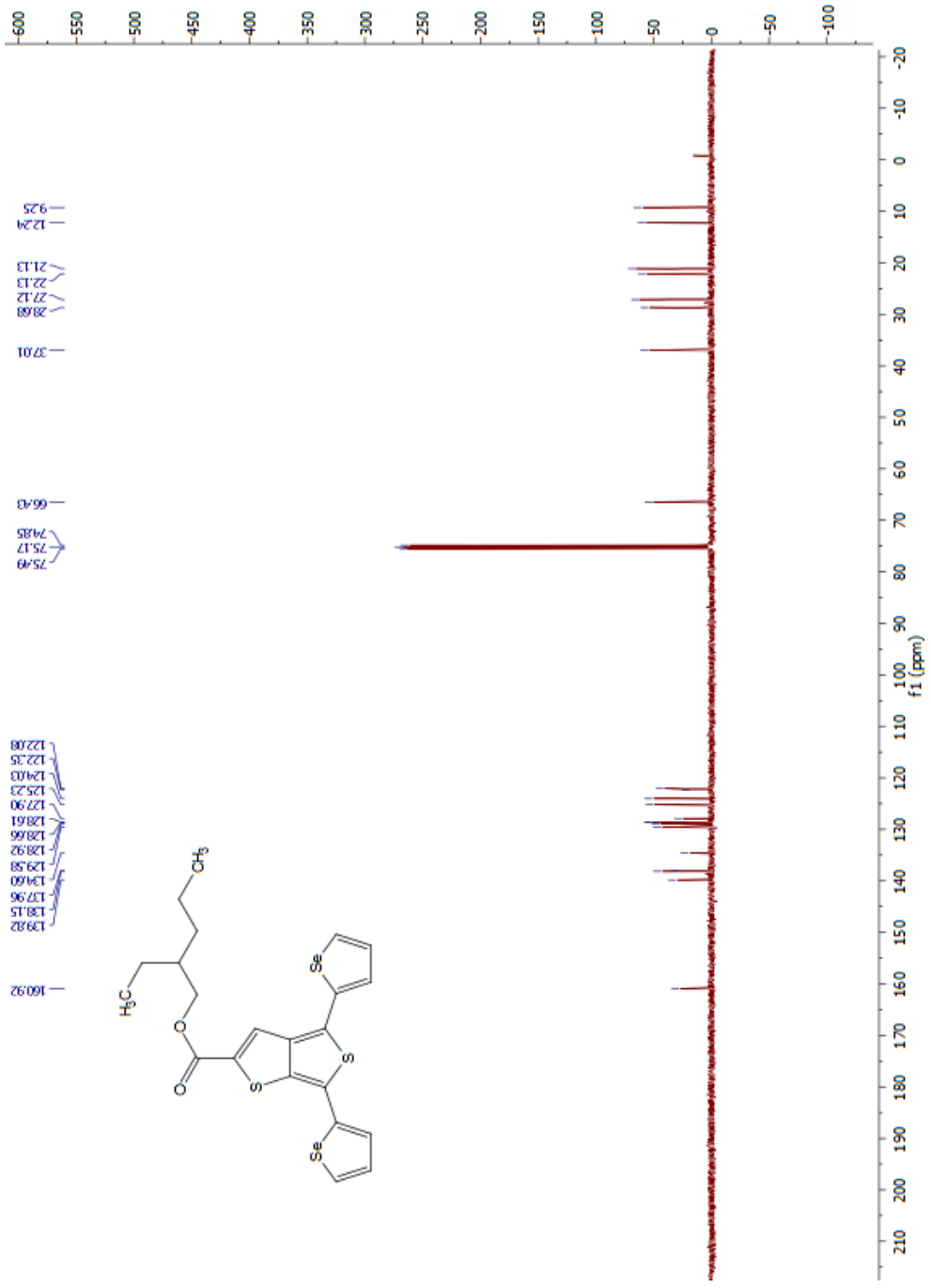

Figure A.16 ^{13}C NMR Spectrum of 2-Ethylhexyl 4,6-di(selenophene-2-yl)thieno[3,4-b]thiophene-2-carboxylate

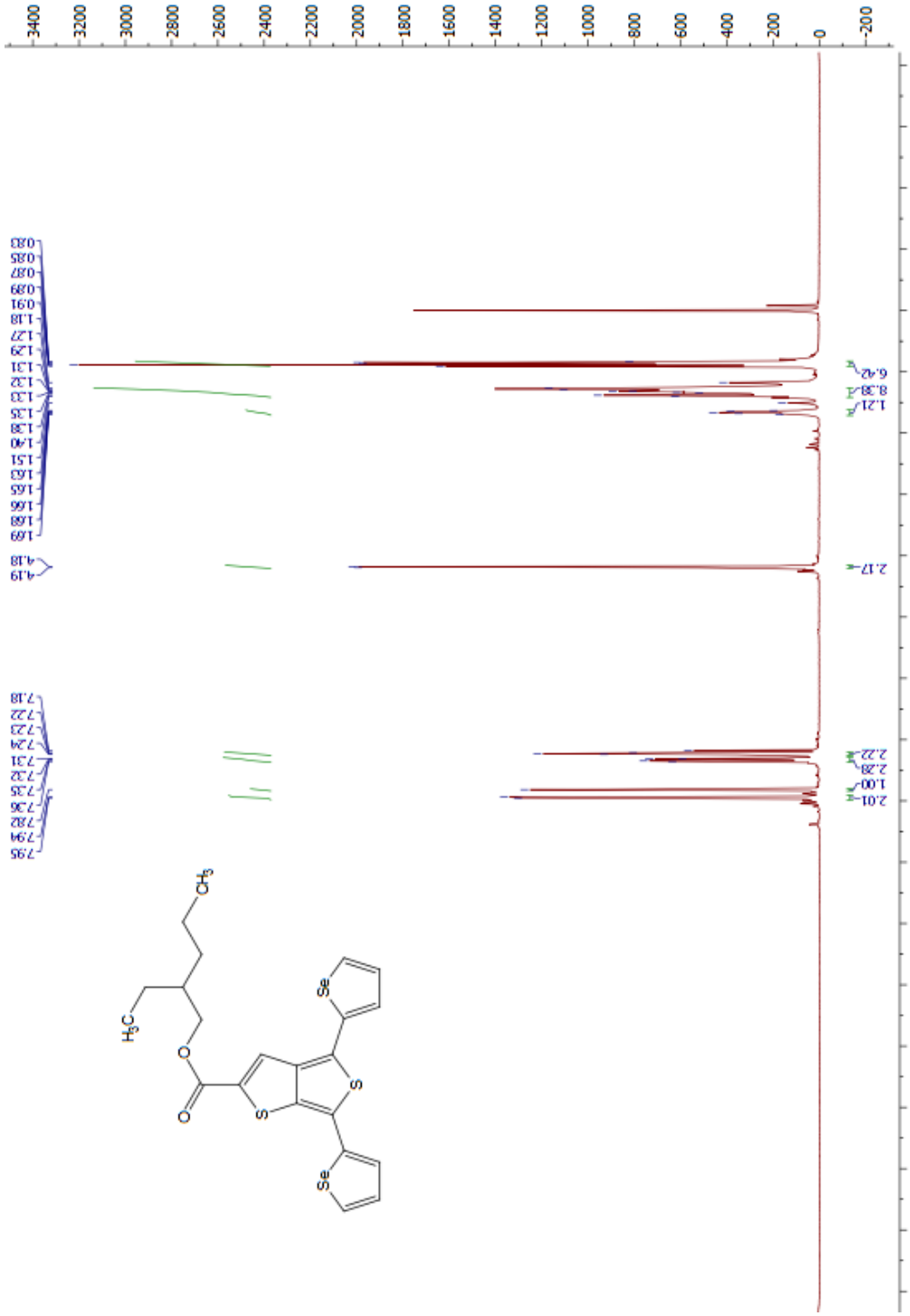

Figure A.17 ^{1}H NMR Spectrum of 2-Ethylhexyl 4,6-di(selenophene-2-yl)thieno[3,4-b]thiophene-2-carboxylate

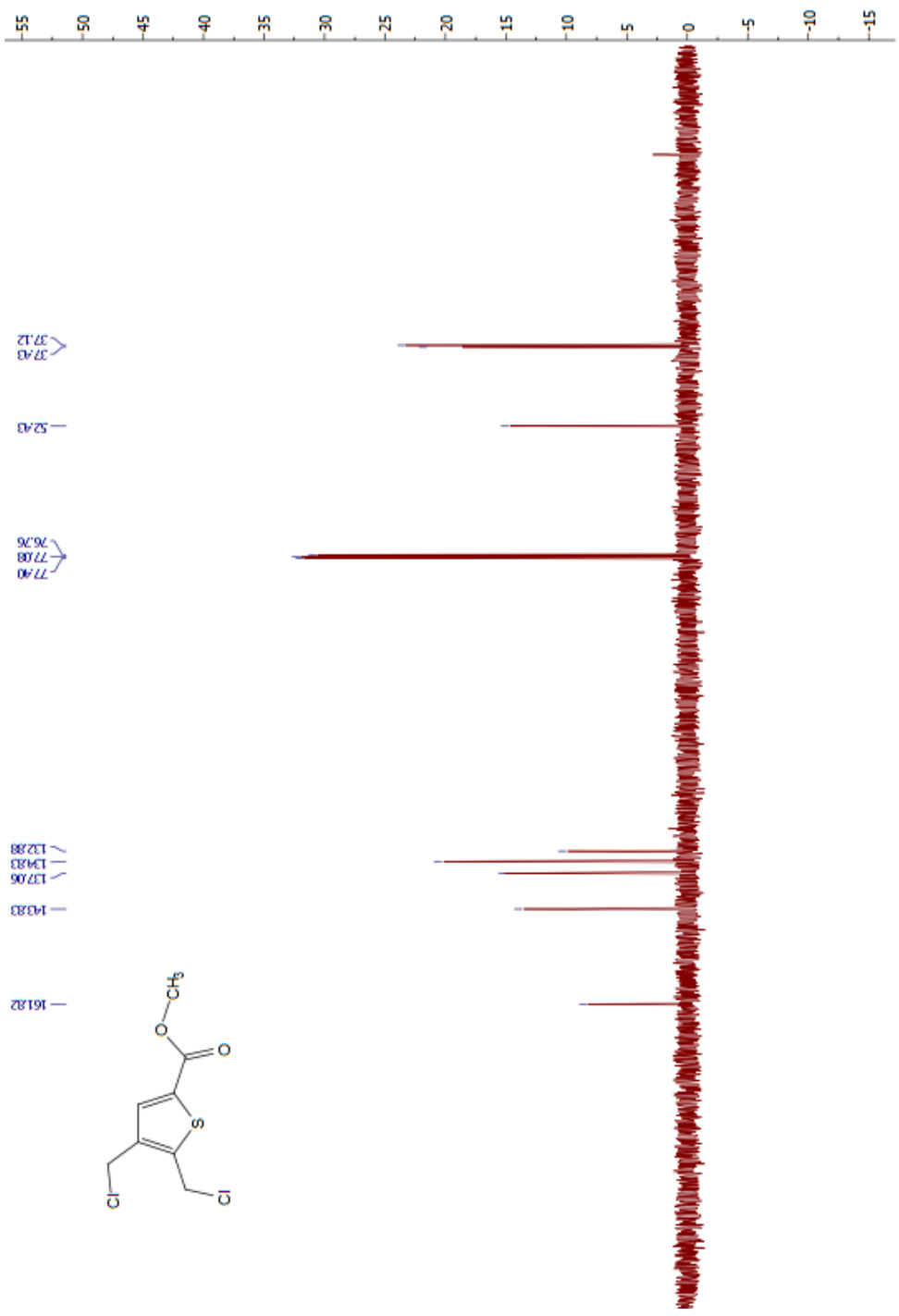

Figure A.18 ^{13}C NMR Spectrum of Methyl 2, 3 –bis (chloromethyl) thiophene-2-carboxylate

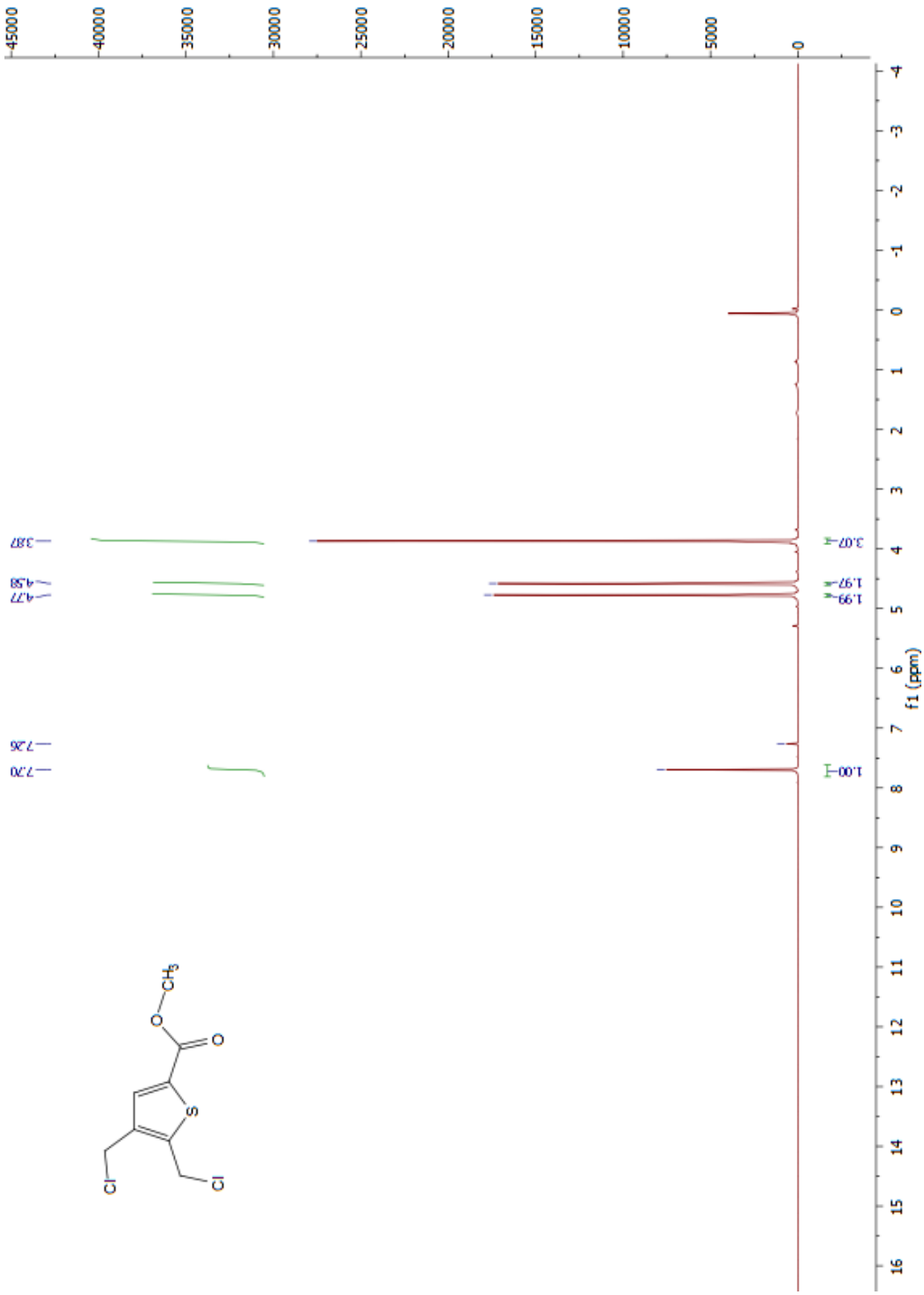

Figure A.19 ^{1}H NMR Spectrum of Methyl 2, 3 –bis (chloromethyl) thiophene-2-carboxylate

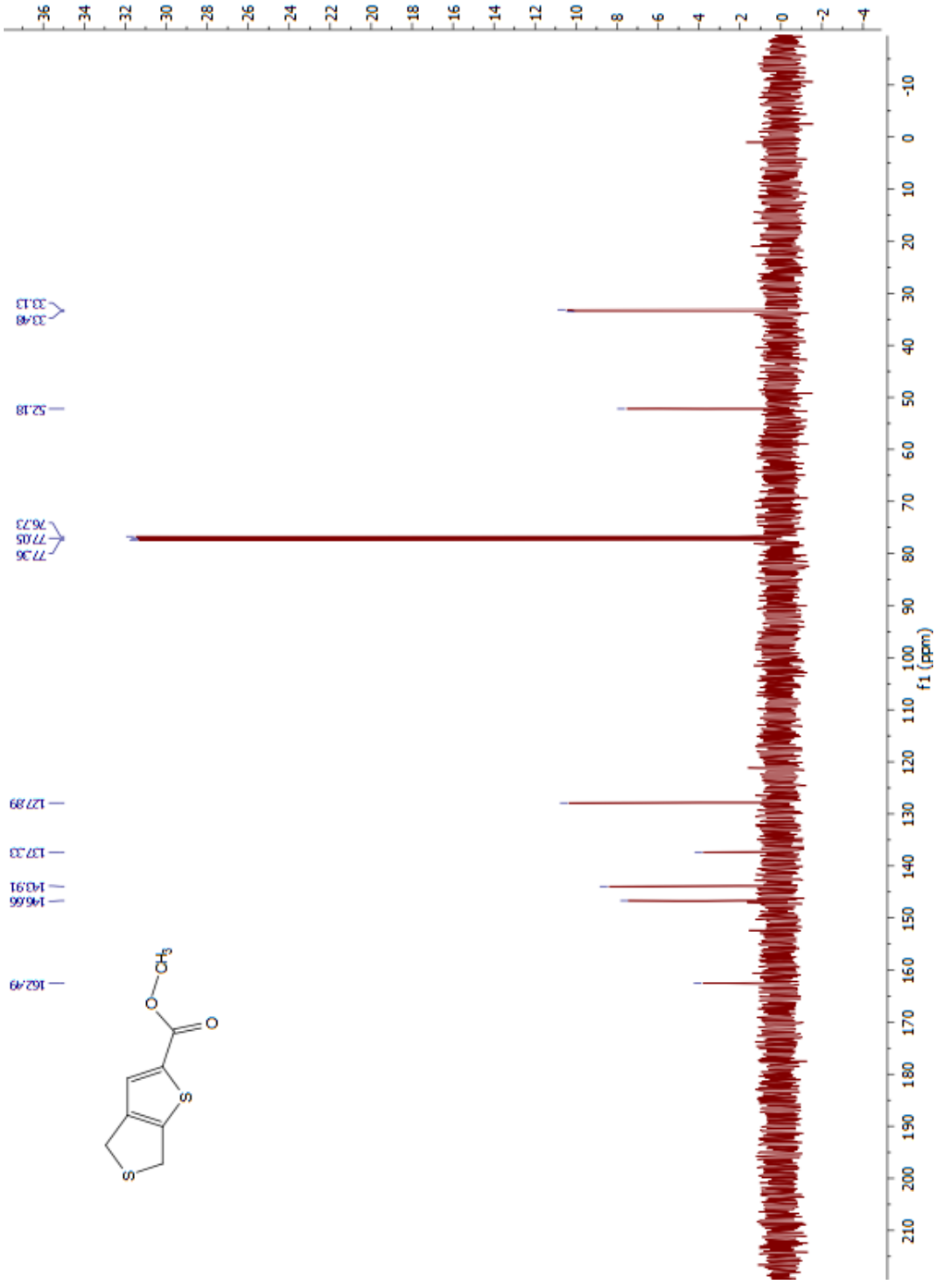

Figure A.20 ^{13}C NMR Spectrum of Methyl 4, 6-dihydrothieno[3,4-b]thiophene-2-carboxylate

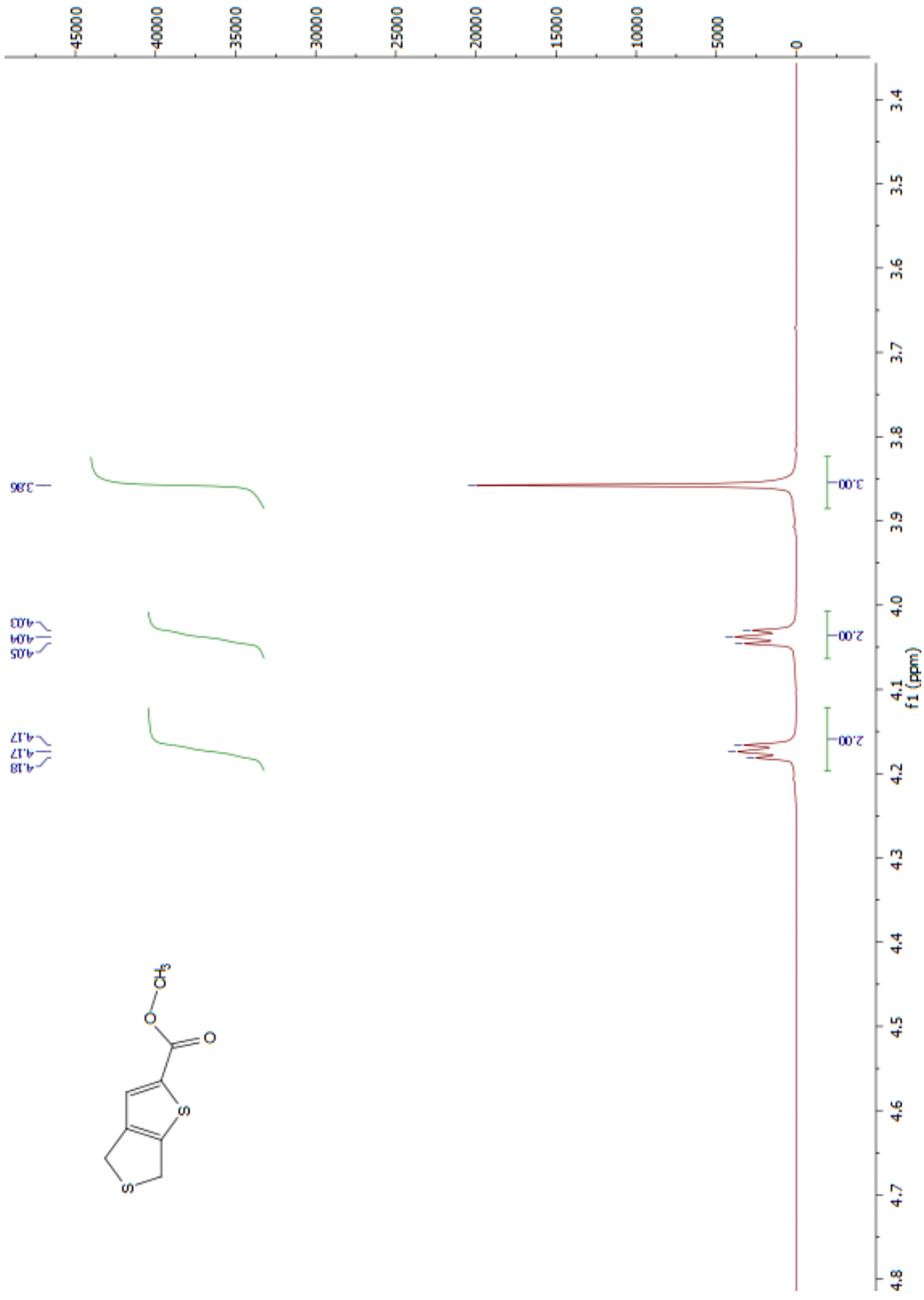

Figure A.21 ^{13}H NMR Spectrum of Methyl 4, 6-dihydrothieno[3,4-b]thiophene-2-carboxylate

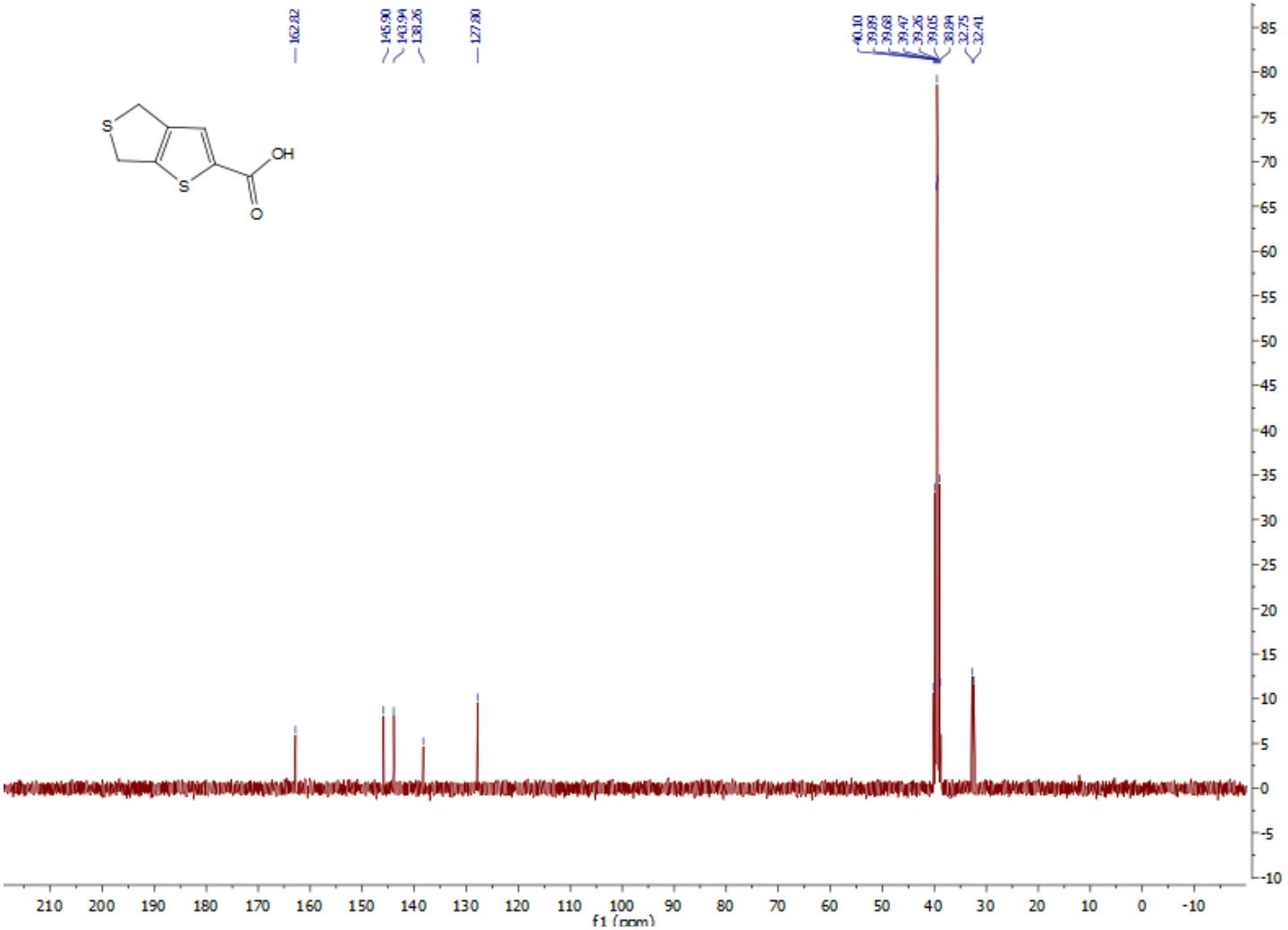

Figure A.22 ^{13}C NMR Spectrum of Methyl 4, 6-dihydrothieno[3,4-b]thiophene-2-carboxylic acid

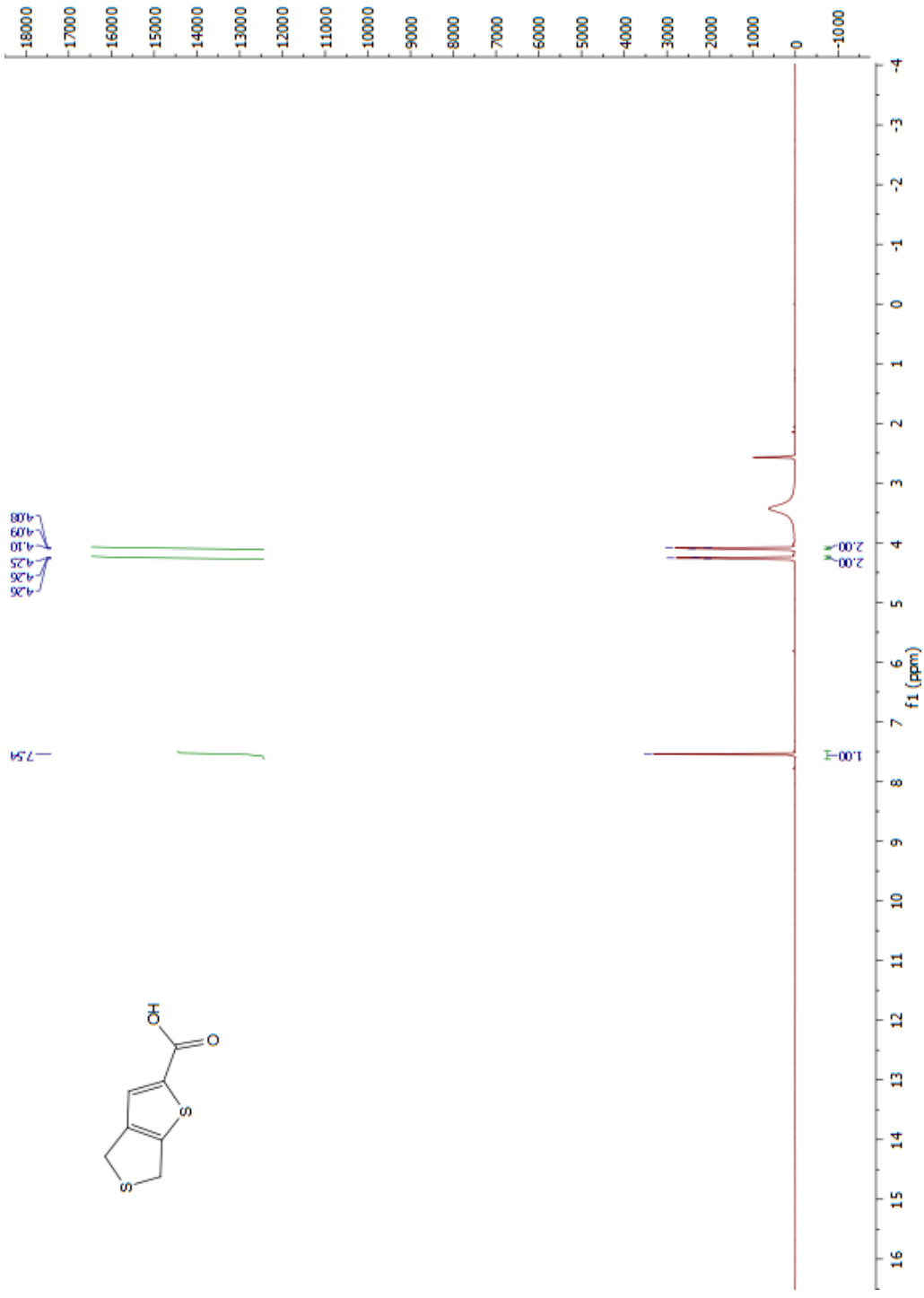

Figure A.9 ^{1}H NMR Spectrum of 4,6-Dihydro[3,4-b]thiophene-2-carboxylic acid

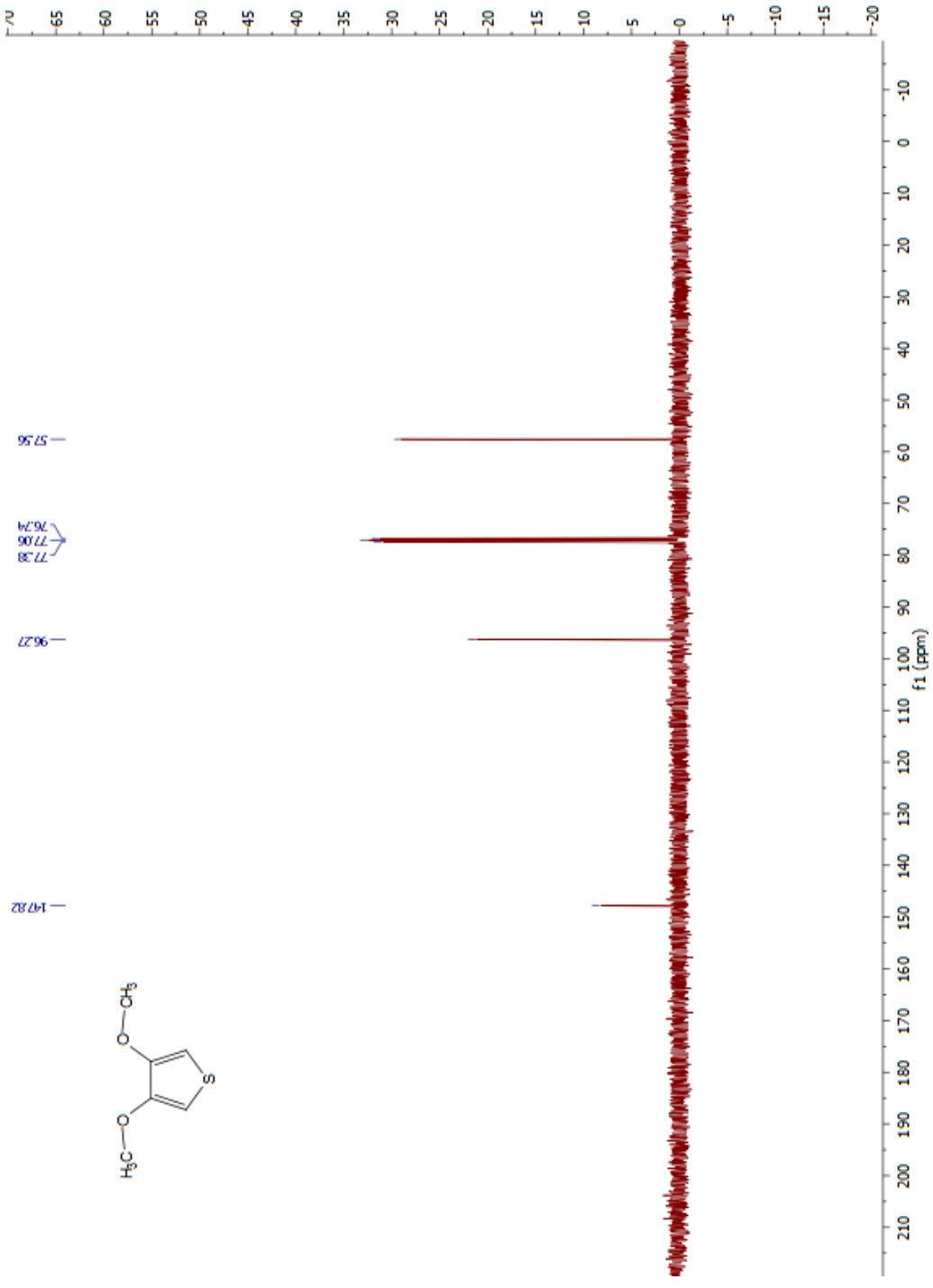

Figure A.24 ^{13}C NMR Spectrum of 3,4-Dimethoxythiophene

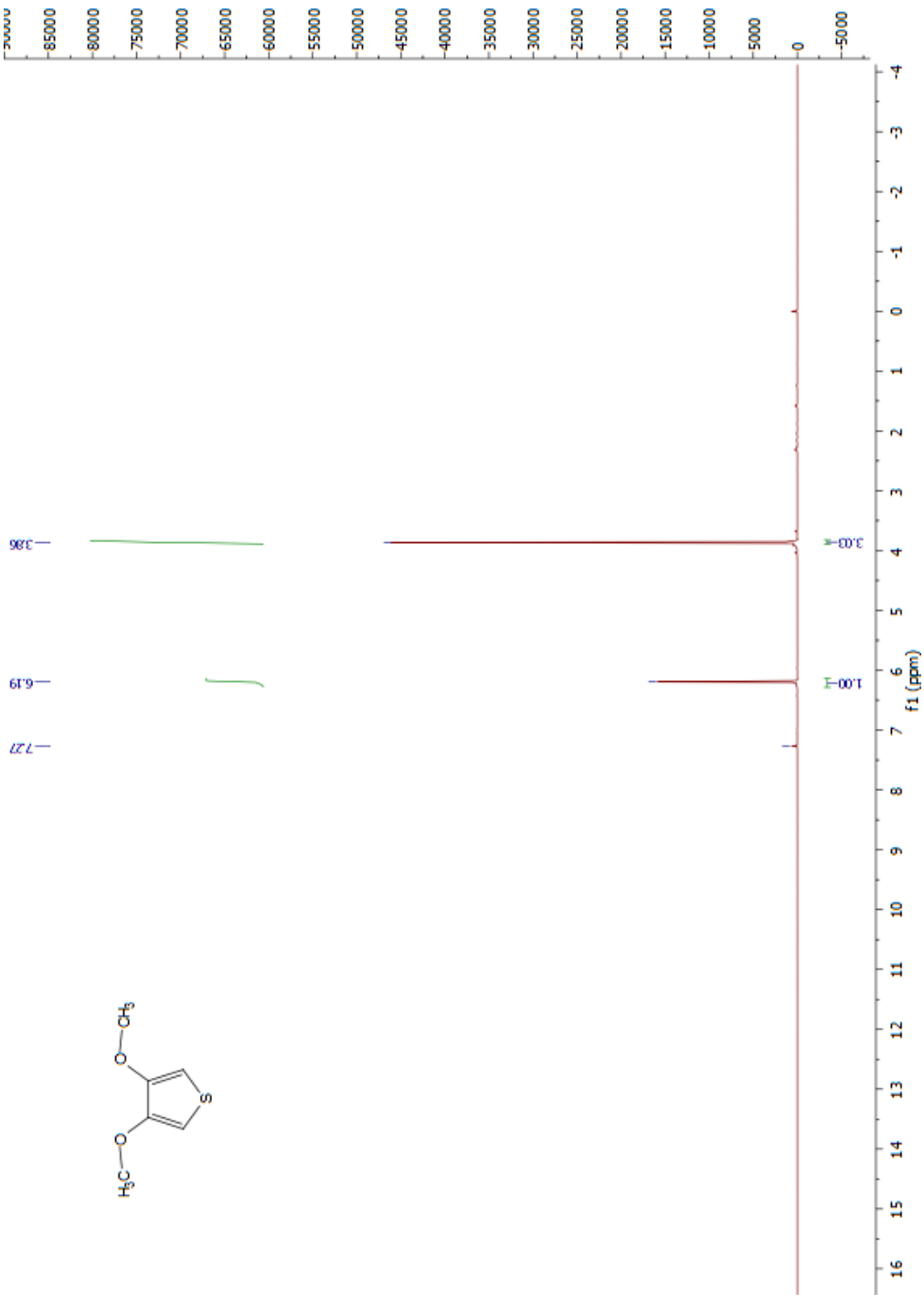

Figure A.25 ^{13}H NMR Spectrum of 3,4-Dimethoxythiophene

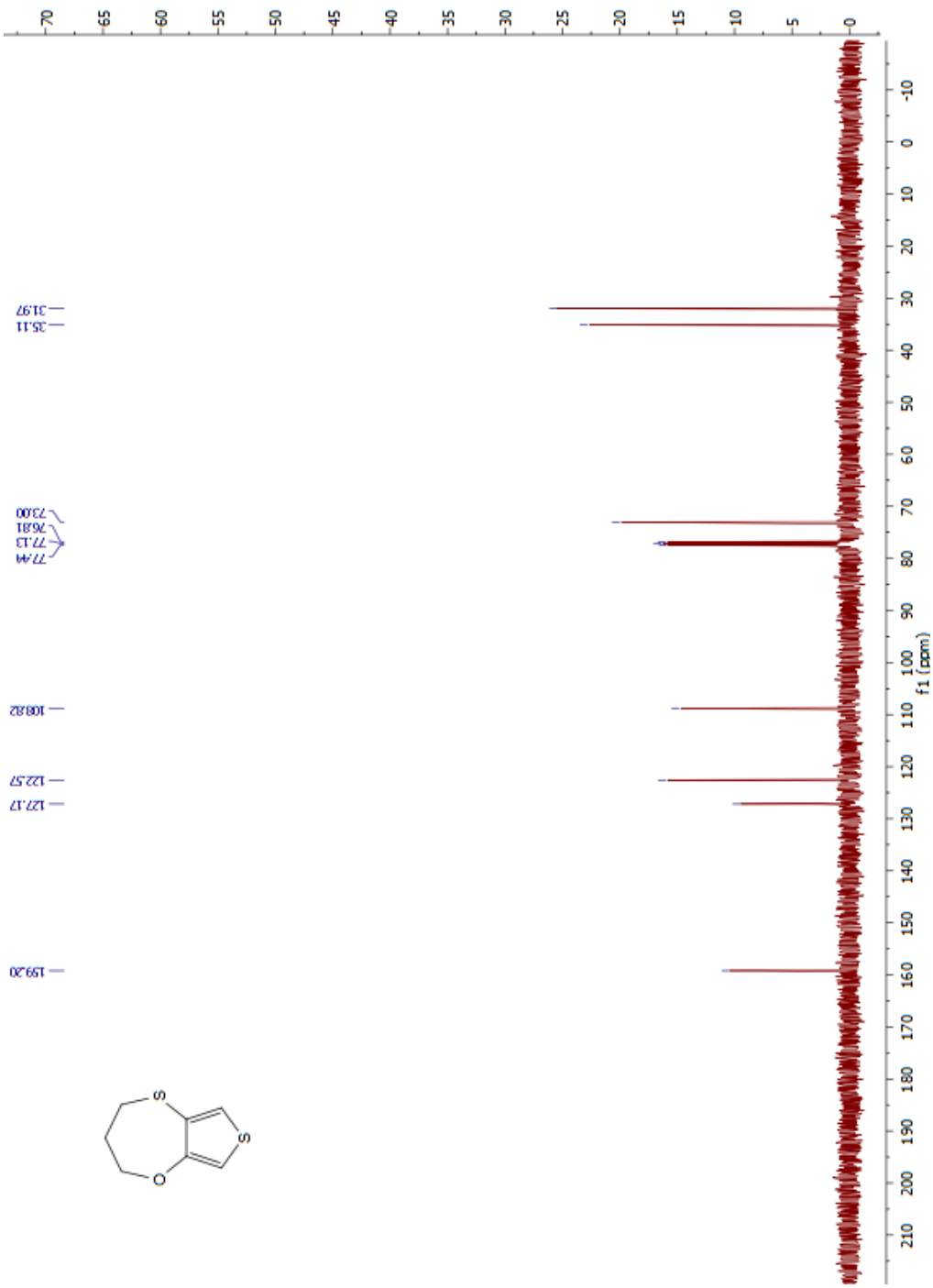

Figure A.26 ^{13}C NMR Spectrum of 3,4-Dihydro-2H-thieno[3,4-b][1,4]oxathiepine

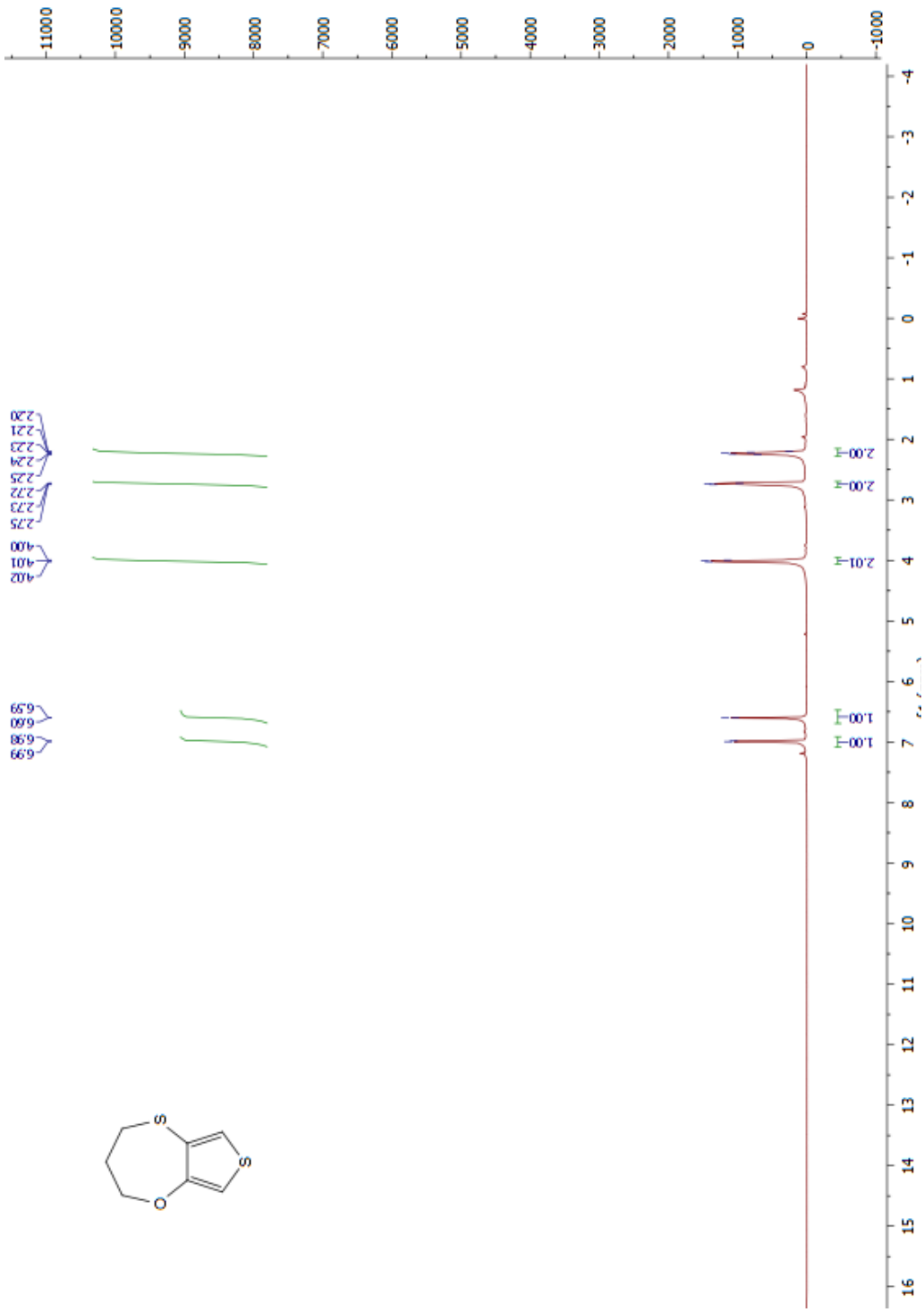

Figure A.27 ^{1}H NMR Spectrum of 3,4-Dihydro-2H-thieno[3,4-b][1,4]oxathiepine

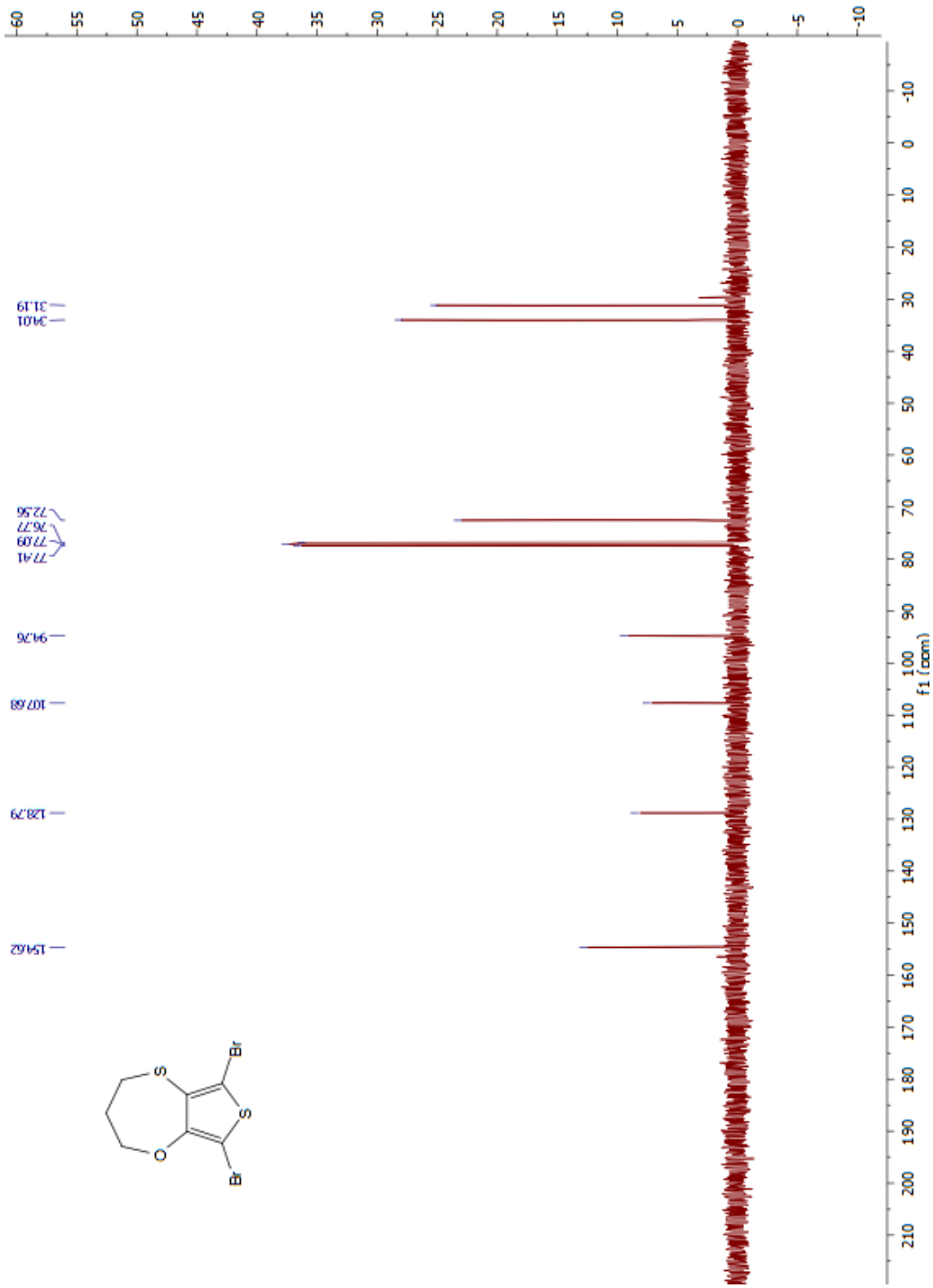

Figure A.28 ^{13}C NMR Spectrum of 6,8–Dibromo-3,4-dihydro-2H-thieno[3,4b][1,4] oxathiephine

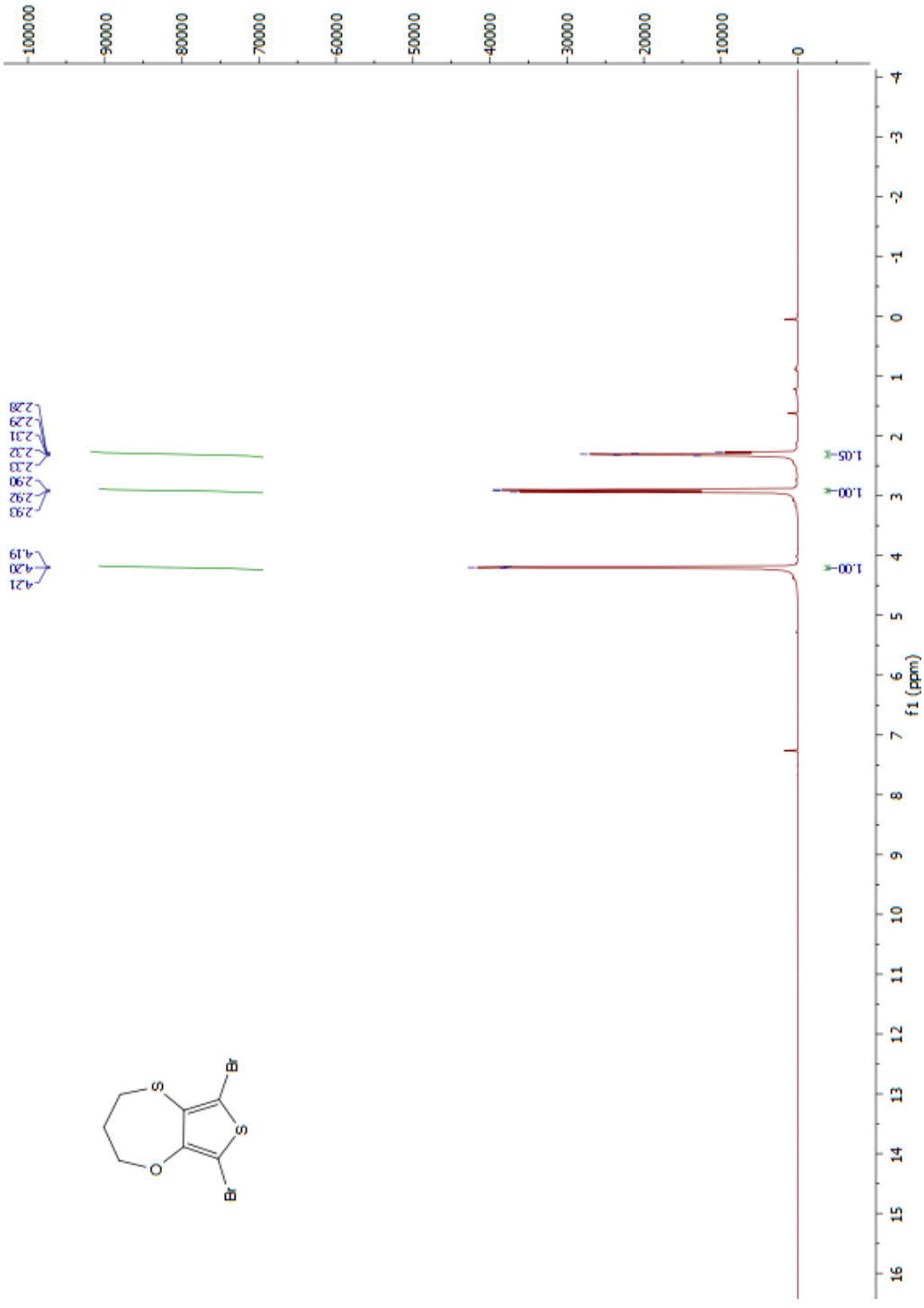

Figure A.29 ^{1}H NMR Spectrum of 6,8–Dibromo-3,4-dihydro-2H-thieno[3,4b][1,4] oxathiephine

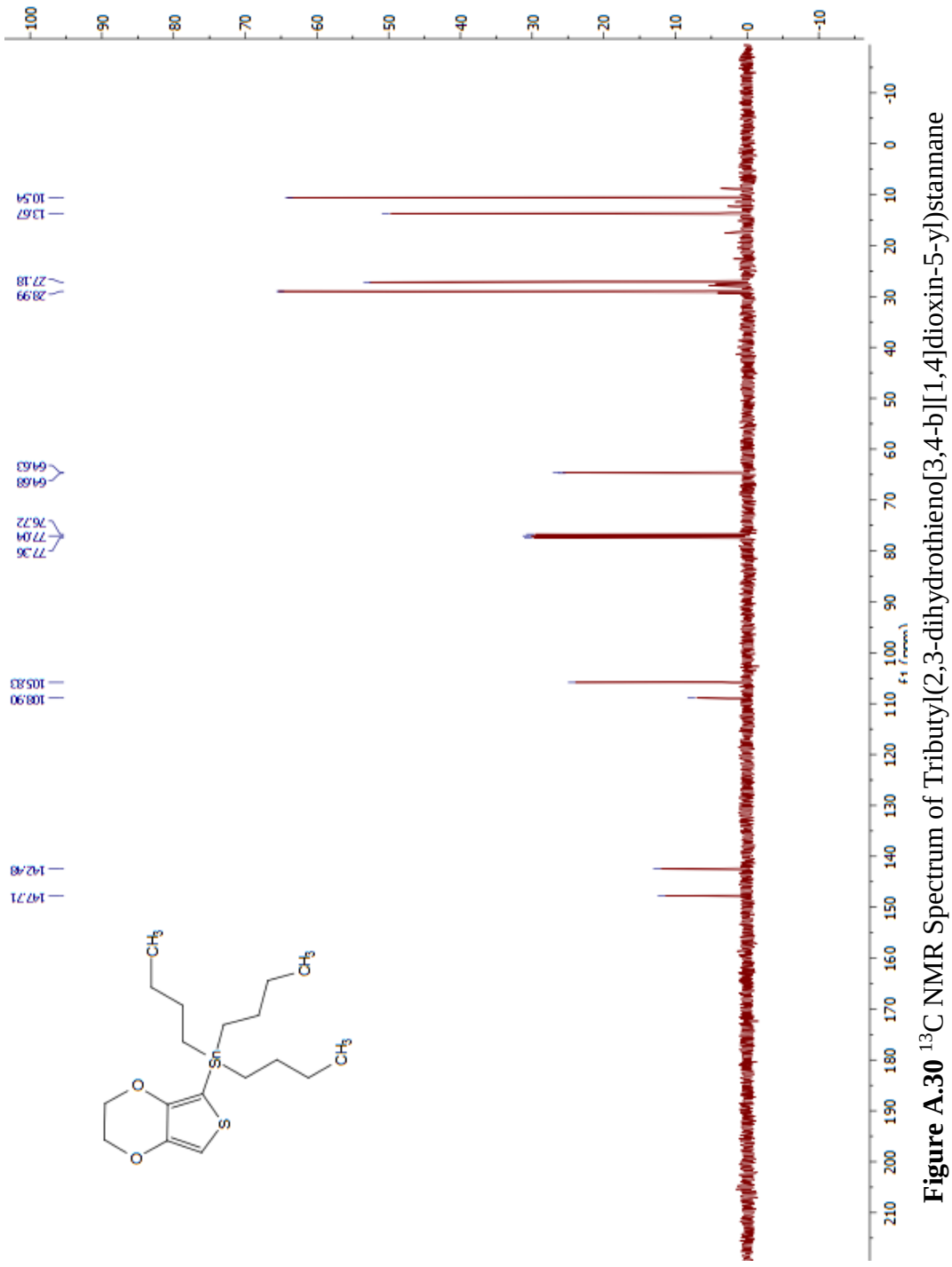

Figure A.30 ^{13}C NMR Spectrum of Tributyl(2,3-dihydrothieno[3,4-b][1,4]dioxin-5-yl)stannane

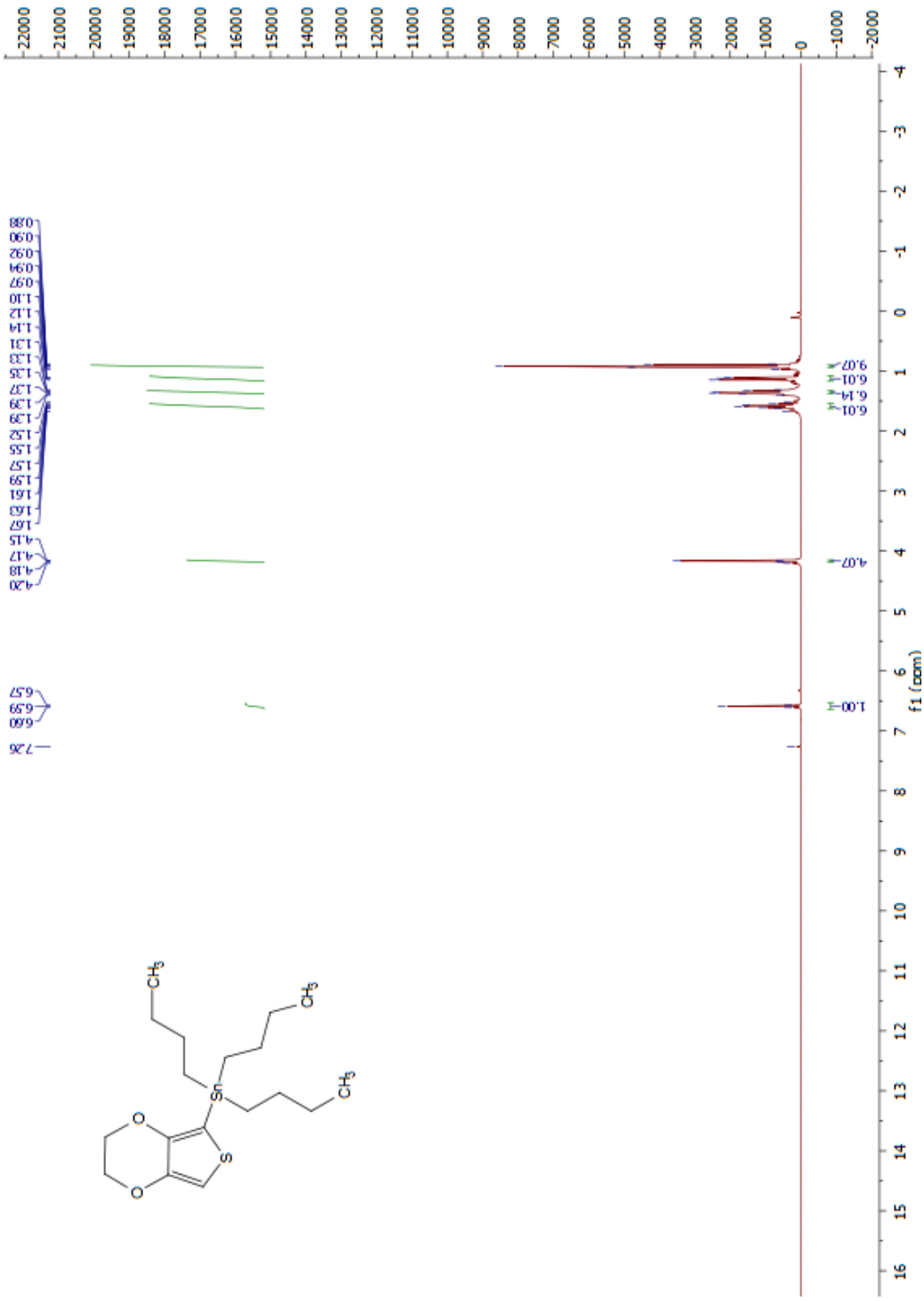

Figure A.10 ^{1}H NMR Spectrum of Tributyl(2,3-dihydrothieno[3,4-b][1,4]dioxin-5-yl)stannane

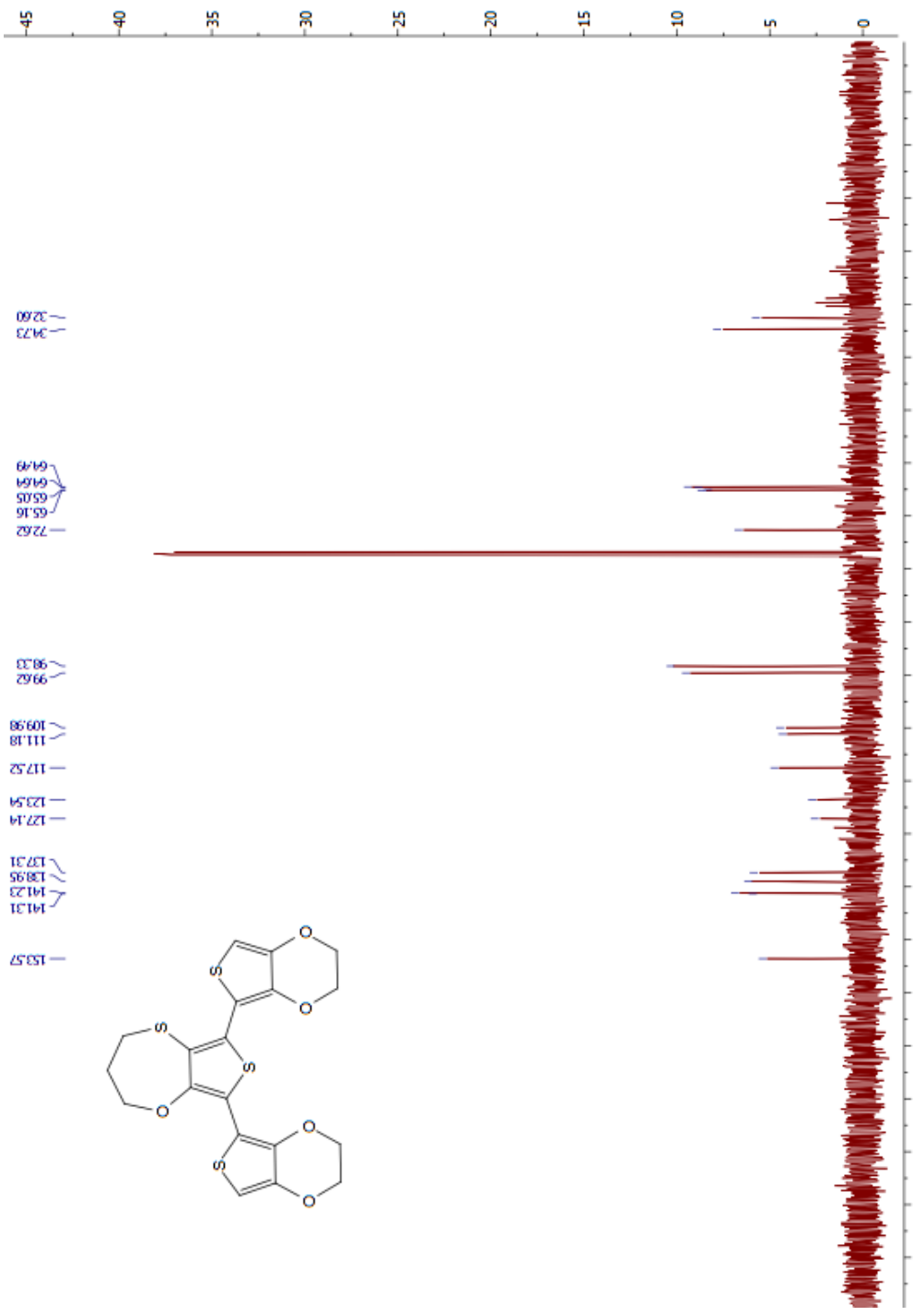

Figure A.11 ^{13}C NMR Spectrum of 6,8-Bis(2,3-dihydrothieno[3,4-b][1,4]dioxin-5-yl)-3,4-dihydro-2H-thieno[3,4-b][1,4]oxathiepine

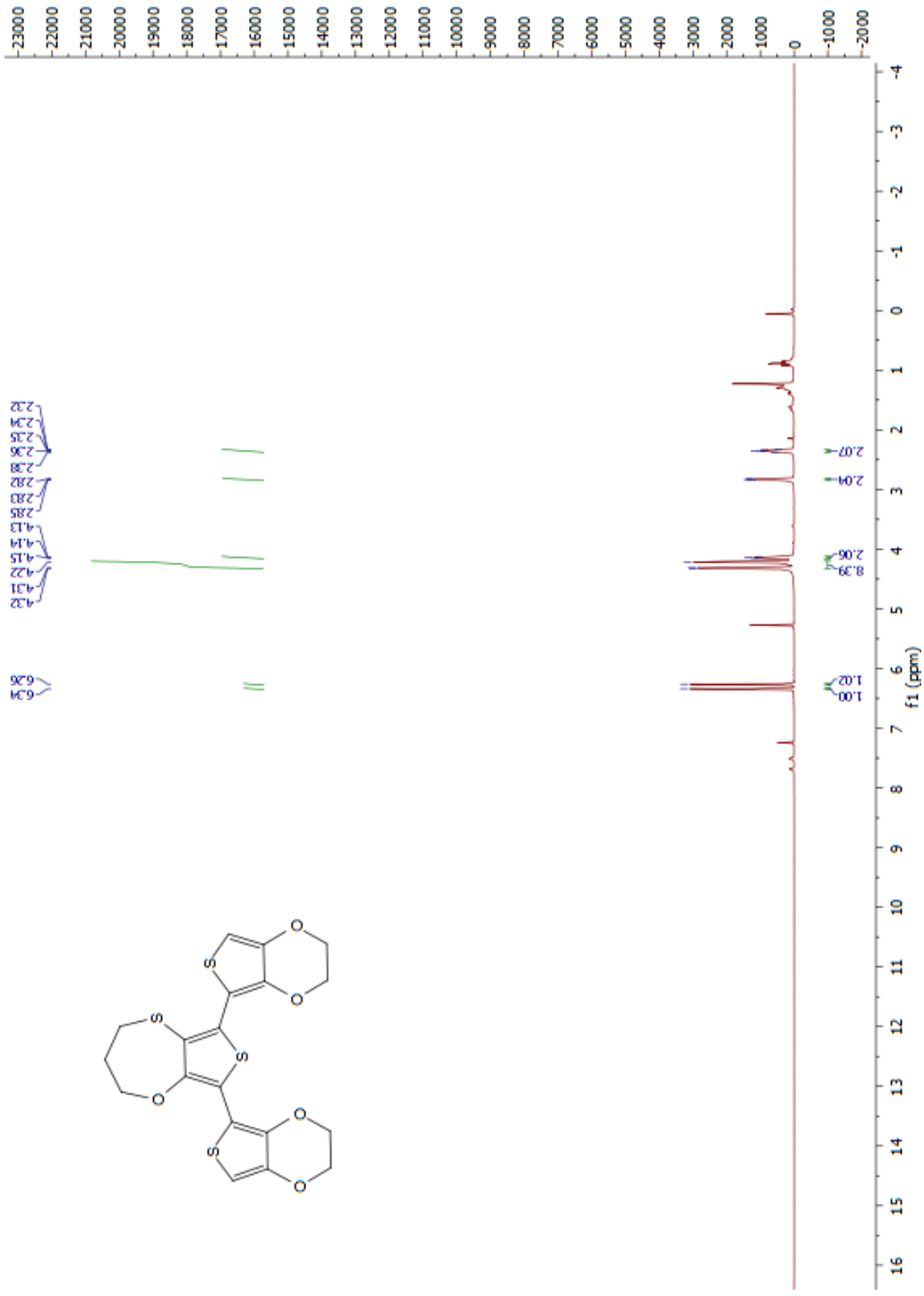

Figure A.33 ^{1}H NMR Spectrum of 6,8-Bis(2,3-dihydrothieno[3,4-b][1,4]dioxin-5-yl)-3,4-dihydro-2H-thieno[3,4-b][1,4]oxathiepine

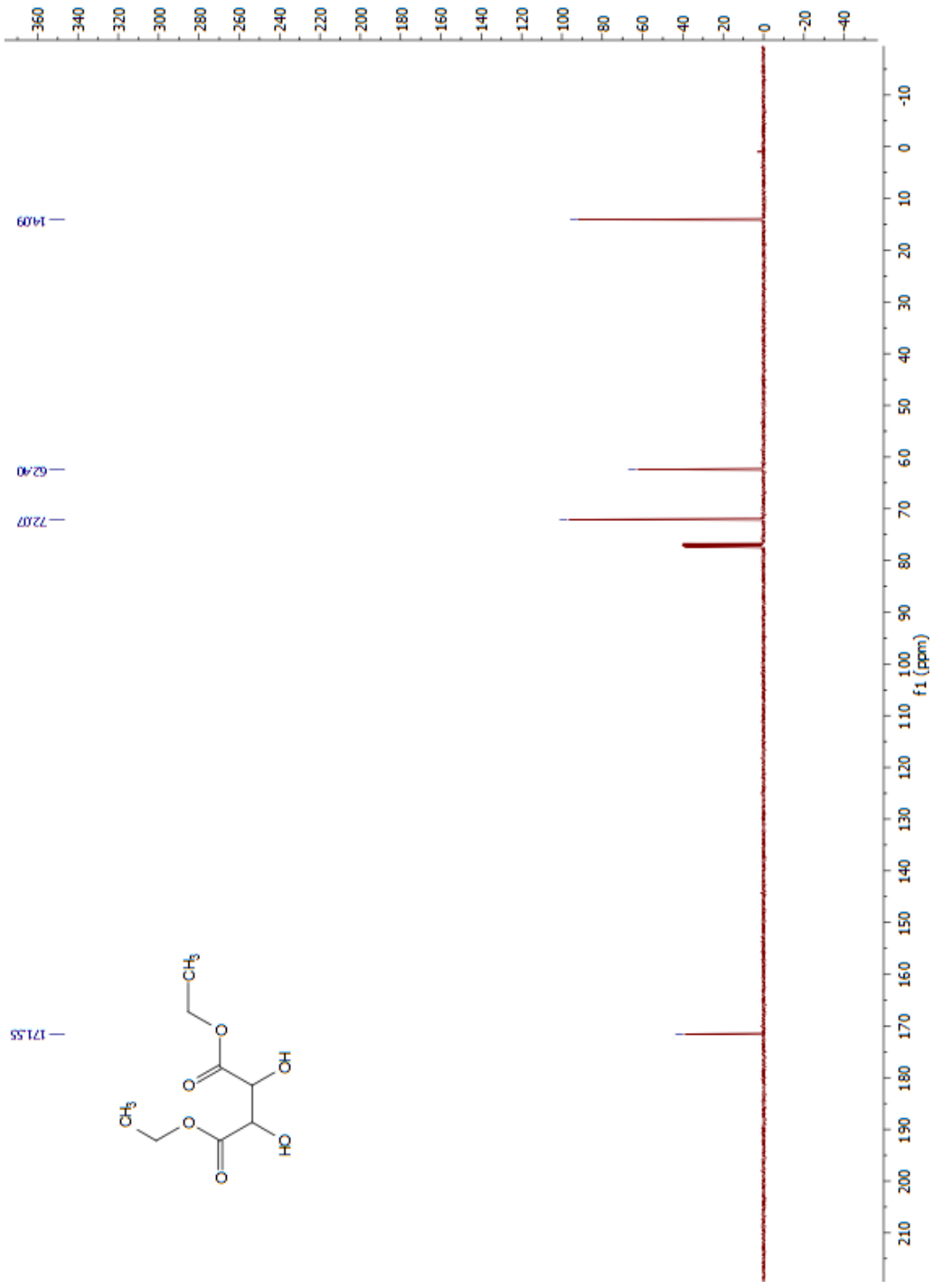

Figure A.12 ^{13}C NMR Spectrum of L(+)-Diethyl L-tartrate

Figure A.35 ^{1}H NMR Spectrum of L(+)-Diethyl L-tartrate

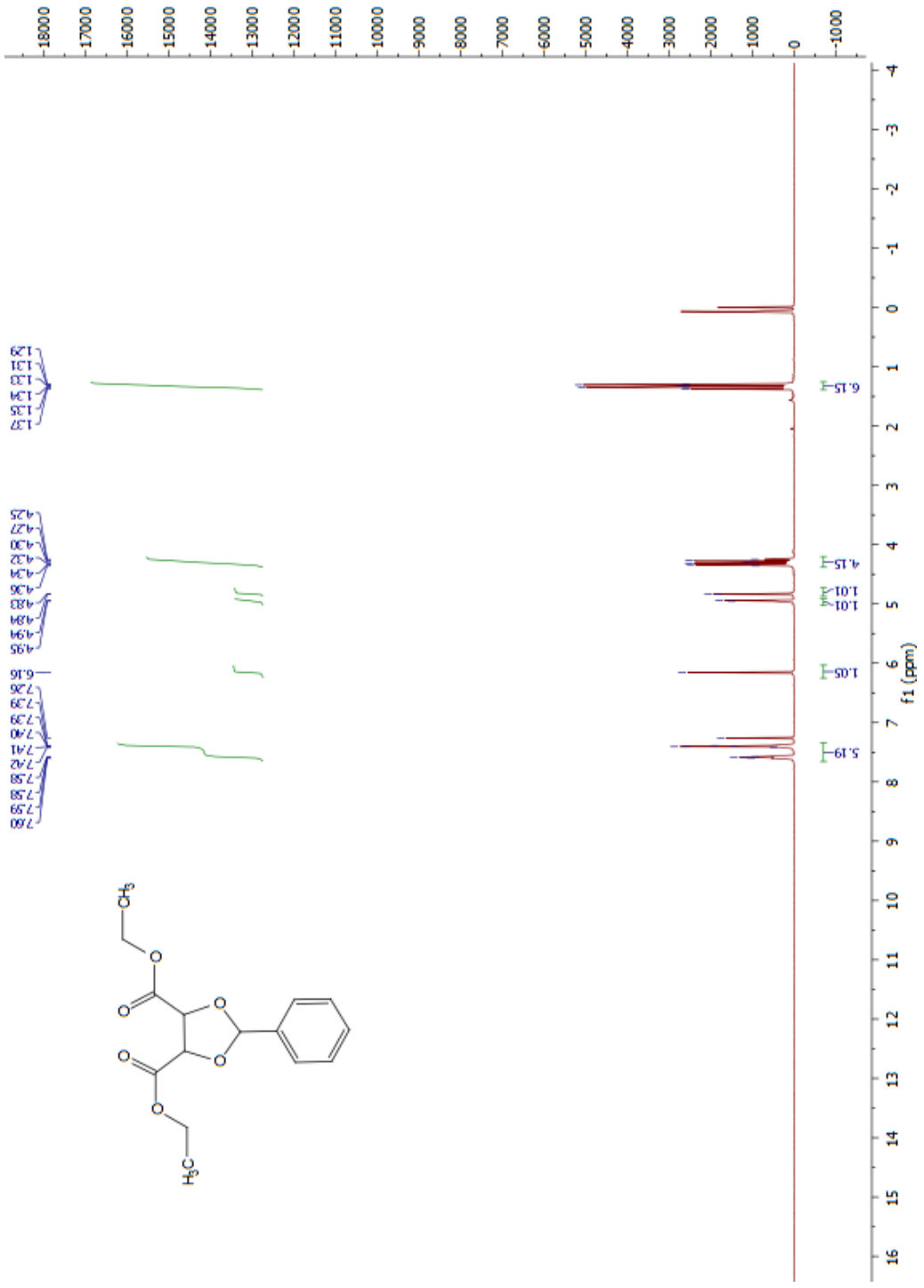

Figure A.36 ^{13}C NMR Spectrum of Diethyl 2-phenyl-1,3-dioxolane-4,5-dicarboxylate

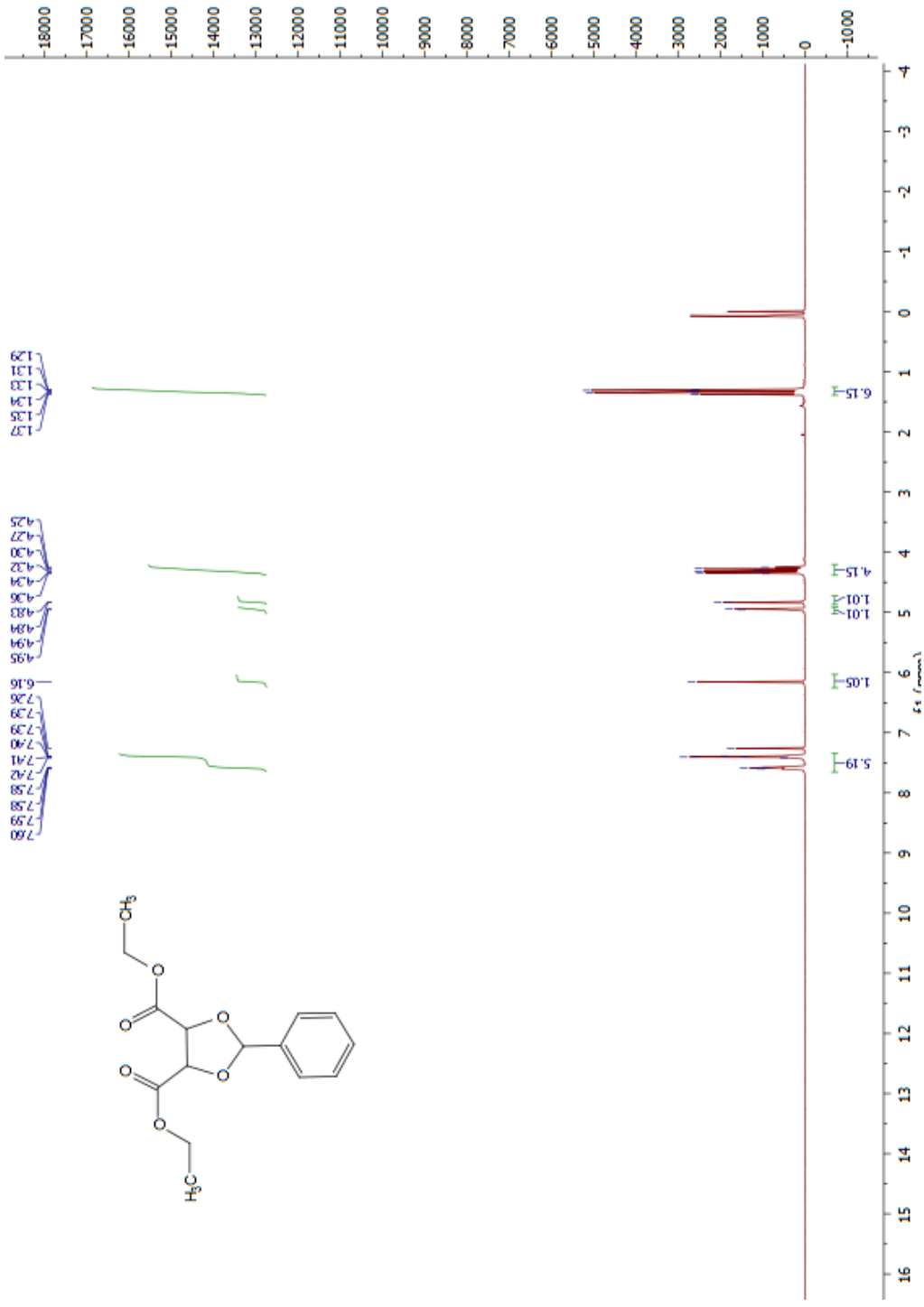

Figure A.3713 ^{1}H NMR Spectrum of Diethyl 2-phenyl-1,3-dioxolane-4,5-dicarboxylate

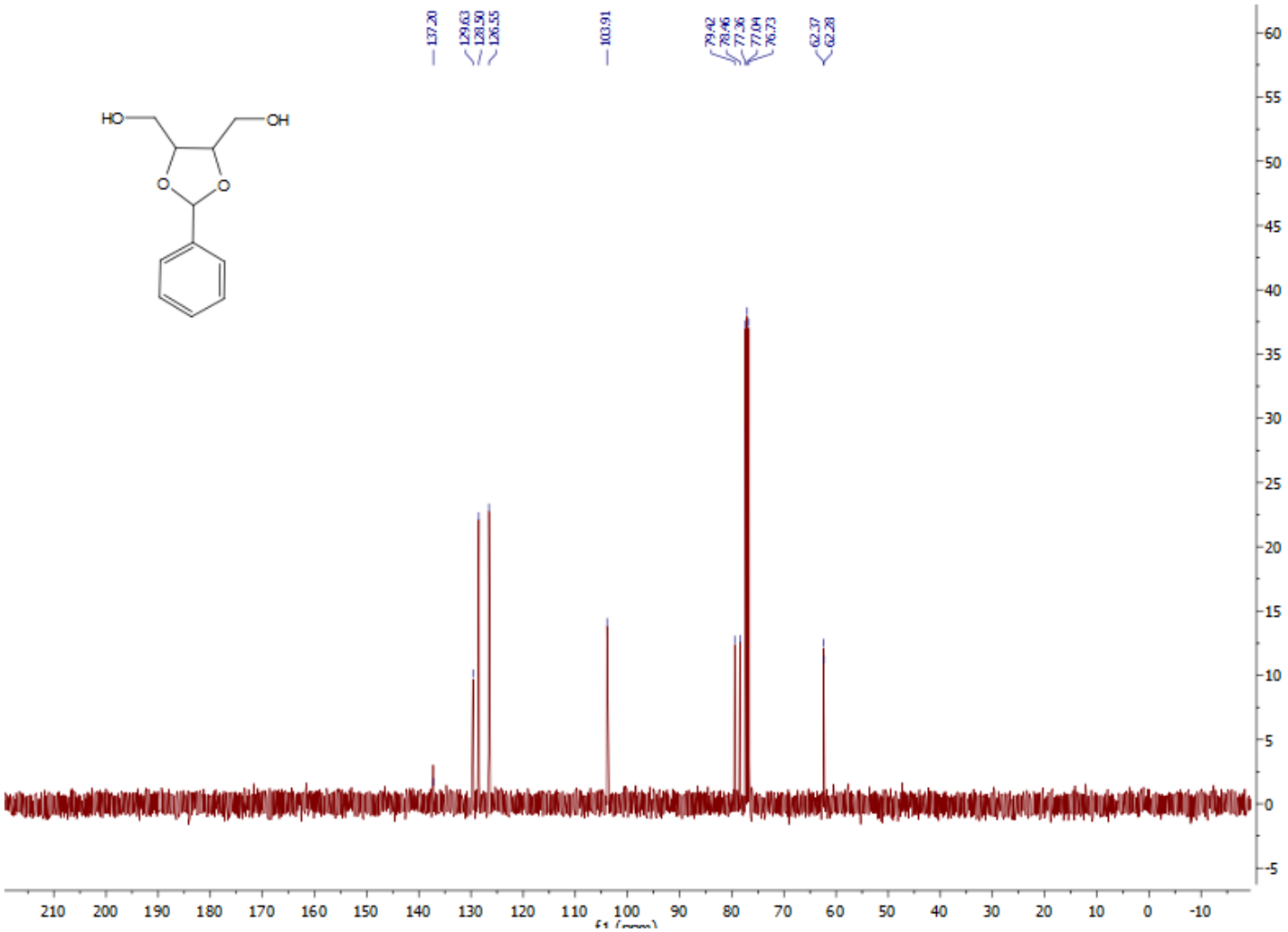

Figure A.38 ^{13}C NMR Spectrum of (2-phenyl-1,3-dioxolane-4,5-diyl)dimethanol

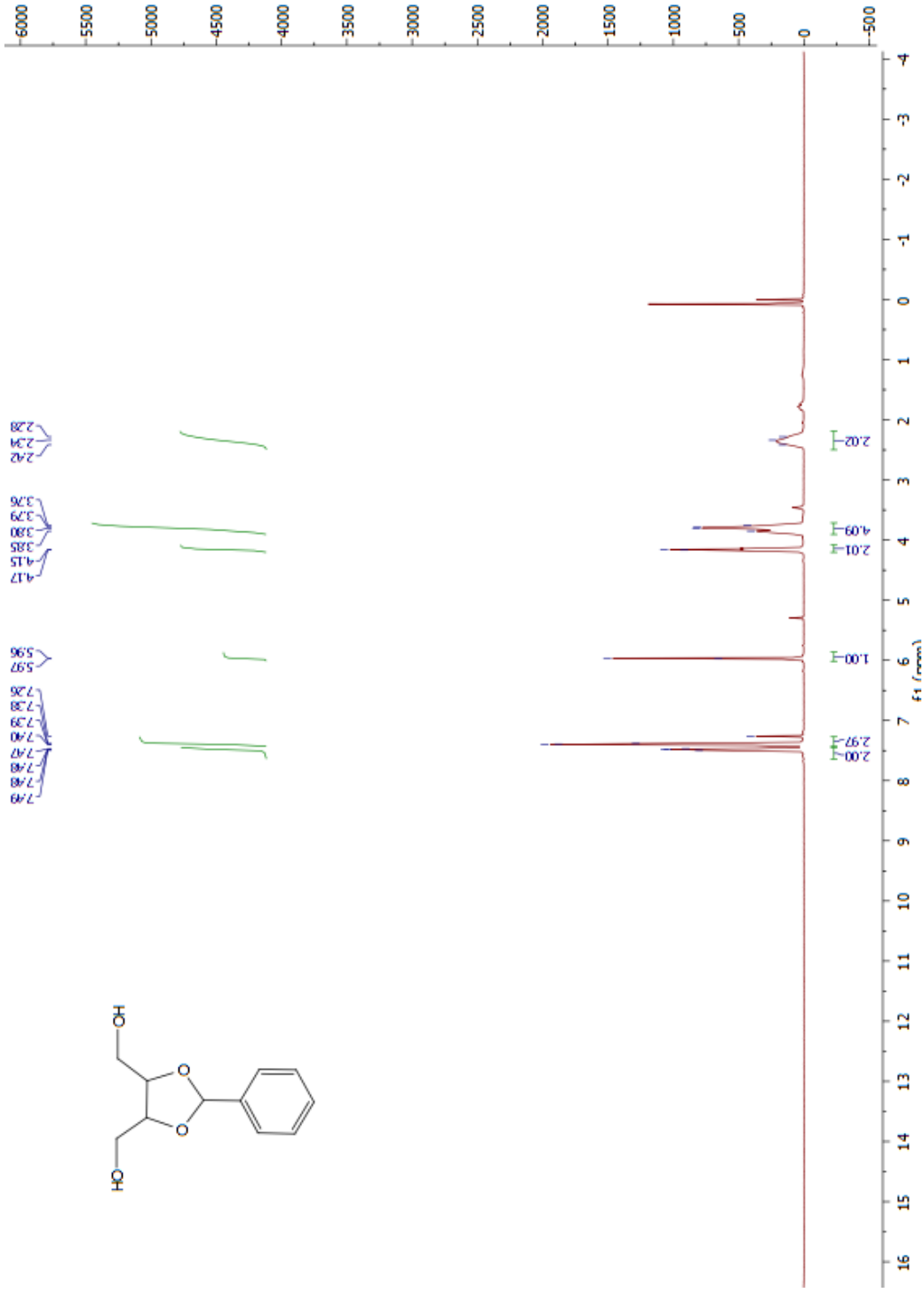

Figure A.39 ^{1}H NMR Spectrum of (2-phenyl-1,3-dioxolane-4,5-diyl)dimethanol

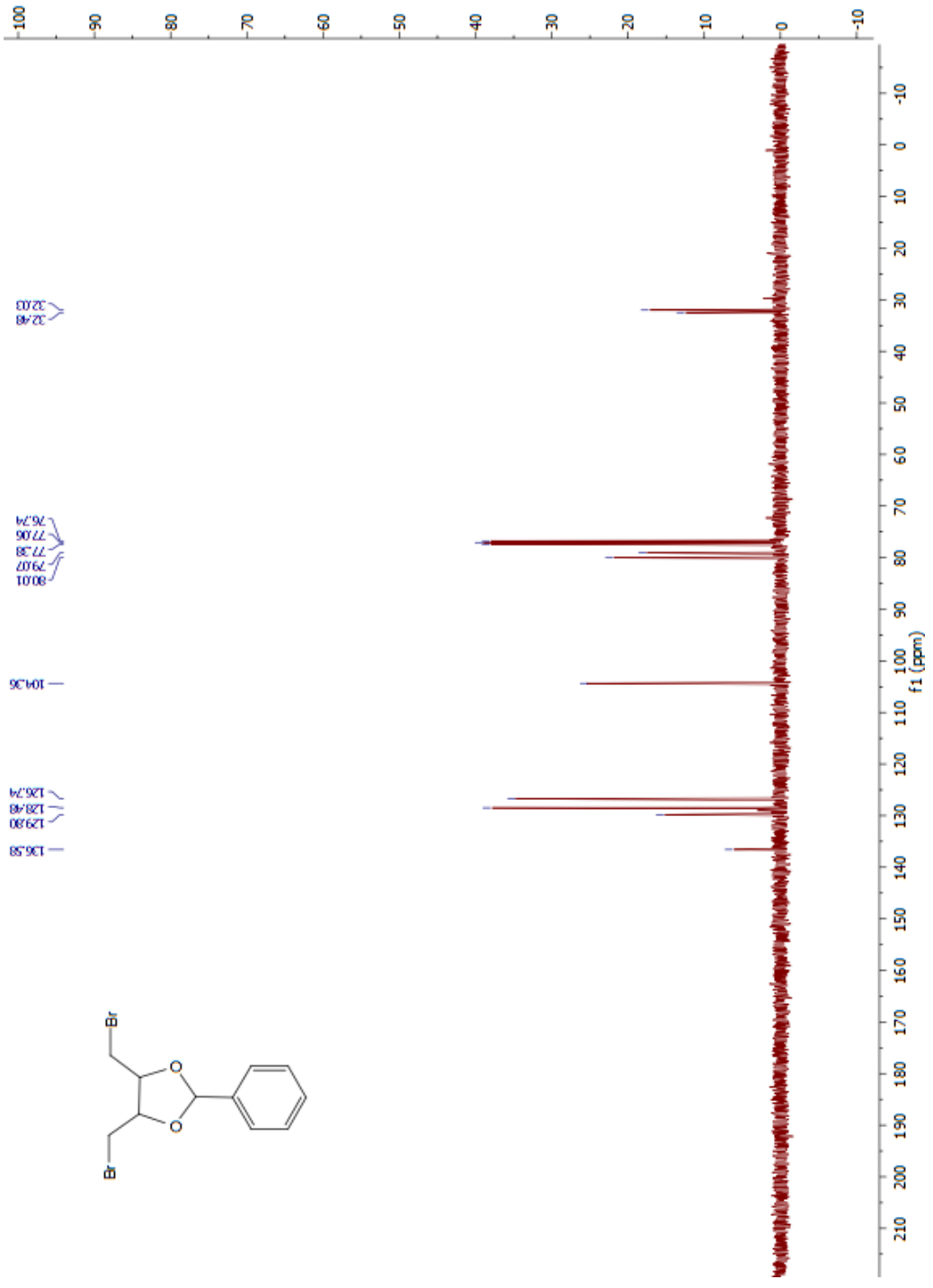

Figure A.40 ^{13}C NMR Spectrum of 4,5-Bis(bromomethyl)-2-phenyl-1,3-dioxolane

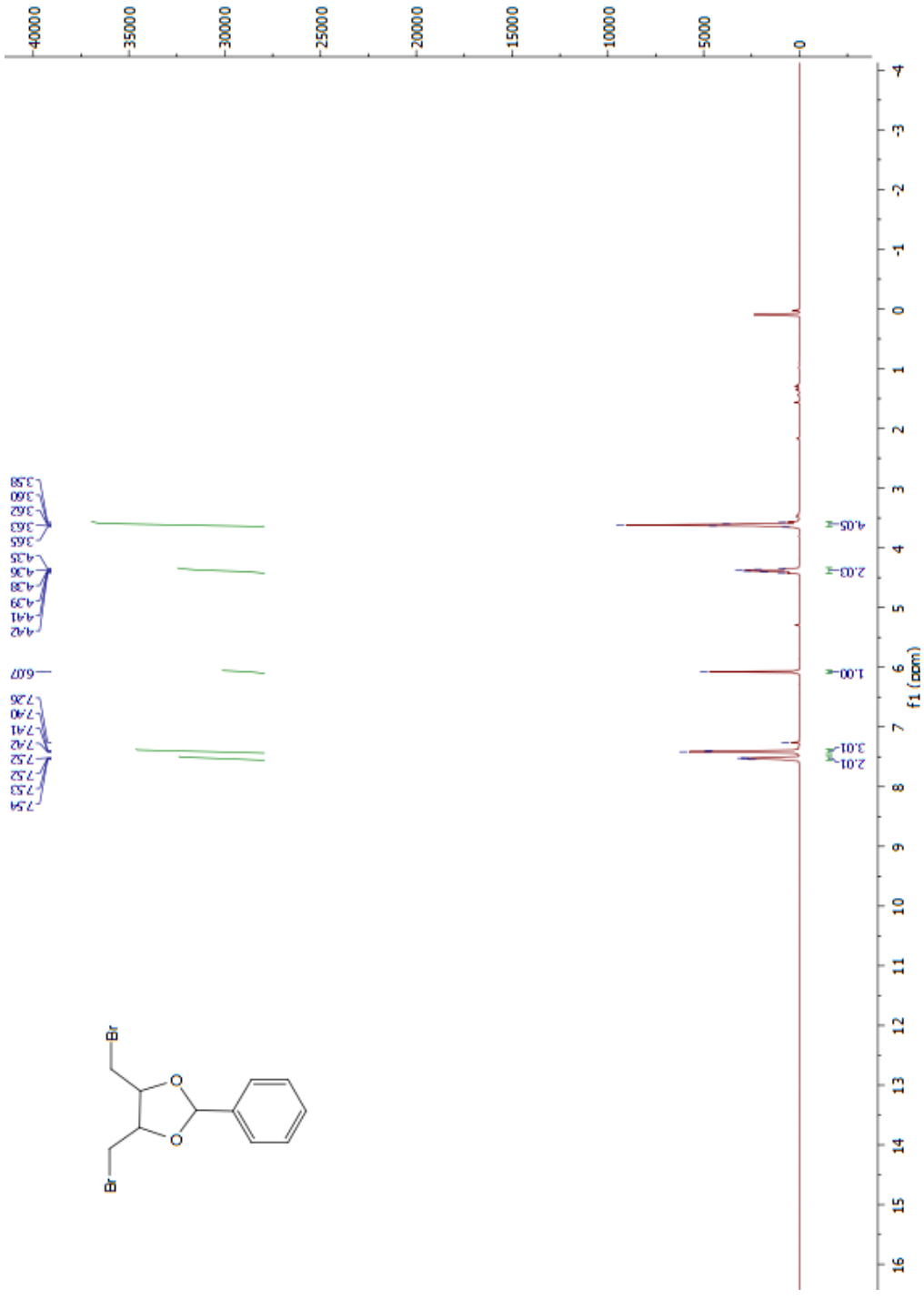

Figure A.41 ^{1}H NMR Spectrum of 4,5-Bis(bromomethyl)-2-phenyl-1,3-dioxolane

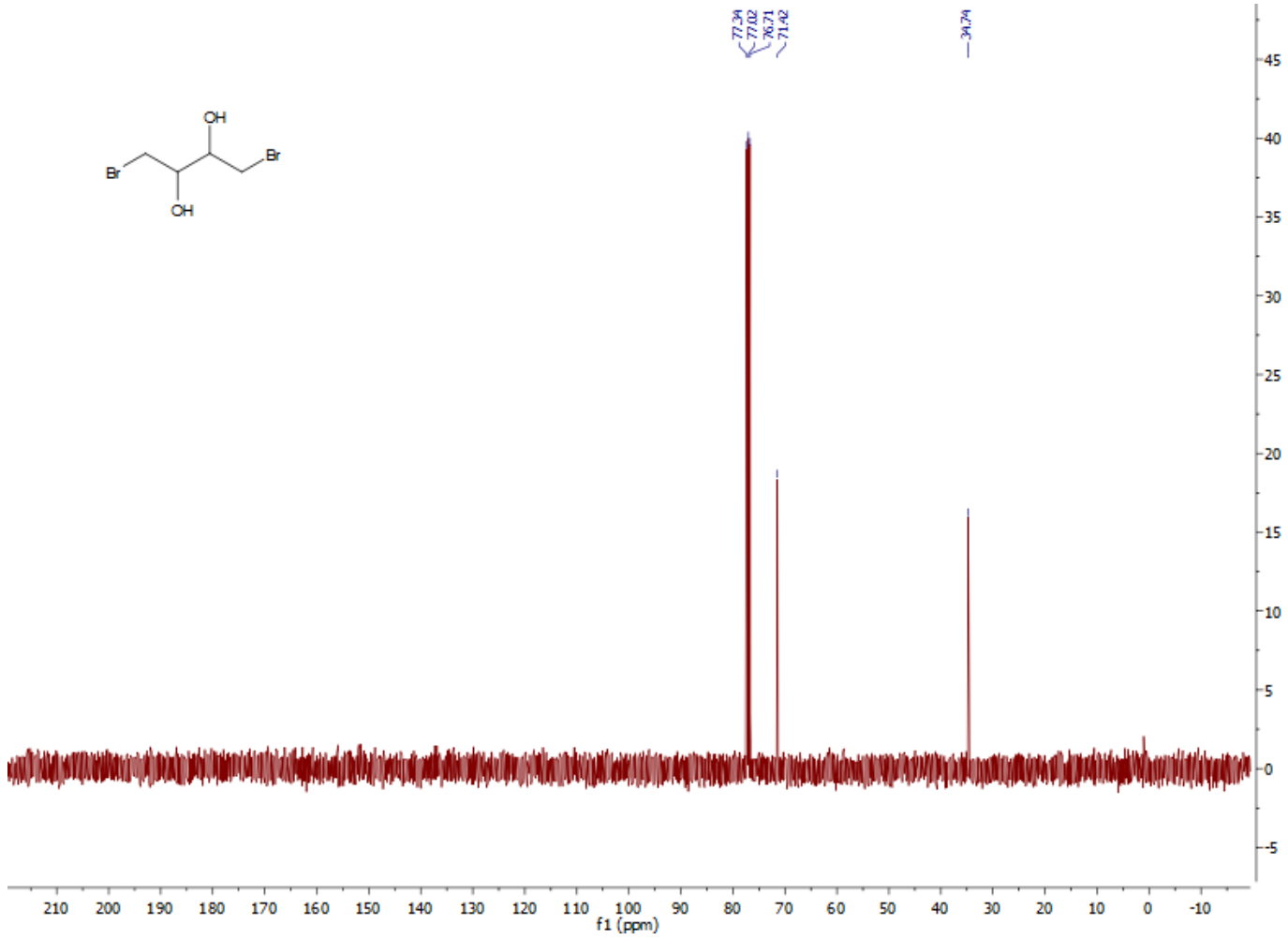

Figure A.14 ^{13}C NMR Spectrum of 1,4-Dibromobutane-2,3-diol

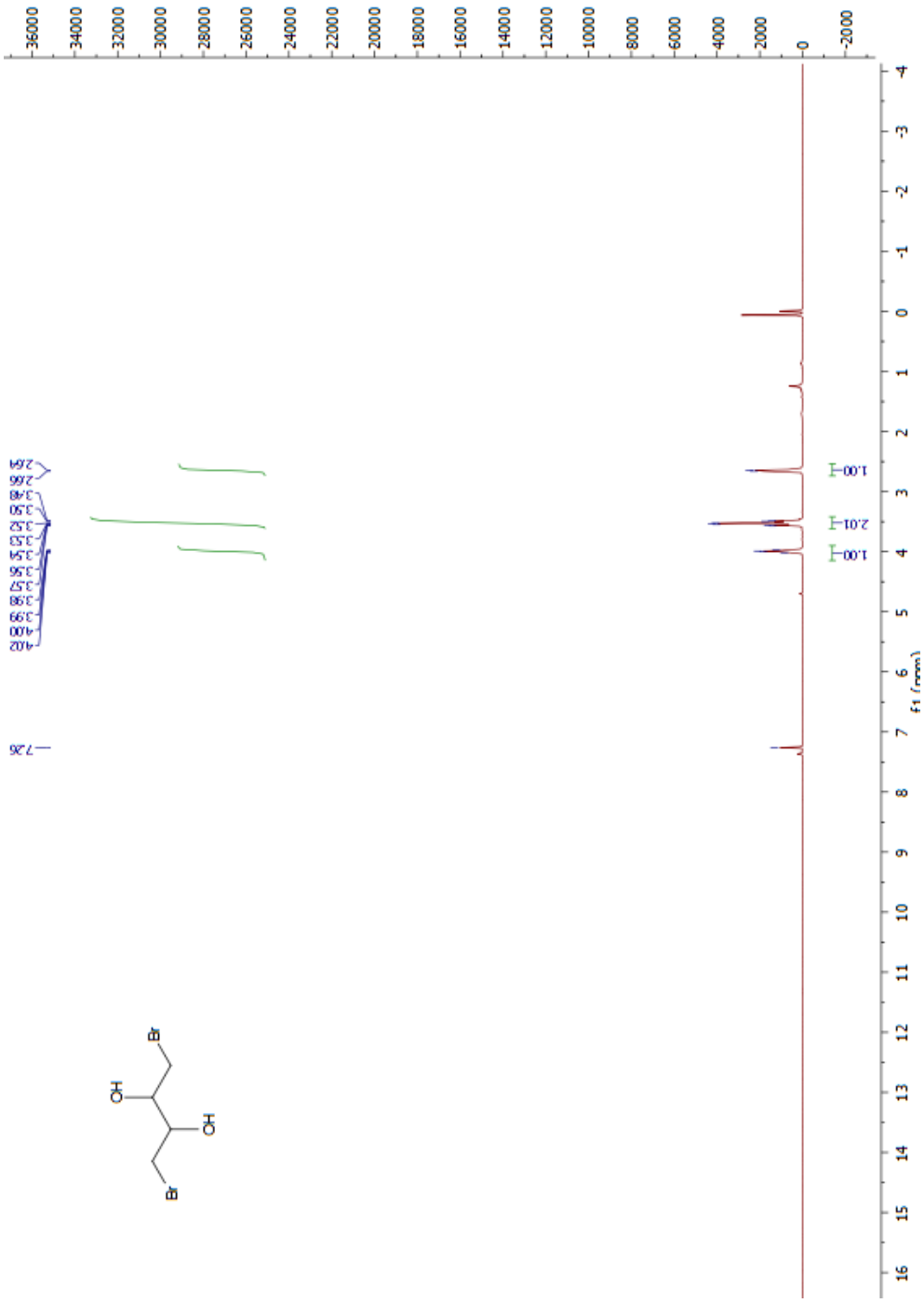

Figure A.43 ^{1}H NMR Spectrum of 1,4-Dibromobutane-2,3-diol

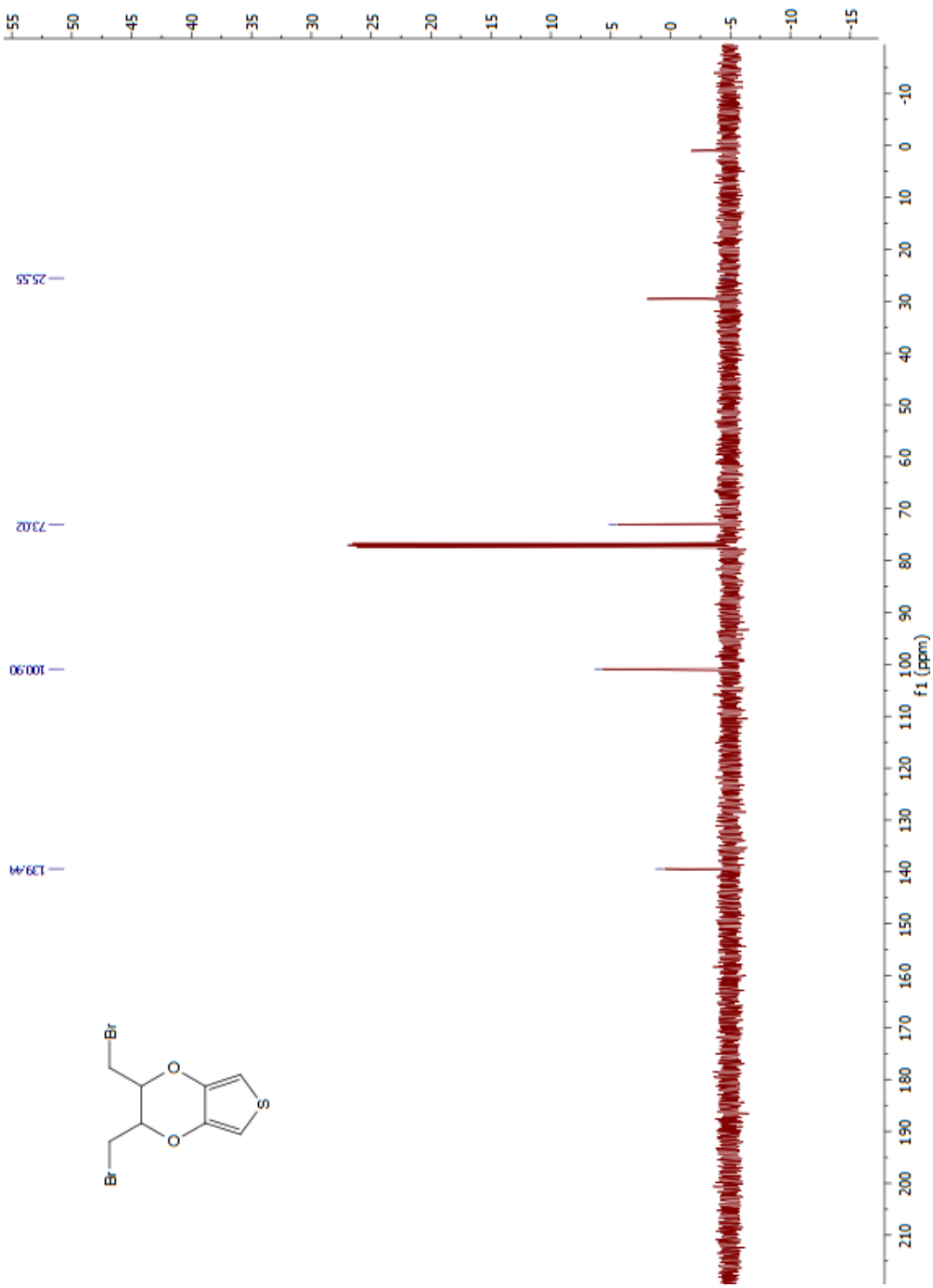

Figure A.44 ^{13}C NMR Spectrum of 2,3-Bis(bromomethyl)-2,3-dihydrothieno[3,4-b][1,4]dioxine

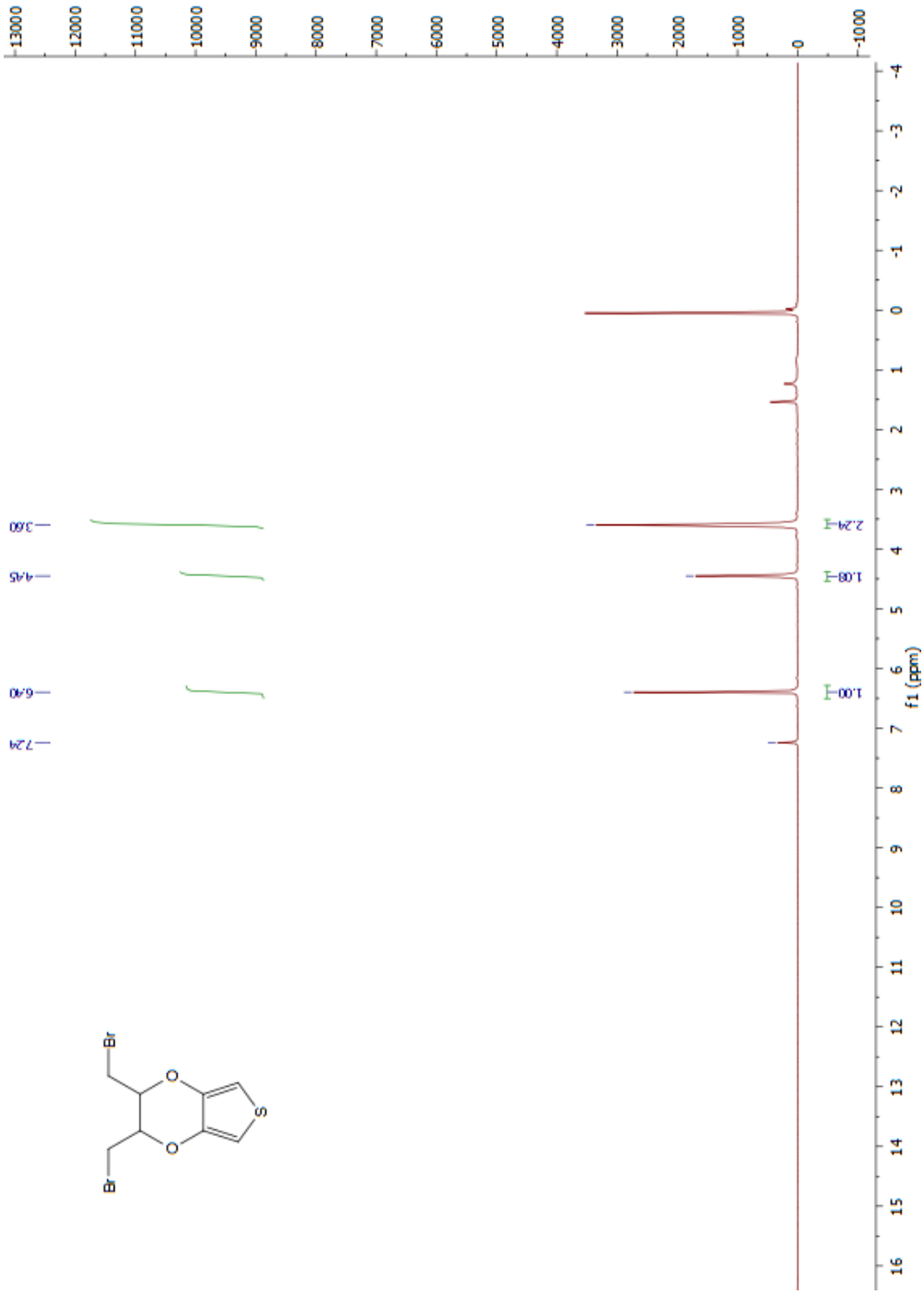

Figure A.45 ^{1}H NMR Spectrum of 2,3-Bis(bromomethyl)-2,3-dihydrothieno[3,4-b][1,4]dioxine

B. HRMS RESULTS OF SYNTHESIZED MONOMERS

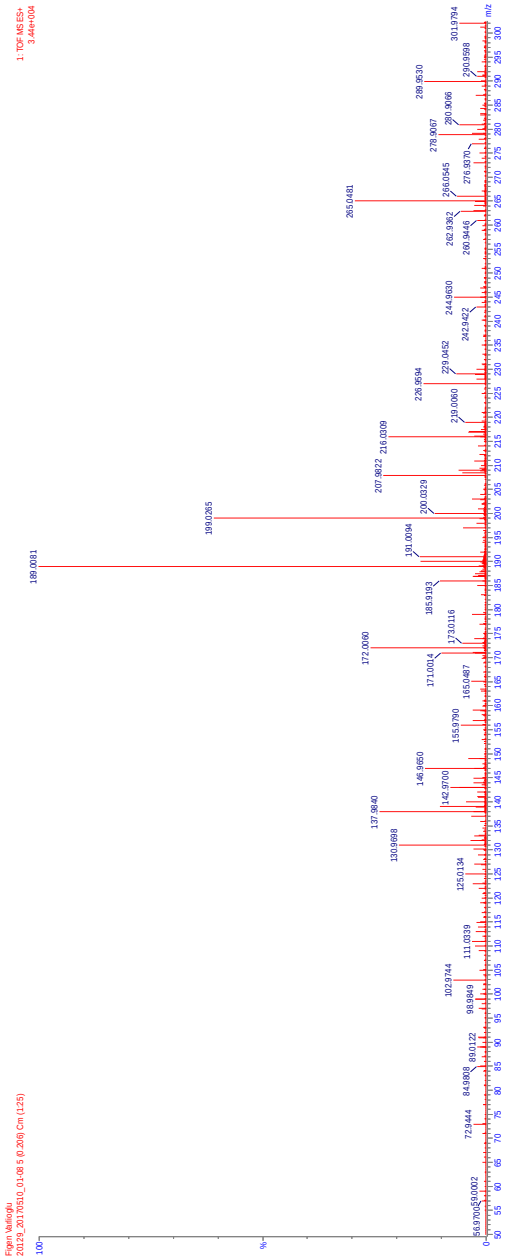

Figure B.1HRMS Result of 3,4-Dihydro-2H-thieno[3,4-b][1,4]oxathiepine

Calculated for $C_7H_8OS_2$: 172.0060 founded: 172.0017

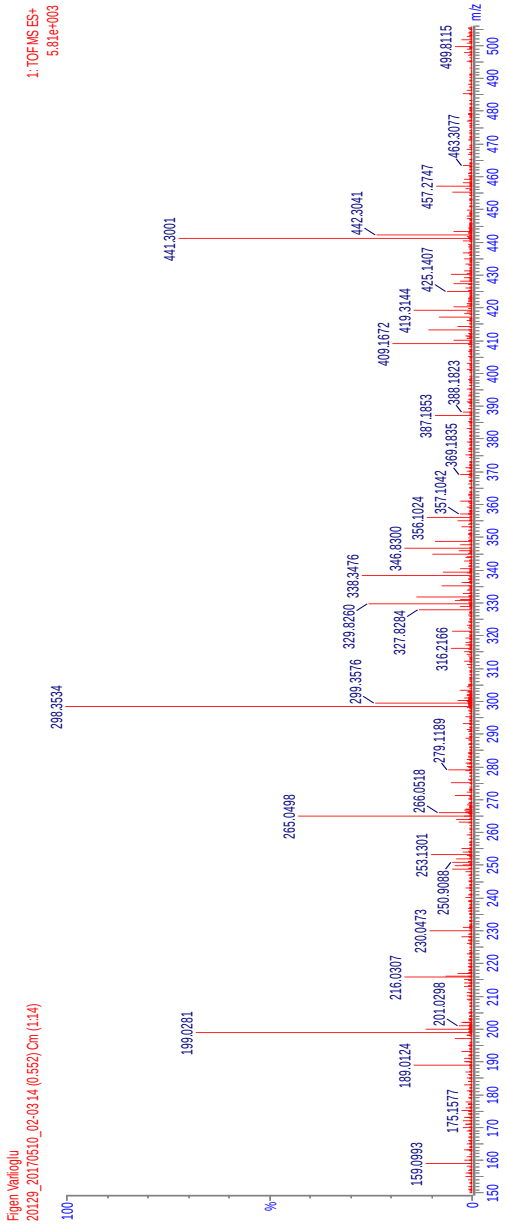

Figure B.2 HRMS Result of 6,8–Dibromo-3,4-dihydro-2H-thieno[3,4b][1,4] oxathiephine

Calculated for $C_7H_6OS_2Br_2$: 329.8260 founded: 329.8206

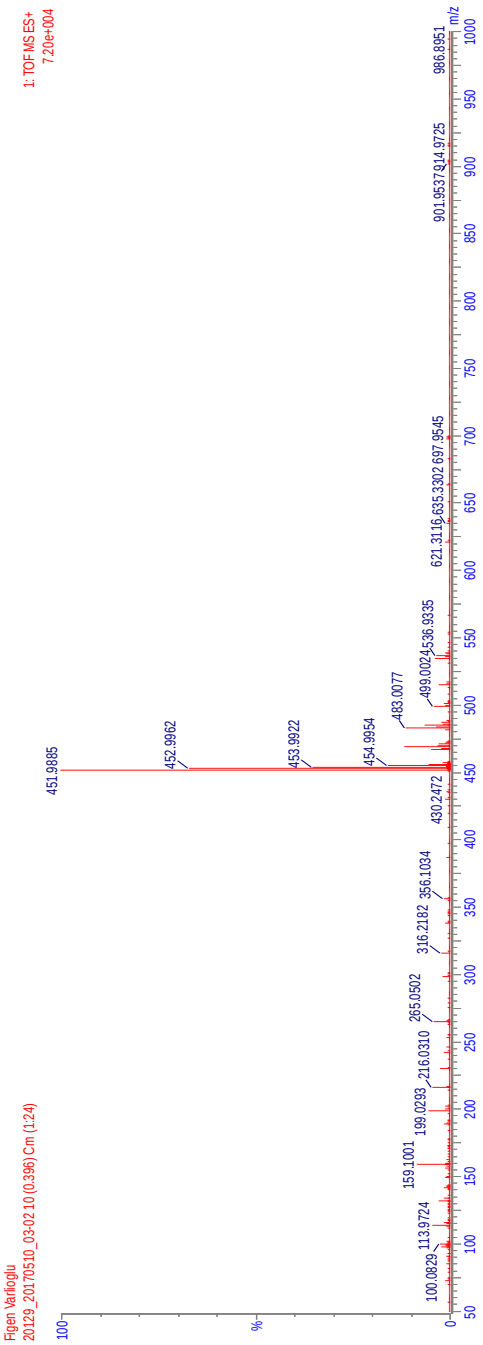

Figure B.3 HRMS Result of 6,8-Bis(2,3-dihydrothieno[3,4-b][1,4]dioxin-5-yl)-3,4-dihydro-2H-thieno[3,4-b][1,4]oxathiepine

Calculated for $C_{19}H_{16}O_5S_4$: 451.9885 founded: 451.9881

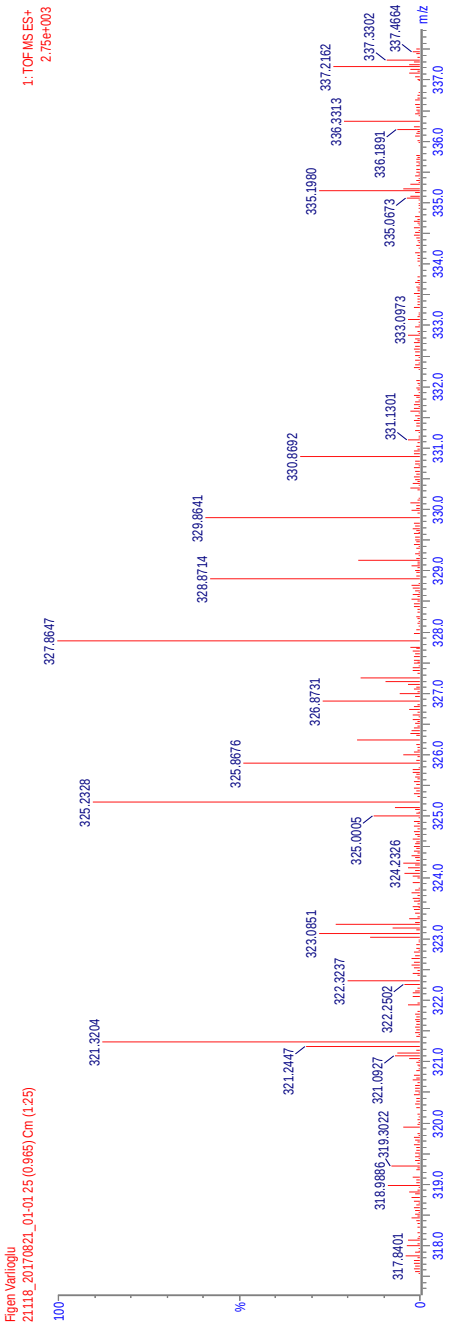

Figure B.15 HRMS Result of 2,3-Bis(bromomethyl)-2,3-dihydrothieno[3,4-b][1,4]dioxine

Calculated for $C_8H_8O_2SBr_2$: 327.8647 founded: 327.8591